

# Barium Tagging in Solid Xenon for nEXO



Tim Walton  
PhD Defense  
2015-12-08



committee:

William Fairbank  
Bruce Berger

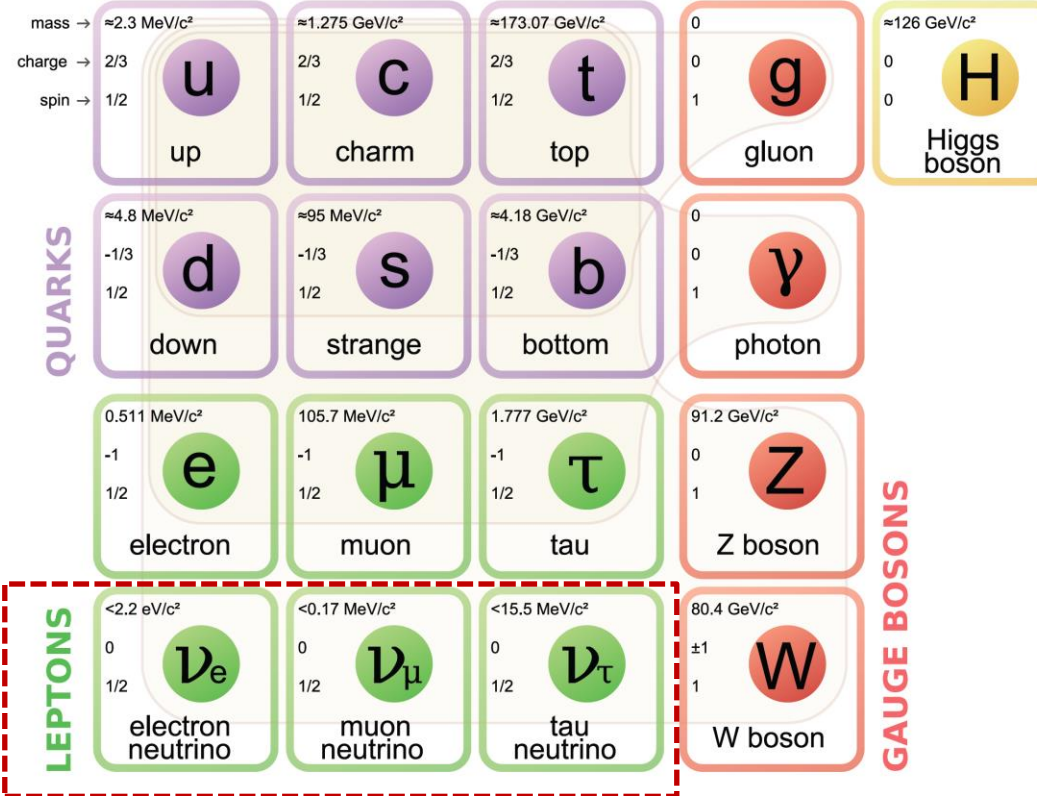
Robert Wilson  
Alan Van Orden



# Outline

- Neutrinos and neutrinoless double beta decay
- EXO-200 experiment
- nEXO and barium tagging
- Barium tagging in solid xenon (SXe):
  - Part 1: Spectroscopy of Ba and Ba<sup>+</sup> in SXe
    - Excitation/emission of Ba in SXe
    - Temperature dependence
    - Bleaching
    - Candidate Ba<sup>+</sup> lines
  - Part 2: Imaging Ba atoms in SXe in focused laser
    - Images of  $\sim 10^3$  atoms w/ 577- and 591-nm lines
    - Single-atom level imaging w/ 619-nm line

# Neutrinos in the Standard Model



- Very small mass
- Interact only via weak force (and gravity)

# Neutrinos in the Standard Model

Charged particles

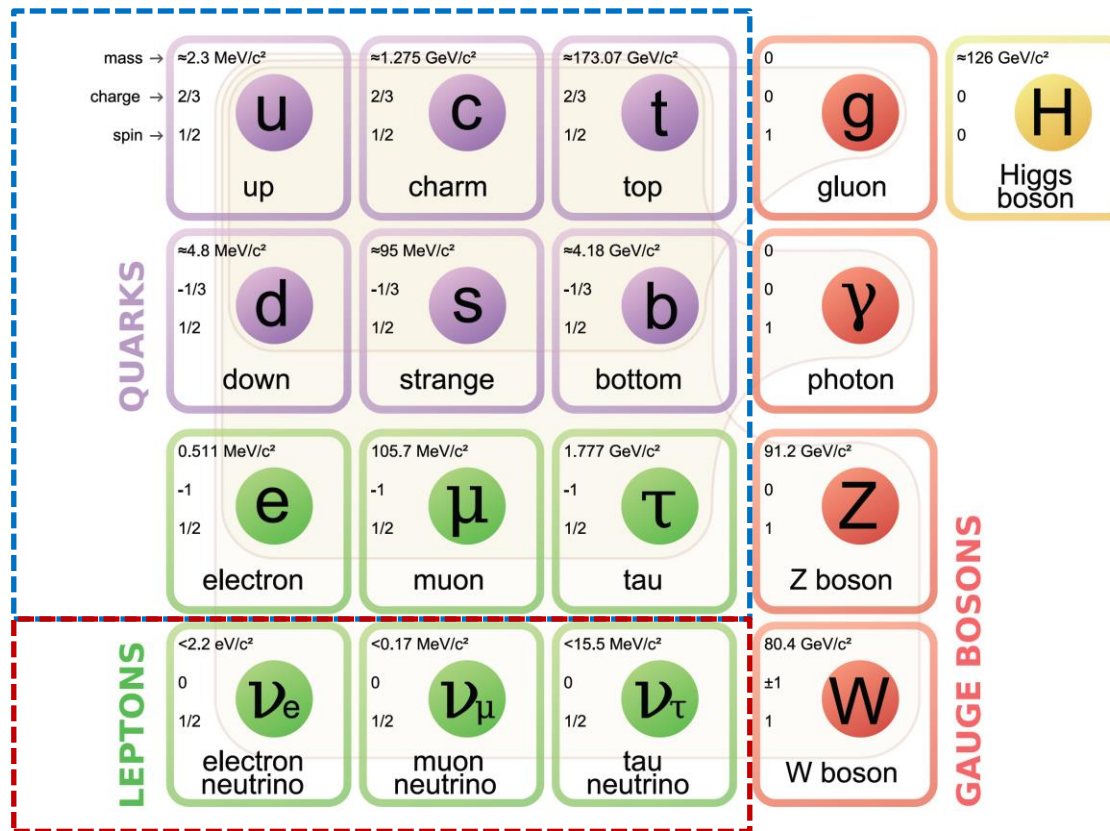


*Distinct  
anti-particles*

No electric charge



*Distinct  
anti-particles??*



Neutrinos could be Majorana particles,  
where particle = anti-particle

# Neutrino Oscillation: neutrinos have mass!

(Nobel prizes: 2002 and 2015)

Oscillation in time between  $\nu_e$ ,  $\nu_\mu$ ,  $\nu_\tau$

Neutrinos interact as flavor states:

$$|\nu_e\rangle, |\nu_\mu\rangle, |\nu_\tau\rangle.$$

which are different from stationary mass states:

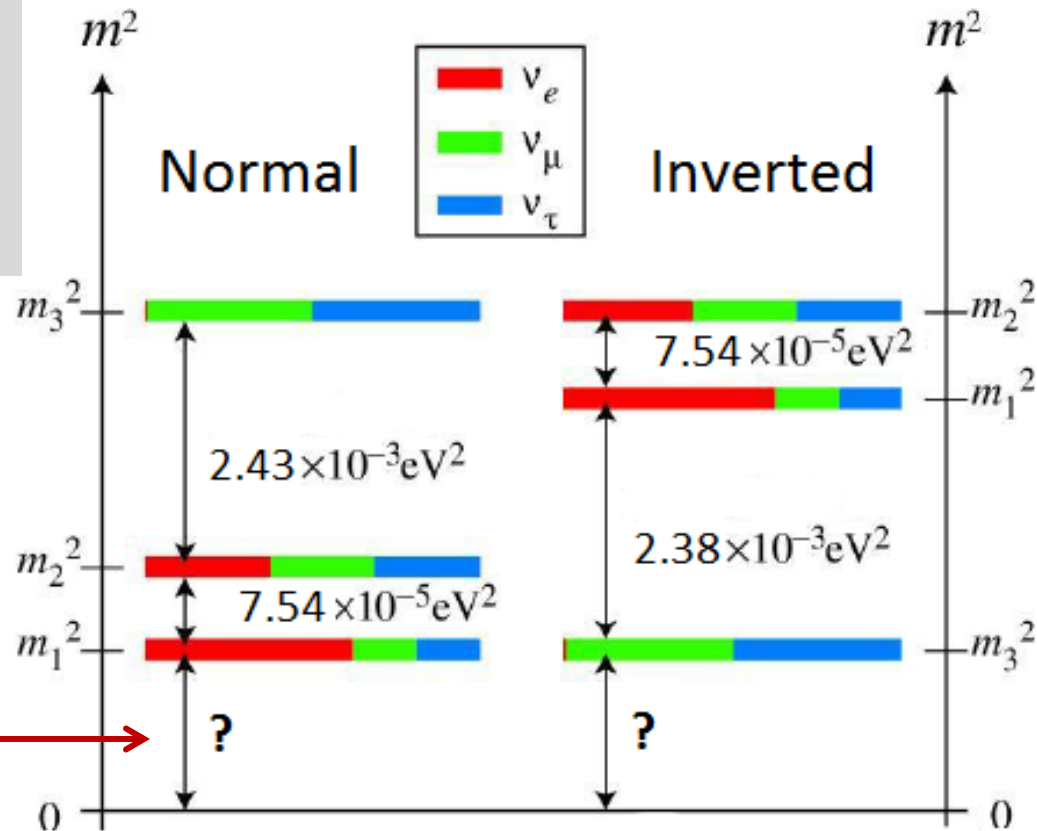
$$|\nu_1\rangle, |\nu_2\rangle, |\nu_3\rangle$$

*Different masses*  $\rightarrow$  oscillations

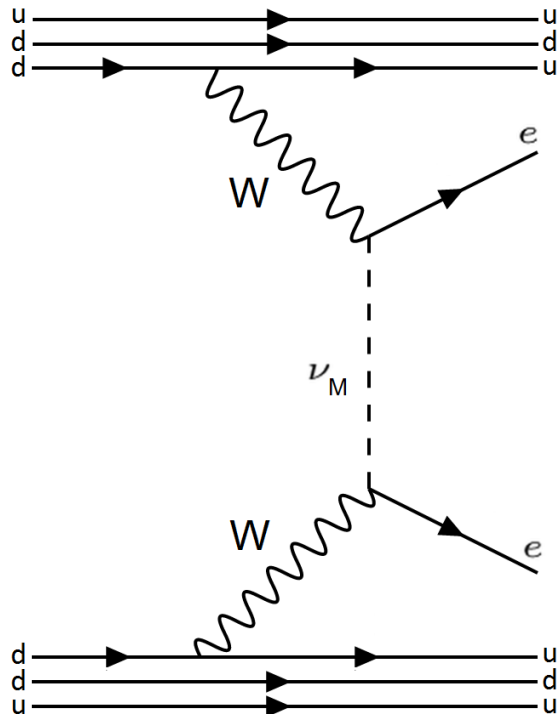
Oscillation experiments have measured difference between squares of neutrino masses:

Absolute mass scale  
yet unknown

Two possible neutrino mass hierarchies:



# Neutrinoless Double Beta Decay ( $0\nu\beta\beta$ )



- Observation would demonstrate Majorana nature of neutrinos
- Violates lepton number conservation
- Could provide measurement of absolute neutrino mass:

$$\langle m_\nu \rangle^2 = [ T_{1/2}^{0\nu} G^{0\nu}(Q,Z) |M^{0\nu}|^2 ]^{-1}$$

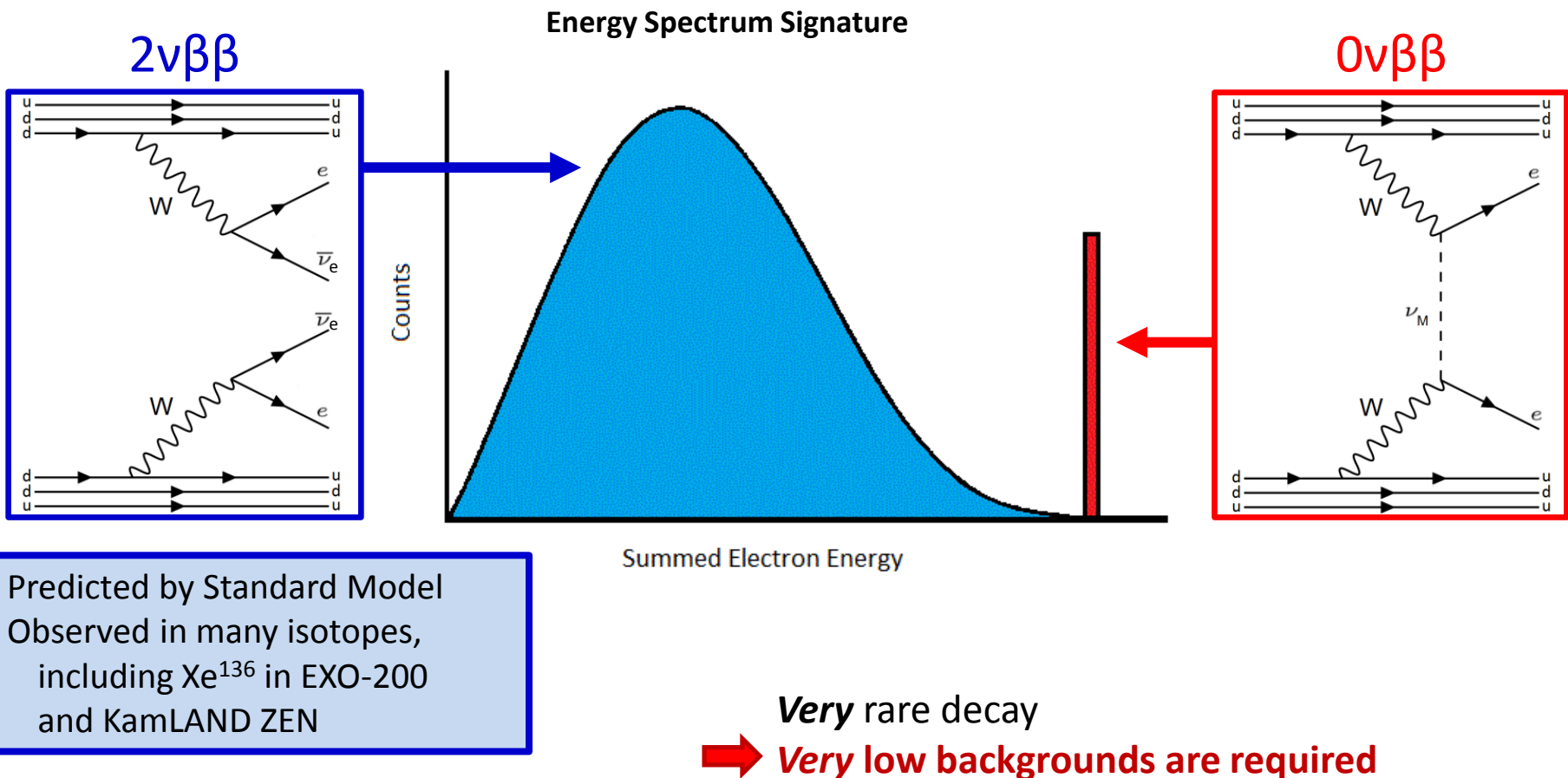
where effective Majorana neutrino mass is  
 $\langle m_\nu \rangle = \sum_i U_{ei}^2 m_i$

$G^{0\nu}$  is a known phase factor

$M^{0\nu}$  is the nuclear matrix element for  $0\nu\beta\beta$

$T_{1/2}^{0\nu}$  is the half-life of  $0\nu\beta\beta$

# Search for $0\nu\beta\beta$

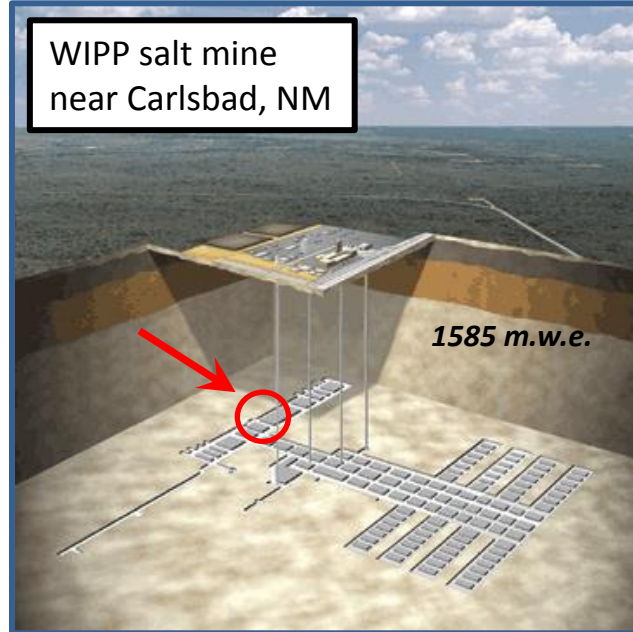


# EXO-200

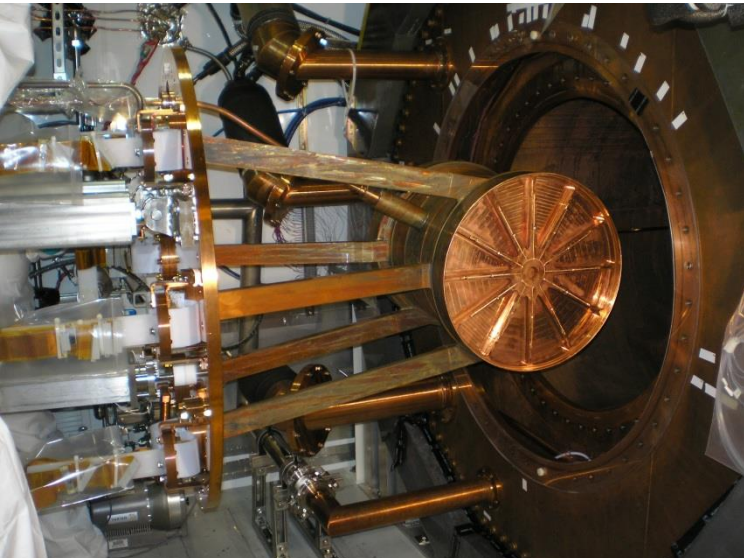
First phase of Enriched Xenon Observatory,  
for the search for  $0\nu\beta\beta$  mode of



- ~170-kg. liquid Xe (LXe) time projection chamber (TPC), enriched to ~80.6% Xe<sup>136</sup>
- operates in class 100 cleanroom, 2,150 ft. underground

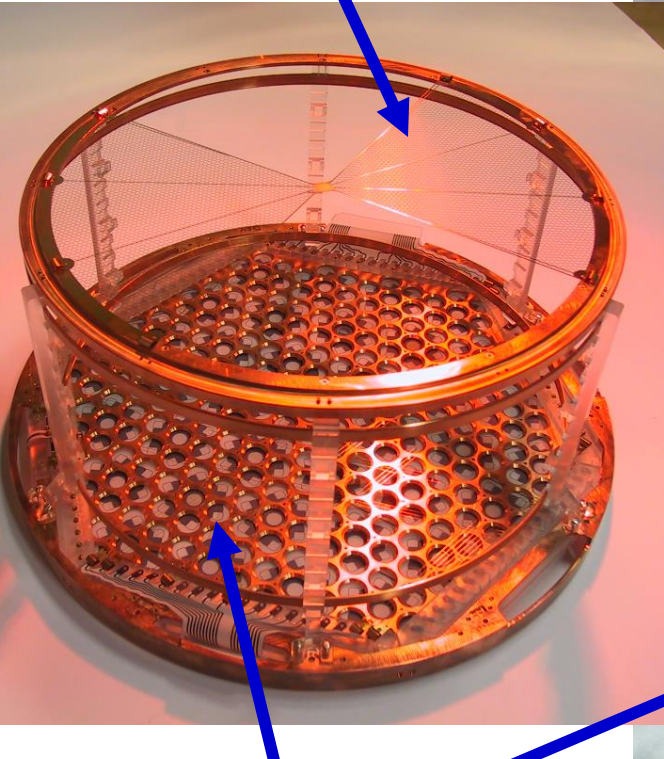


TPC installation into copper cryostat

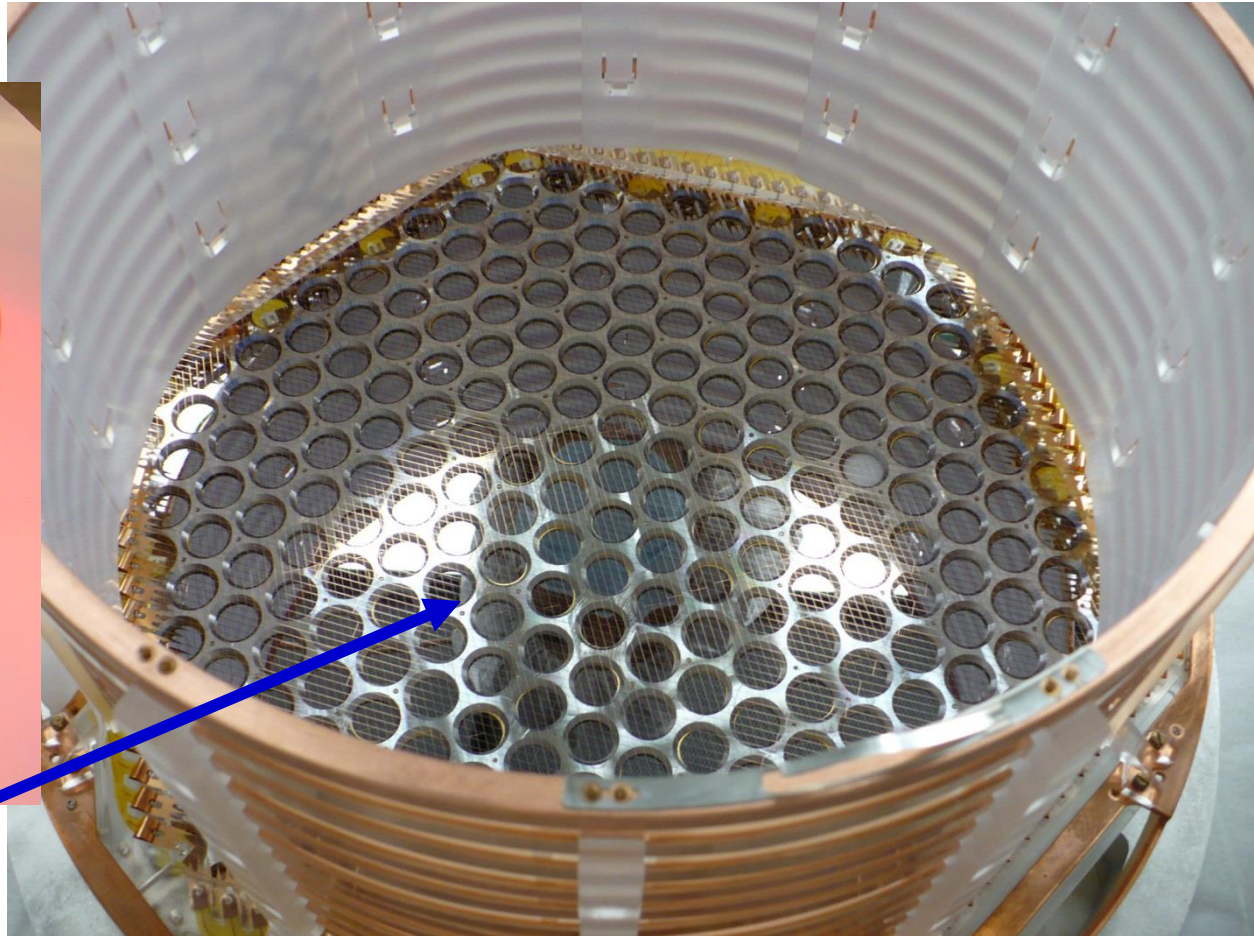


# EXO-200 Time Projection Chamber

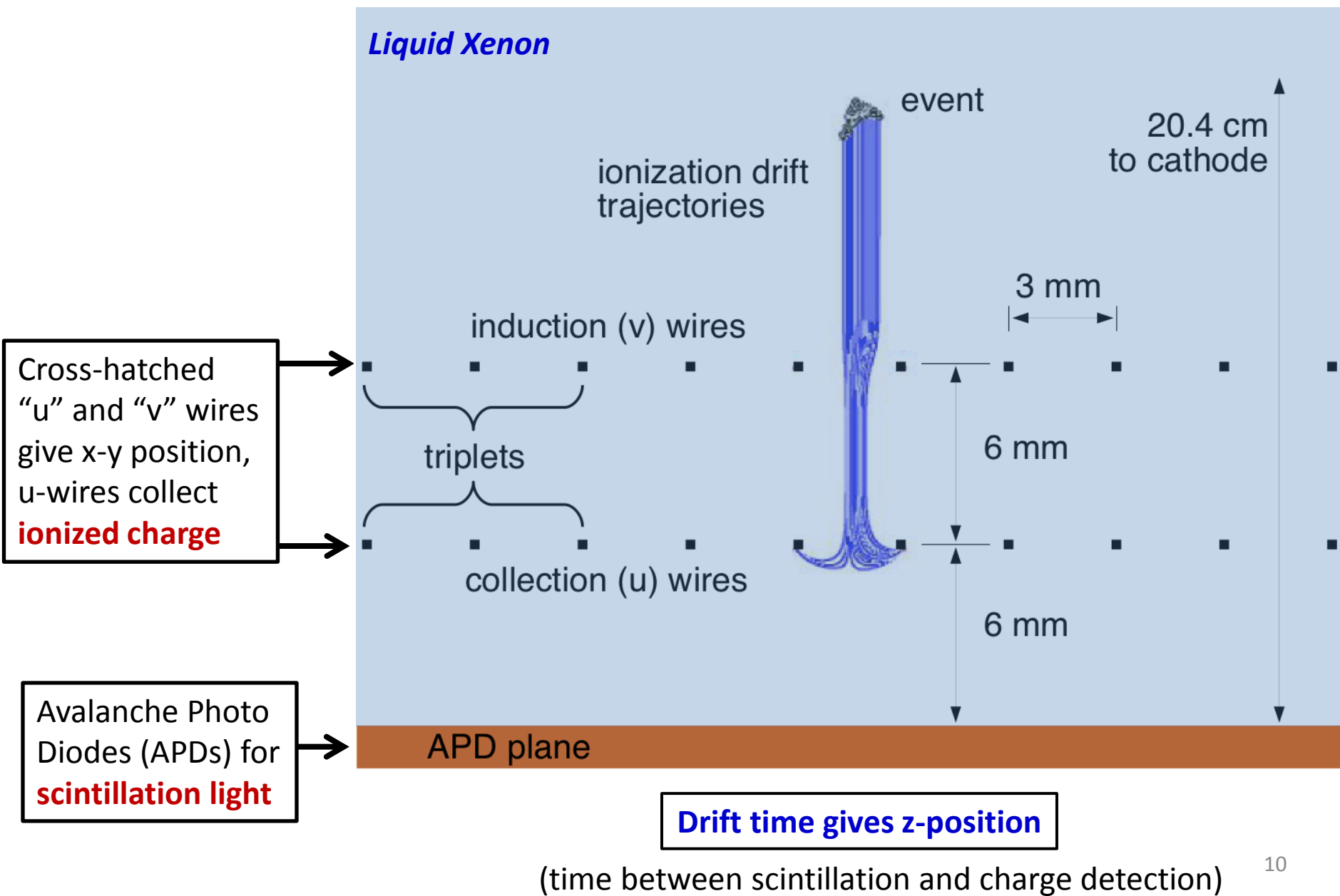
Cathode grid



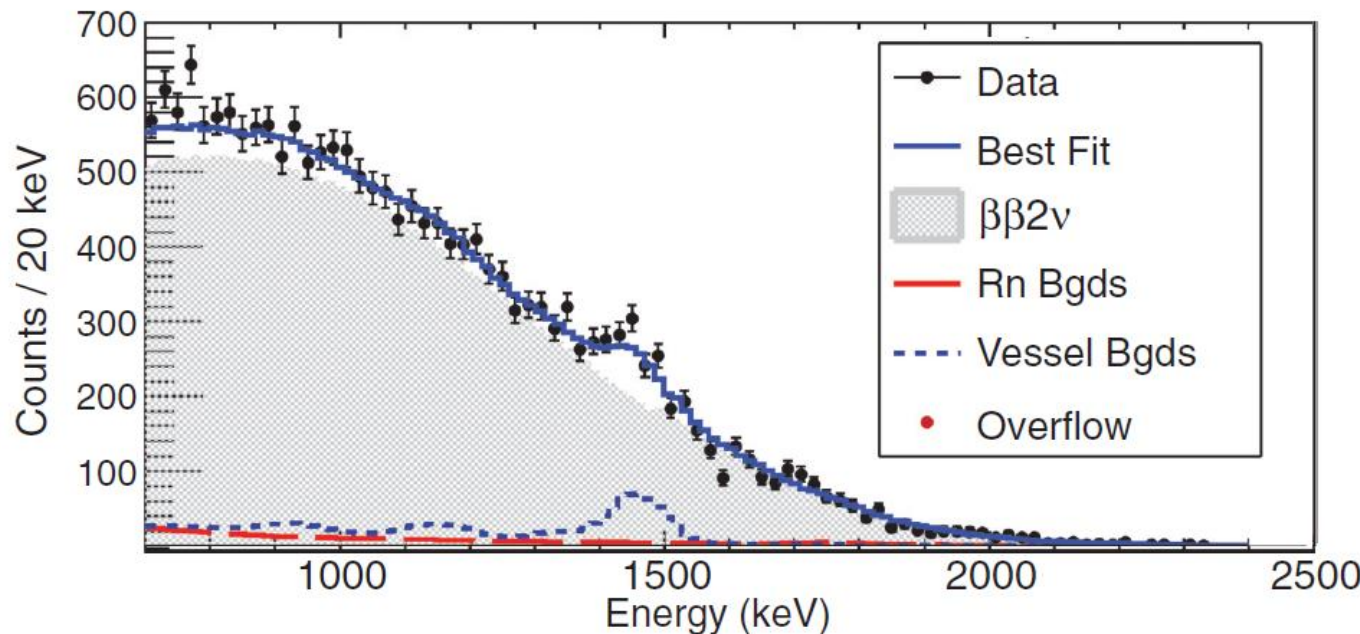
Detection plane for  
charge (wires) and scintillation  
(APDs) from decay events in the LXe



# EXO-200 Time Projection Chamber

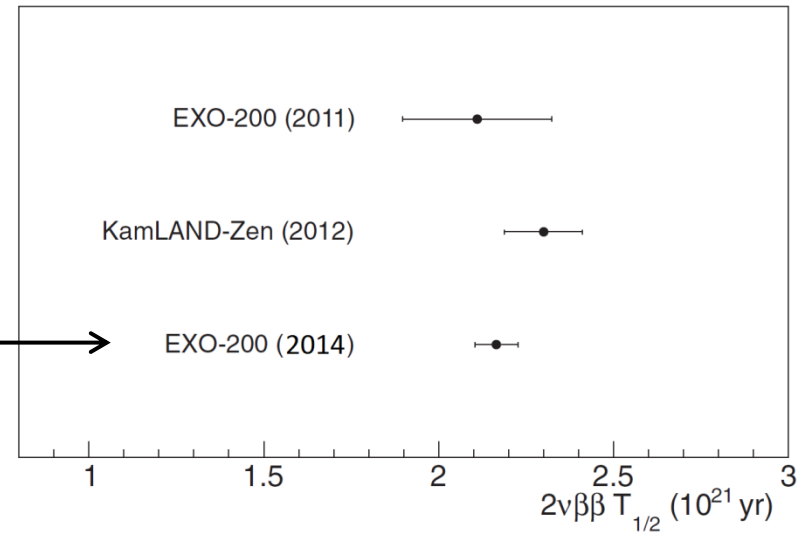


# EXO-200 Results: $2\nu\beta\beta$ Measurement

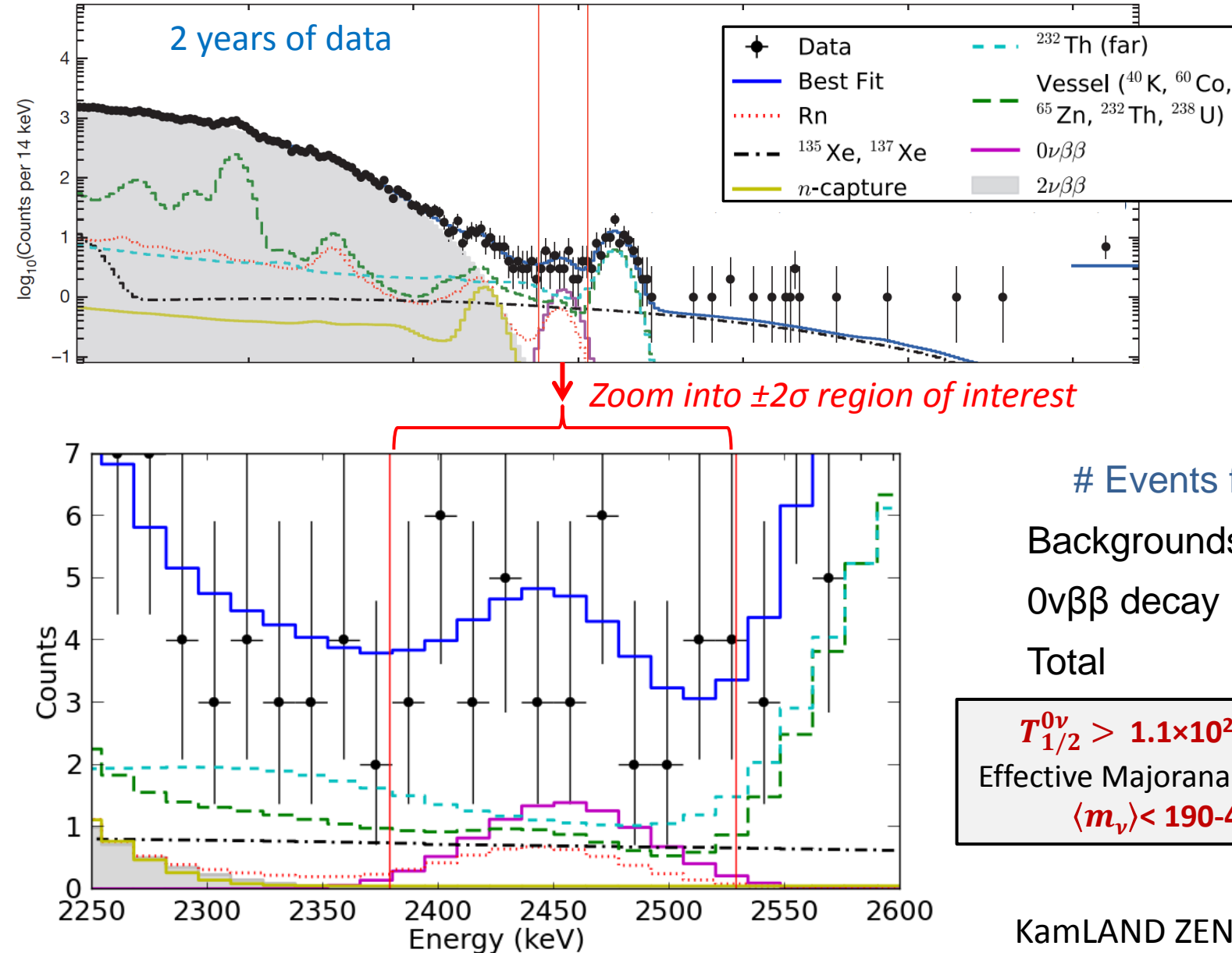


Phys. Rev. C **89**, 015502 (2014)

$$T_{1/2}^{2\nu} = (2.165 \pm 0.016 \text{ stat.} \pm 0.059 \text{ sys.}) \times 10^{21} \text{ yr}$$



# EXO-200 Results: $0\nu\beta\beta$ Search

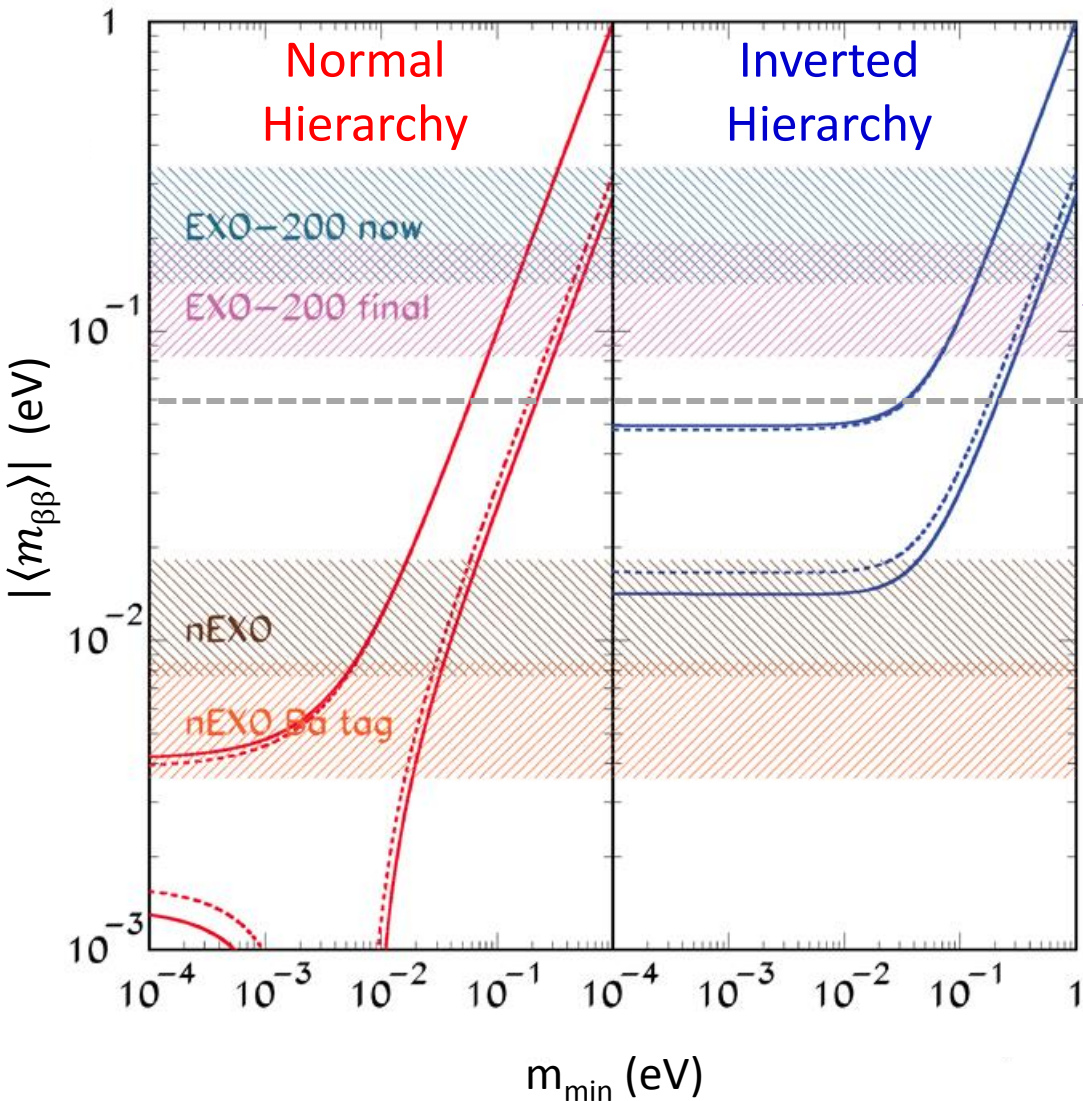


Nature 510, 229 (2014)

KamLAND ZEN:

$T_{1/2}^{0\nu} > 1.9 \times 10^{25} \text{ yr (90\% CL)}$

# $0\nu\beta\beta$ Sensitivity

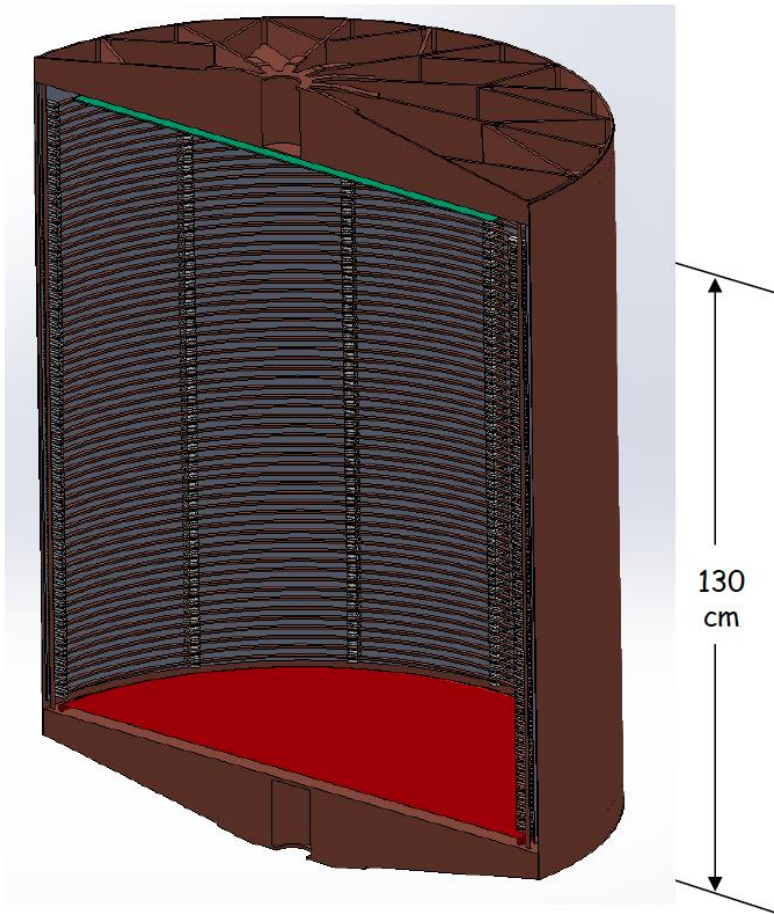


Final (2019) EXO-200 sensitivity in “Quasi-degenerate” region of neutrino masses.

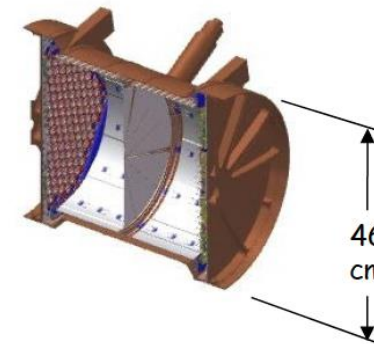
Measurement of  $\langle m_\nu \rangle$  could determine mass hierarchy if below this region.  
But need bigger detector...

# nEXO

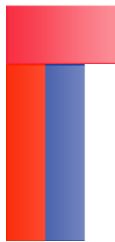
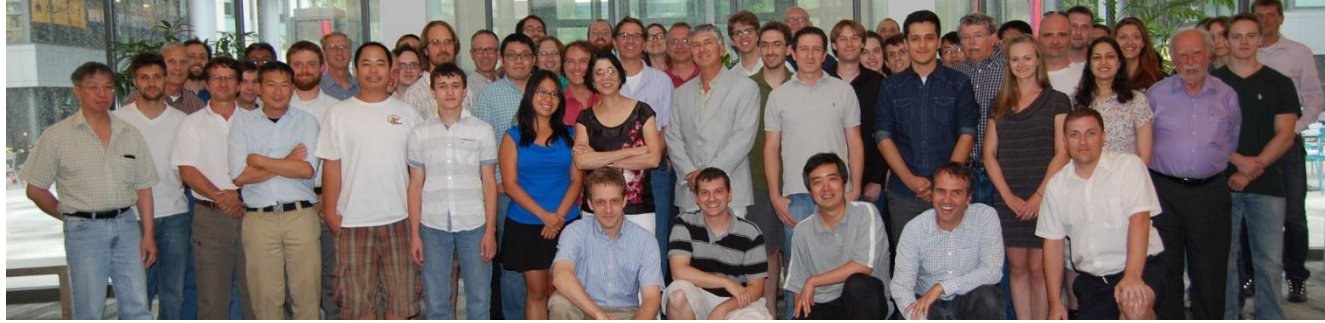
Successor to EXO-200: ~5-ton enriched LXe TPC  
for more sensitive  $0\nu\beta\beta$  search.



EXO-200: 170 kg enriched LXe



# The nEXO Collaboration



University of Alabama, Tuscaloosa AL, USA — T Didberidze, M Hughes, A Piepke, R Tsang

University of Bern, Switzerland — S Delaquis, R Gornea<sup>†</sup>, J-L Vuilleumier

<sup>†</sup>Now at Carleton University

Brookhaven National Laboratory, Upton NY, USA — M Chiu, G De Geronimo, S Li, V Radeka, T Rao, G Smith, T Tsang, B Yu

California Institute of Technology, Pasadena CA, USA — P Vogel

Carleton University, Ottawa ON, Canada — Y Baribeau, V Basque, M Bowcock, M Dunford, M Facina, R Gornea, K Graham, P Gravelle, R Killick, T Koffas, C Licciardi, K McFarlane, R Schnarr, D Sinclair

Colorado State University, Fort Collins CO, USA — C Chambers, A Craycraft, W Fairbank Jr., T Walton

Drexel University, Philadelphia PA, USA — MJ Dolinski, YH Lin, E Smith, T Winick, Y-R Yen

Duke University, Durham NC, USA — PS Barbeau, G Swift

University of Erlangen-Nuremberg, Erlangen, Germany — G Anton, R Bayerlein, J Hoessl, P Hufschmidt, A Jamil, T Michel, T Ziegler

IBS Center for Underground Physics, Daejeon, South Korea — DS Leonard

IHEP Beijing, People's Republic of China — G Cao, W Cen, X Jiang, H Li, Z Ning, X Sun, T Tolba, W Wei, L Wen, W Wu, J Zhao

University of Illinois, Urbana-Champaign IL, USA — D Beck, M Coon, J Walton, L Yang

Indiana University, Bloomington IN, USA — JB Albert, S Daugherty, TN Johnson, LJ Kaufman, G Visser, J Zettlemoyer

University of California, Irvine, Irvine CA, USA — M Moe

ITEP Moscow, Russia — V Belov, A Burenkov, M Danilov, A Dolgolenko, A Karelina, A Kobyakin, A Kuchenkov, V Stekhanov, O Zeldovich

Laurentian University, Sudbury ON, Canada — B Cleveland, A Der Mesrobian-Kabakian, J Farine, B Mong, U Wichoski

Lawrence Livermore National Laboratory, Livermore CA, USA — O Alford, J Brodsky, M Heffner, G Holtmeier, A House, M Johnson, S Sangiorgio

University of Massachusetts, Amherst MA, USA — J Dalmasson, S Feyzakhsh, S Johnston, J King, A Pocar

McGill University, Montreal PQ, Canada — T Brunner

Oak Ridge National Laboratory, Oak Ridge TN, USA — L Fabris, D Hornback, RJ Newby, K Ziack

Rensselaer Polytechnic Institute, Troy NY, USA — E Brown

SLAC National Accelerator Laboratory, Menlo Park CA, USA — T Daniels, - K Fouts, G Haller, R Herbst, M Kwiatkowski, K Nishimura, A Odian, M Oriunno, PC Rowson, K Skarpaas

University of South Dakota, Vermillion SD, USA — R MacLellan

Stanford University, Stanford CA, USA — R DeVoe, D Fudenberg, G Gratta, M Jewell, S Kravitz, D Moore, I Ostrovskiy, A Schubert, K Twelker, M Weber

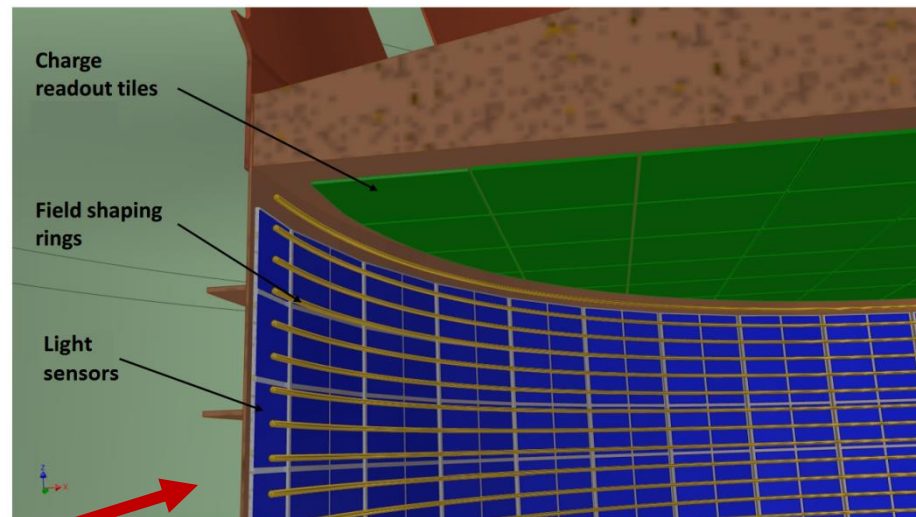
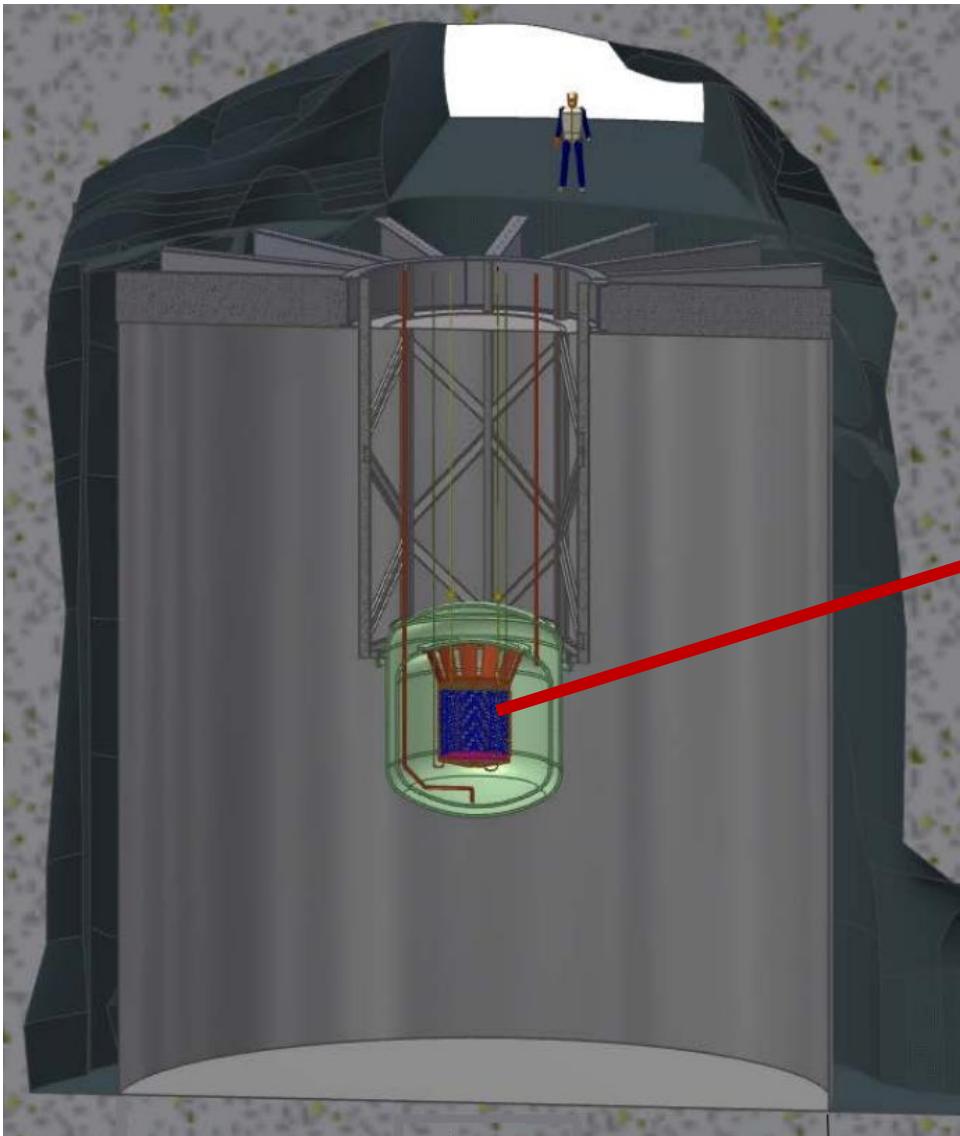
Stony Brook University, SUNY, Stony Brook, NY, USA — K Kumar, O Njoya, M Tarka

Technical University of Munich, Garching, Germany — P Fierlinger, M Marino

TRIUMF, Vancouver BC, Canada — J Dilling, P Gumplinger, R Krücken, F Retière, V Strickland

# nEXO

Successor to EXO-200: ~5-ton enriched LXe TPC  
for more sensitive  $0\nu\beta\beta$  search.

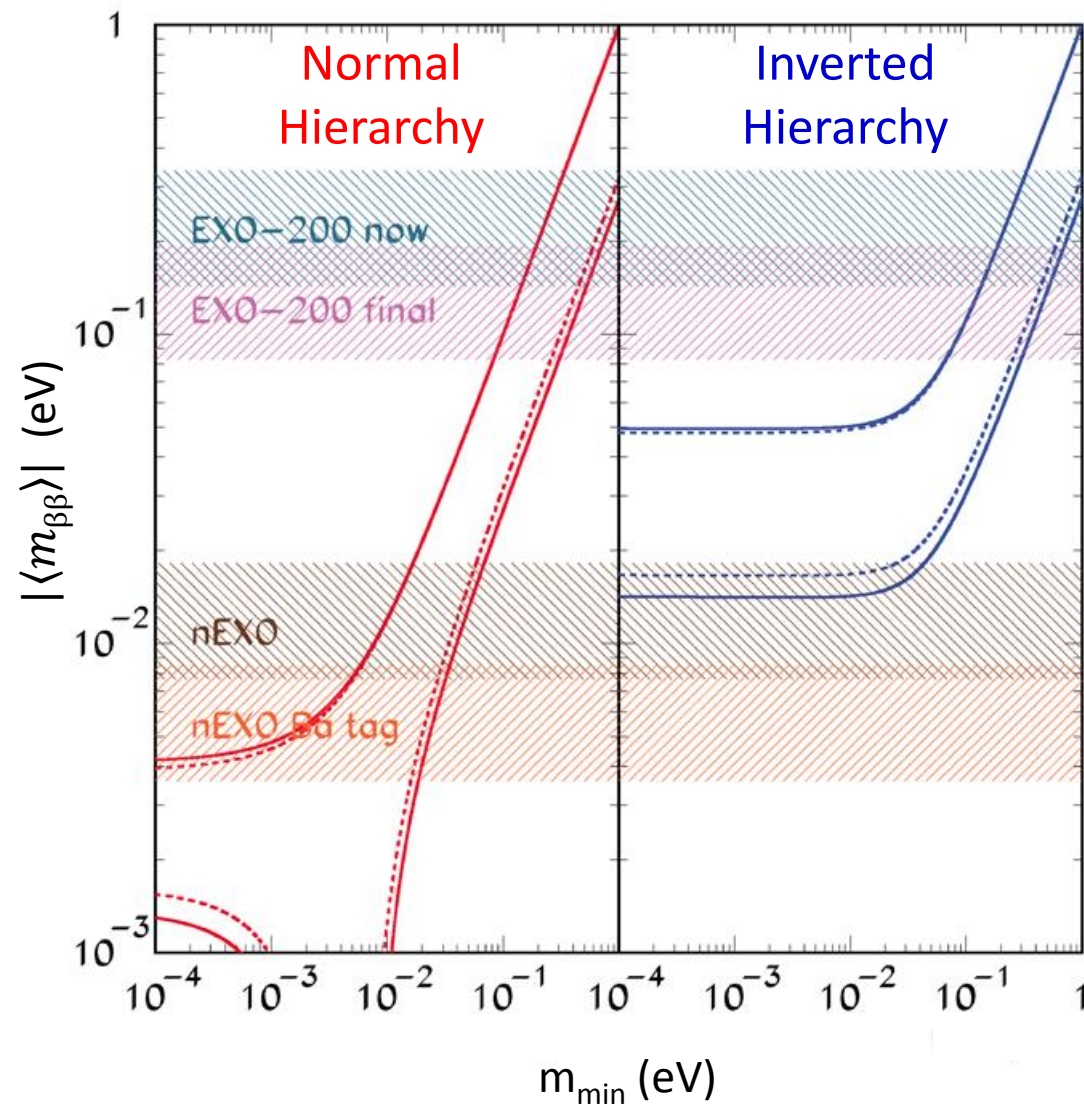


**Ba tagging:** identify barium daughter  
for complete background elimination



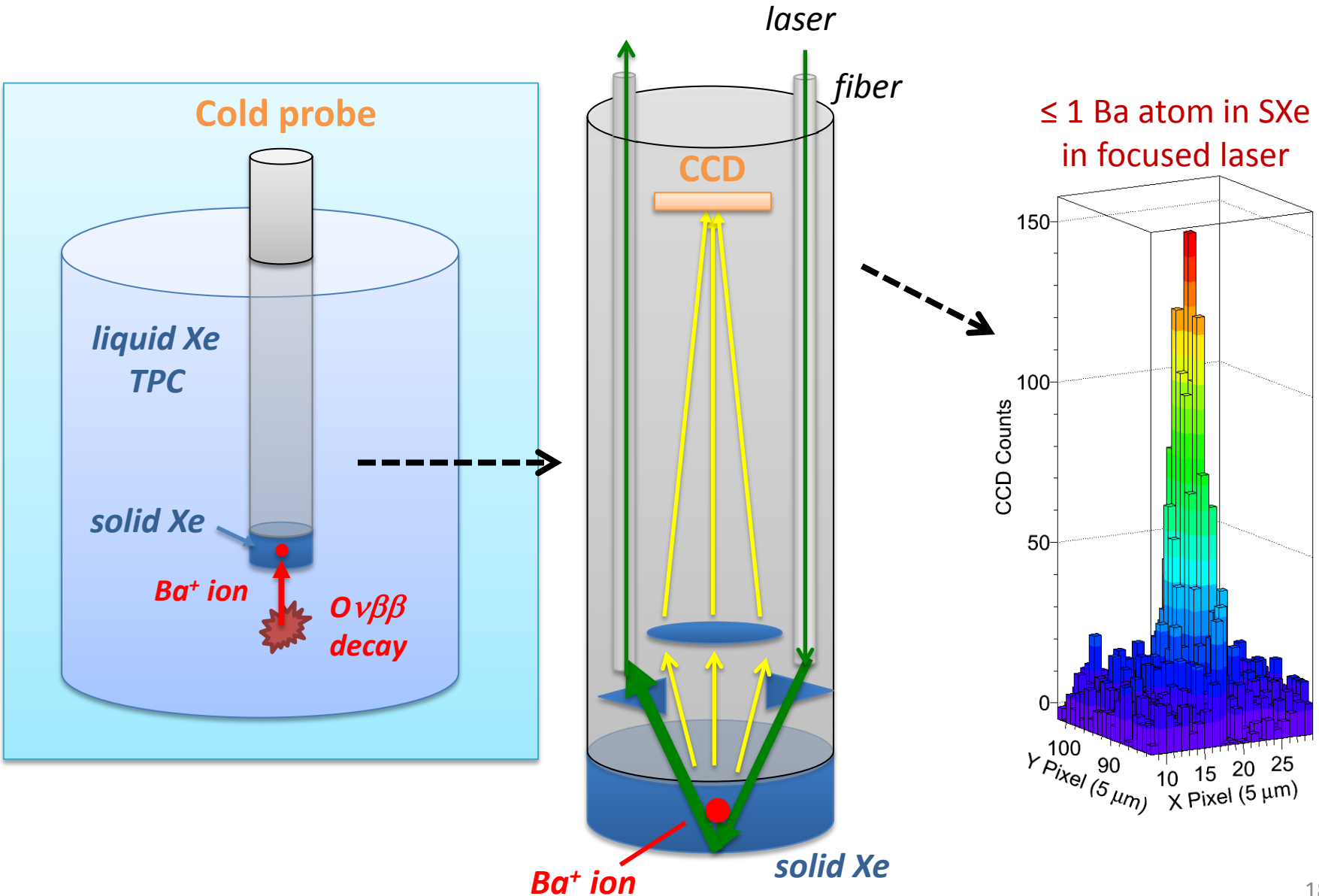
*Will require grabbing/detecting a  
single  $Ba^+$  out of a macroscopic  
volume of LXe!*

# $0\nu\beta\beta$ Sensitivity



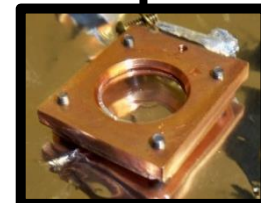
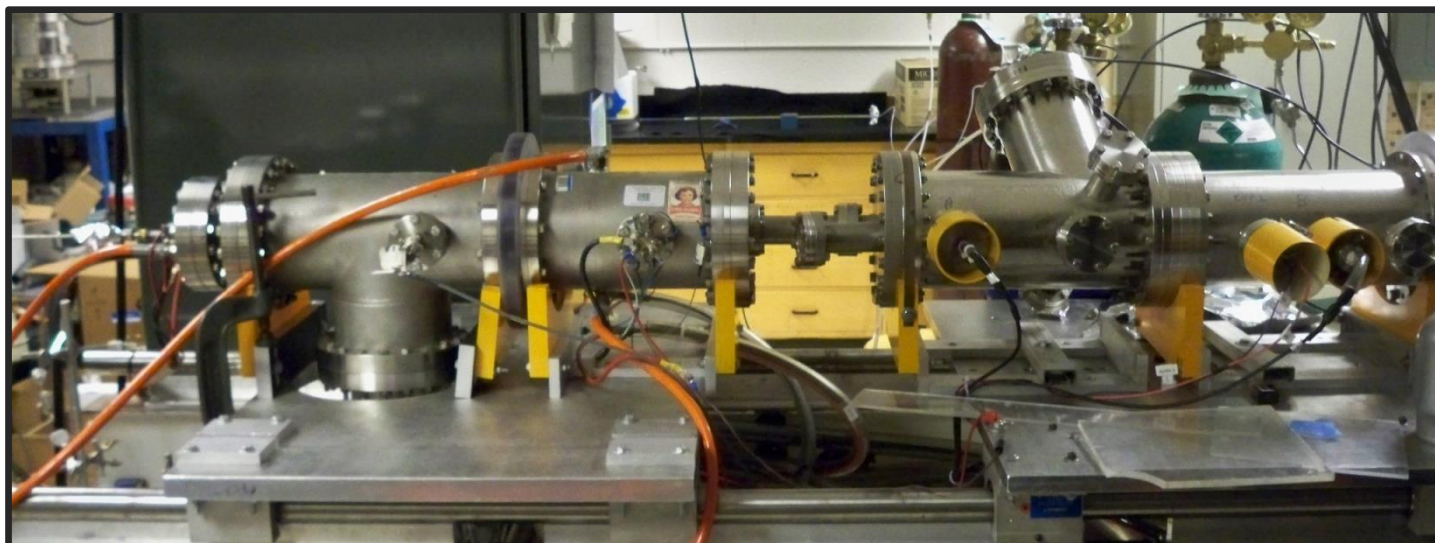
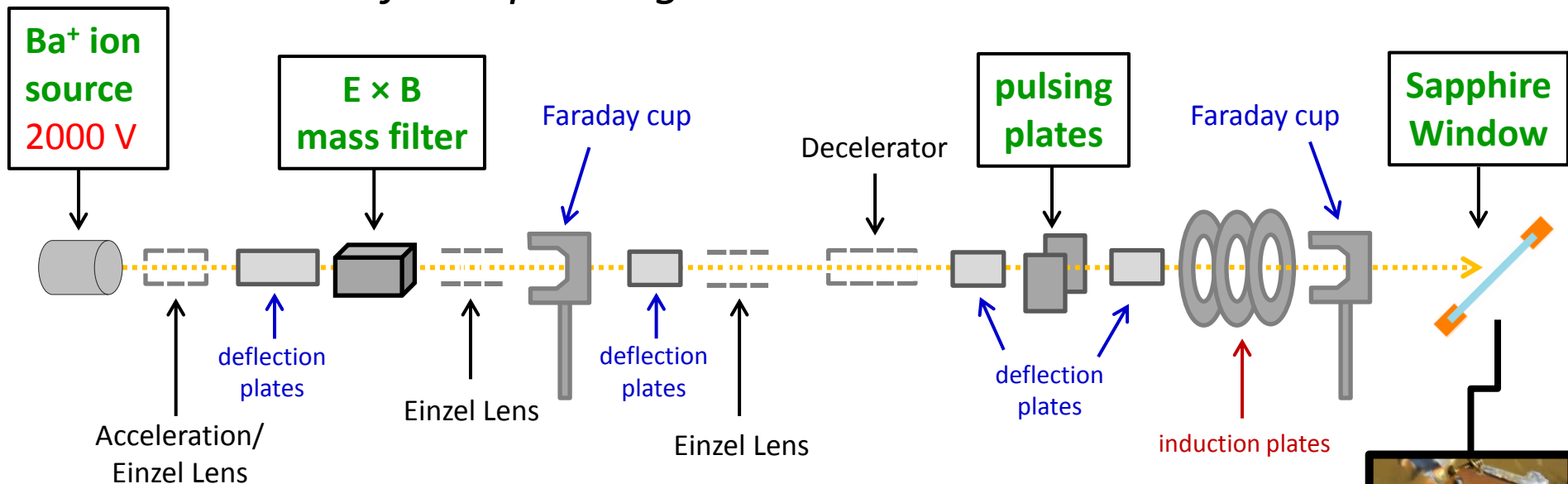
} nEXO will probe entire Inverted Hierarchy, and well into Normal Hierarchy with Ba tagging.

# Barium Tagging in Solid Xenon

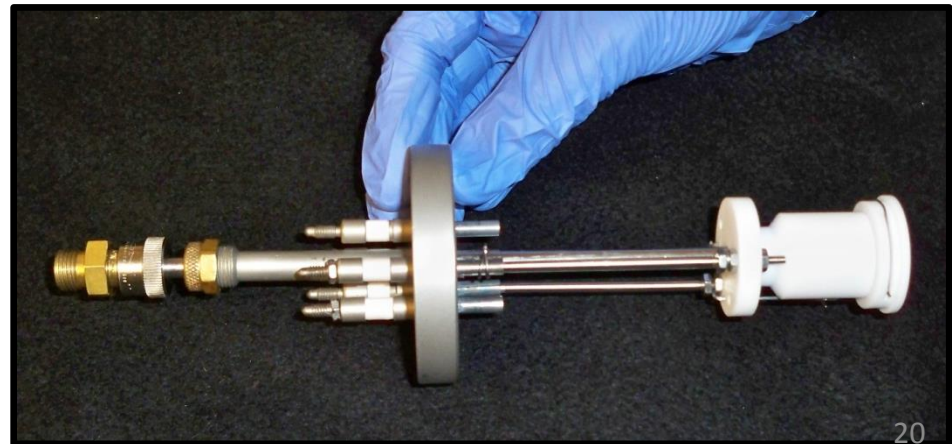
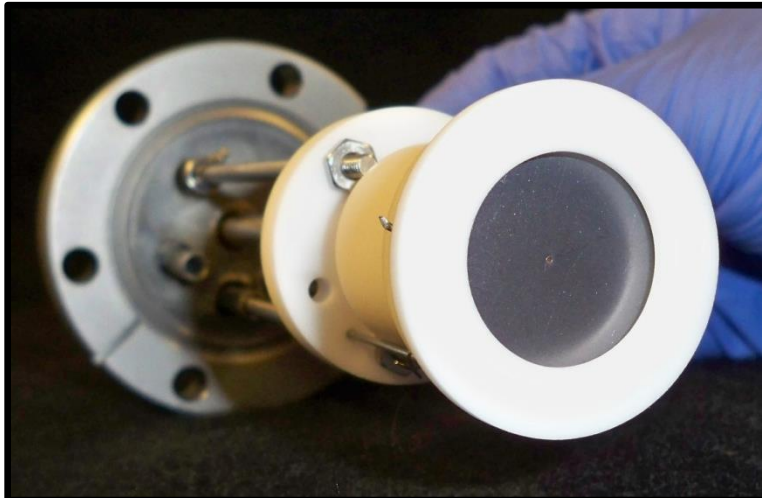
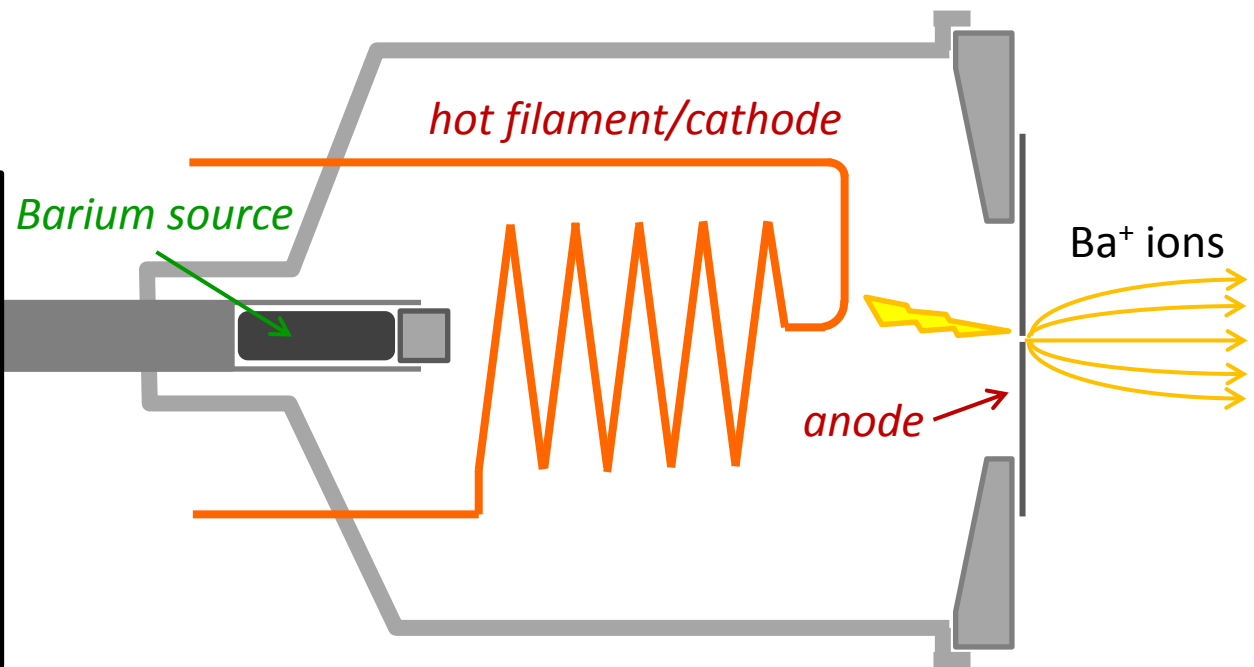


# Ion Beam

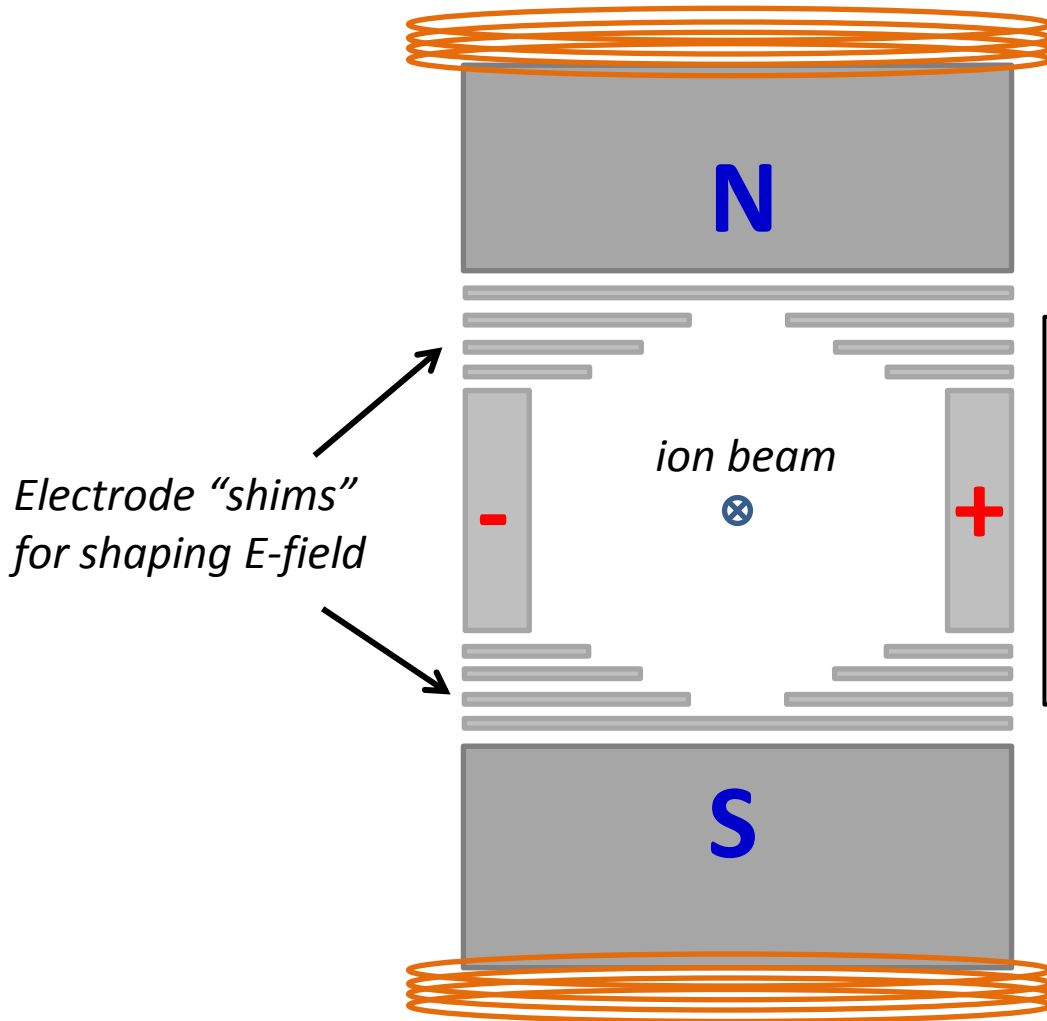
*for depositing Ba<sup>+</sup> ions into Solid Xenon*



# Ion Source

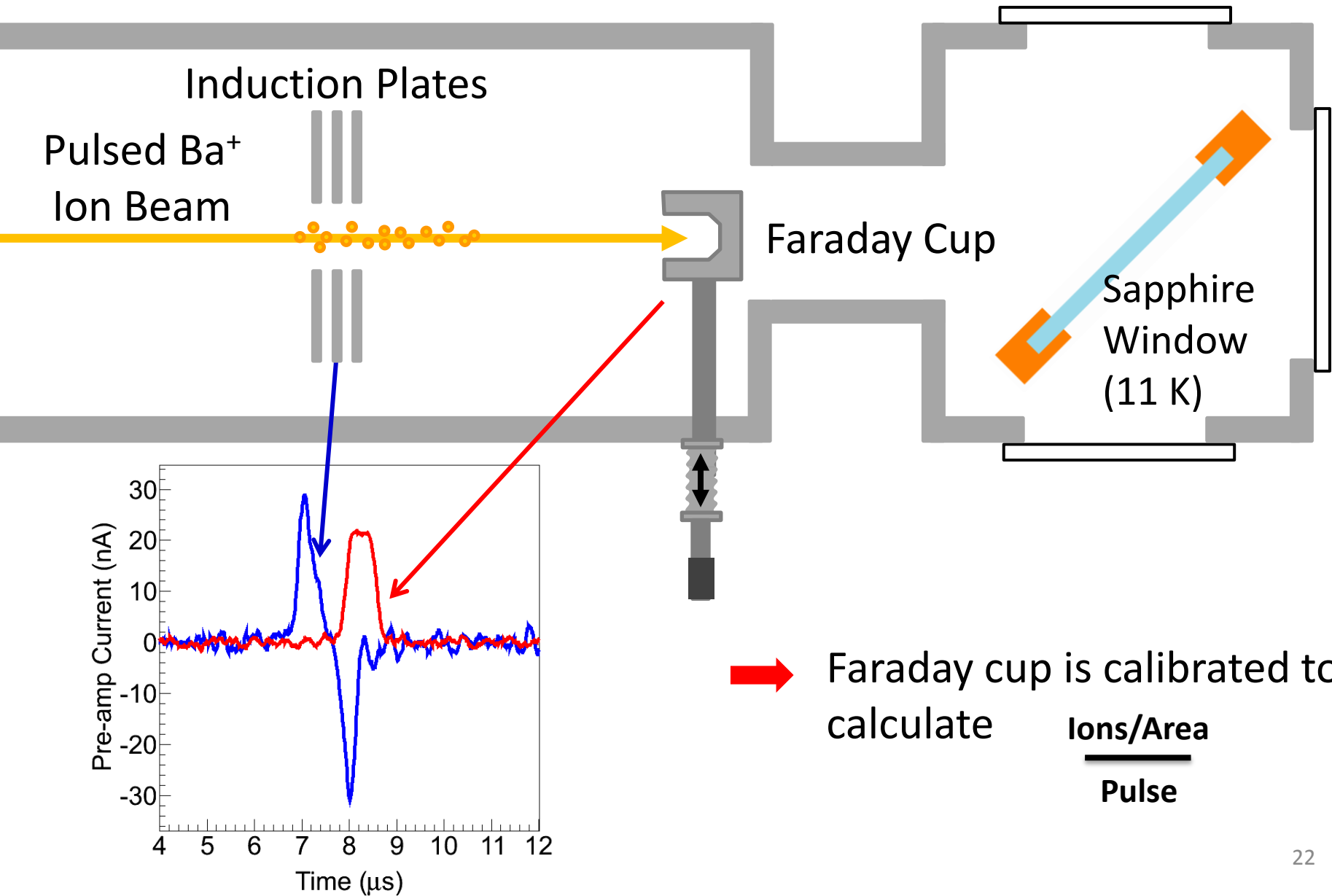


# $E \times B$ Mass Filter for selecting $\text{Ba}^+$

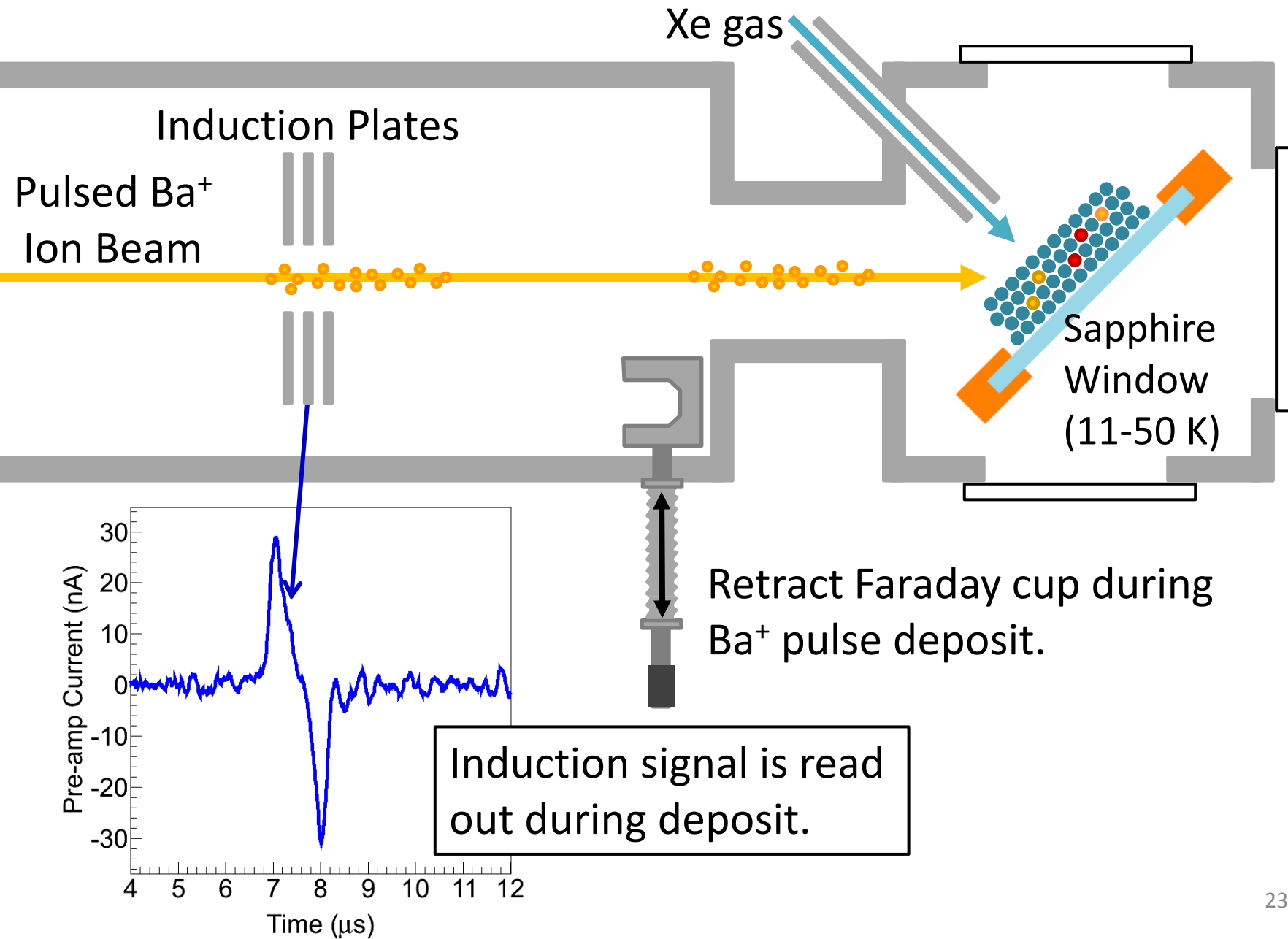


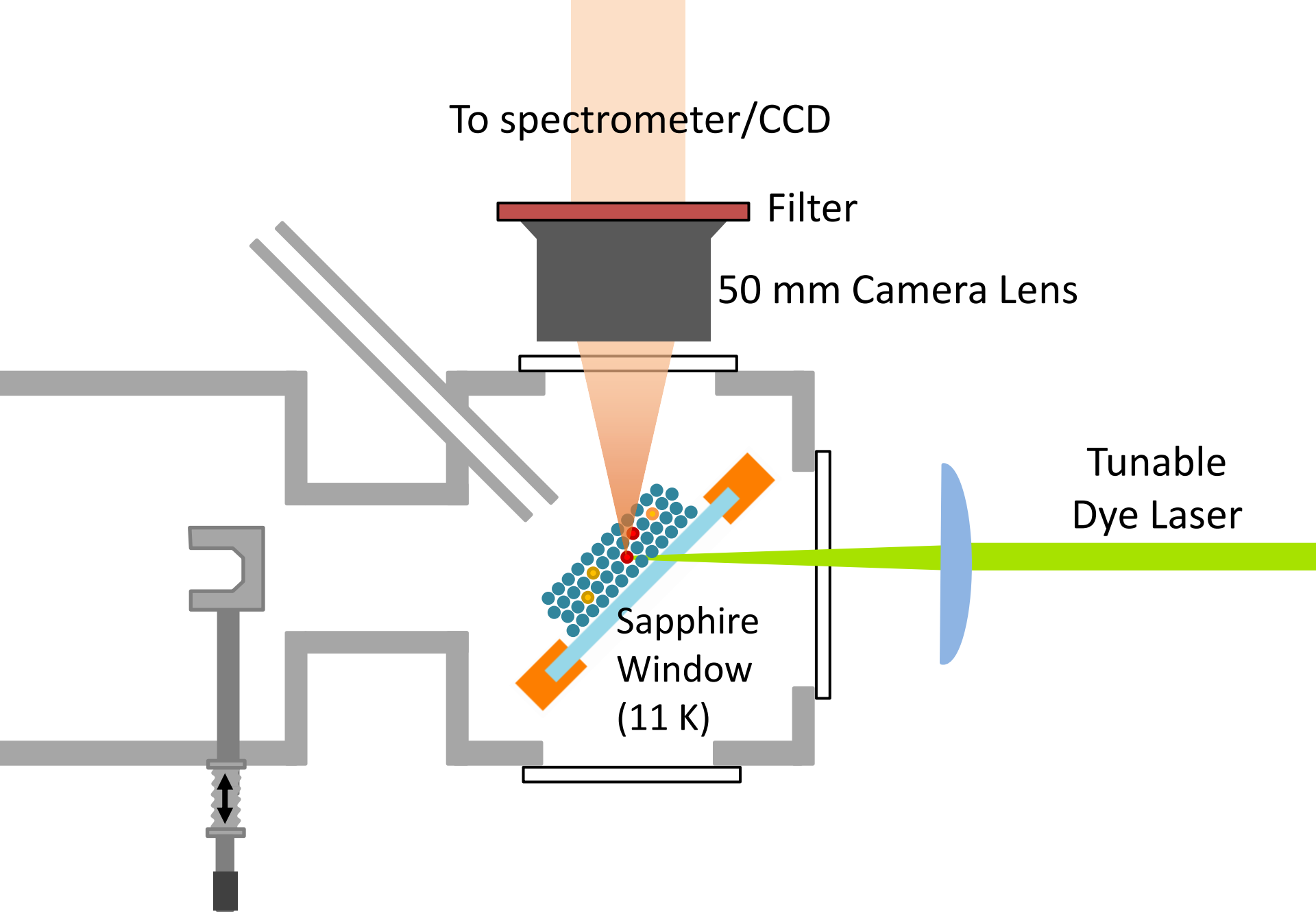
Only ions with velocity satisfying  
 $qE = qvB$   
will move through filter undeflected,  
thus selecting specific  $m/q$ , which  
have different velocities due to  
initial acceleration.

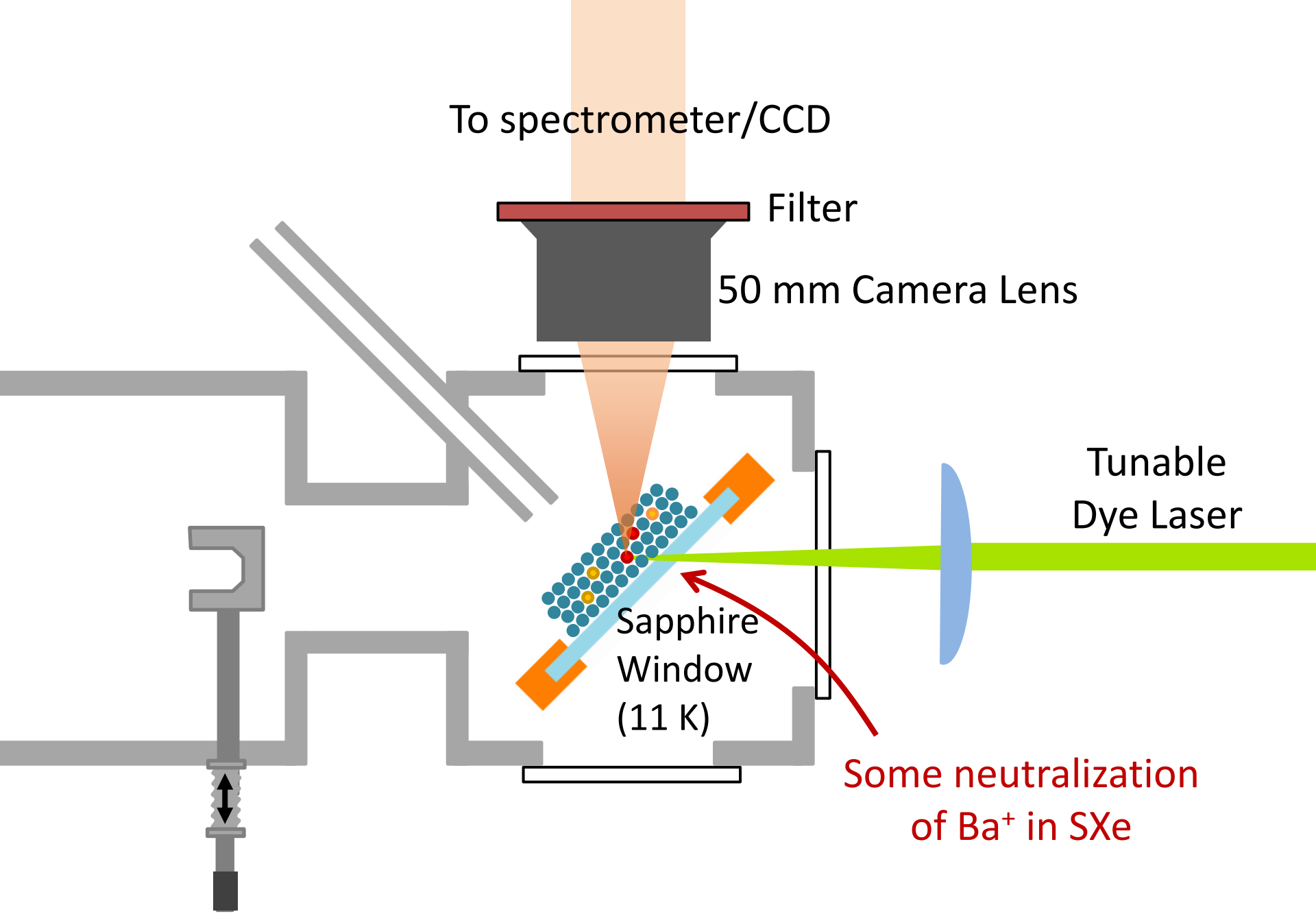
# $\text{Ba}^+$ /Ba Deposition

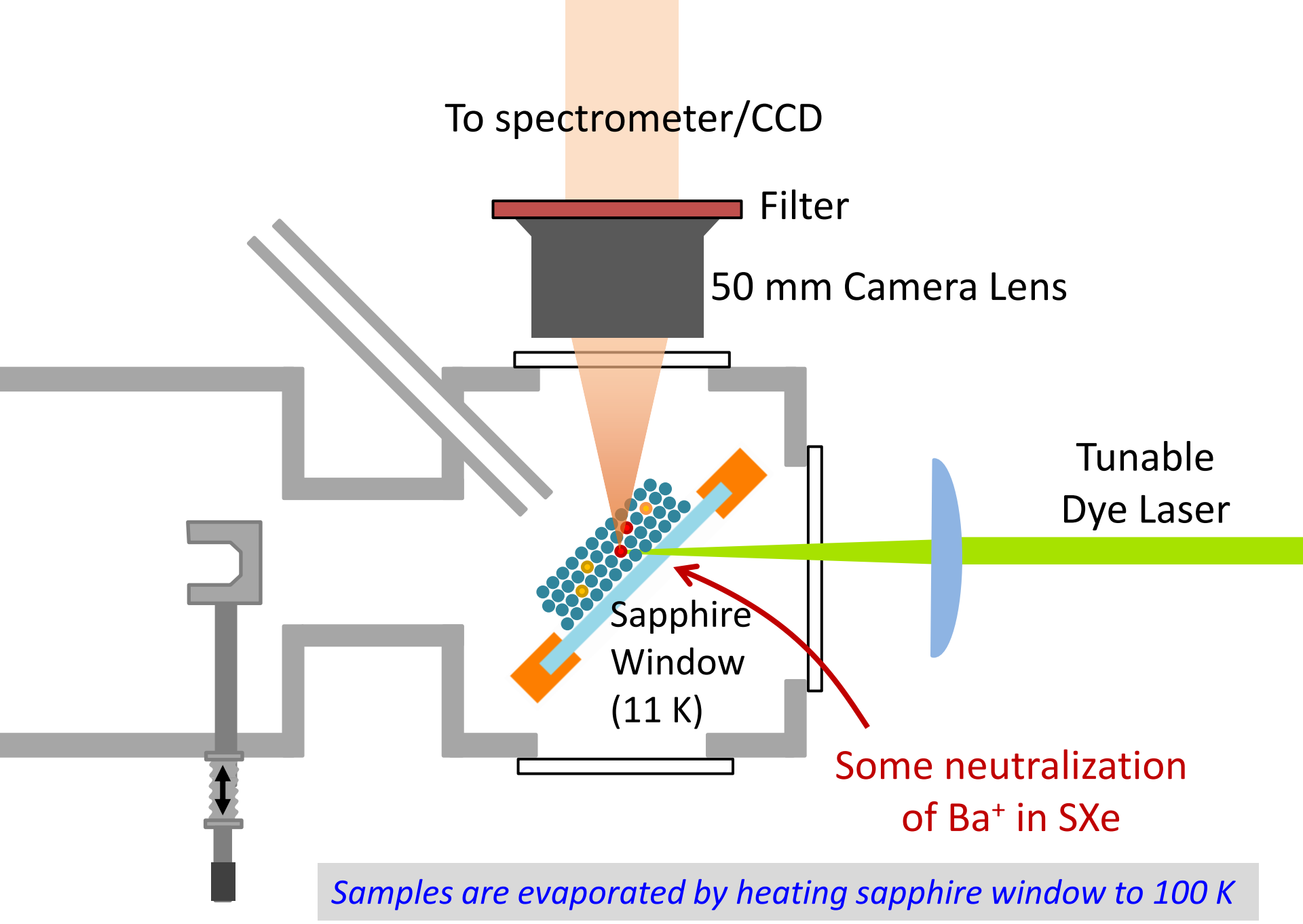


# $\text{Ba}^+/\text{Ba}$ Deposition









# Imaging Ba in SXe on Cold Sapphire Window

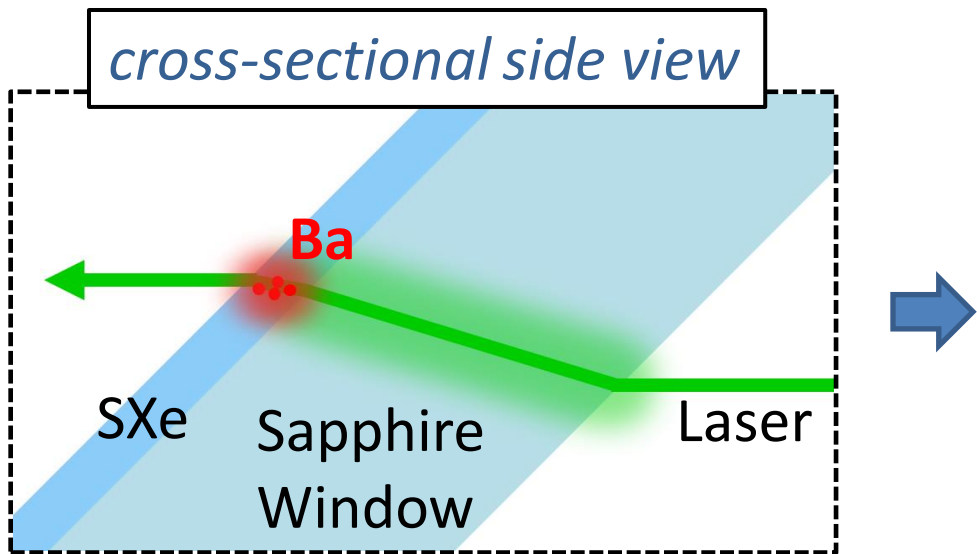
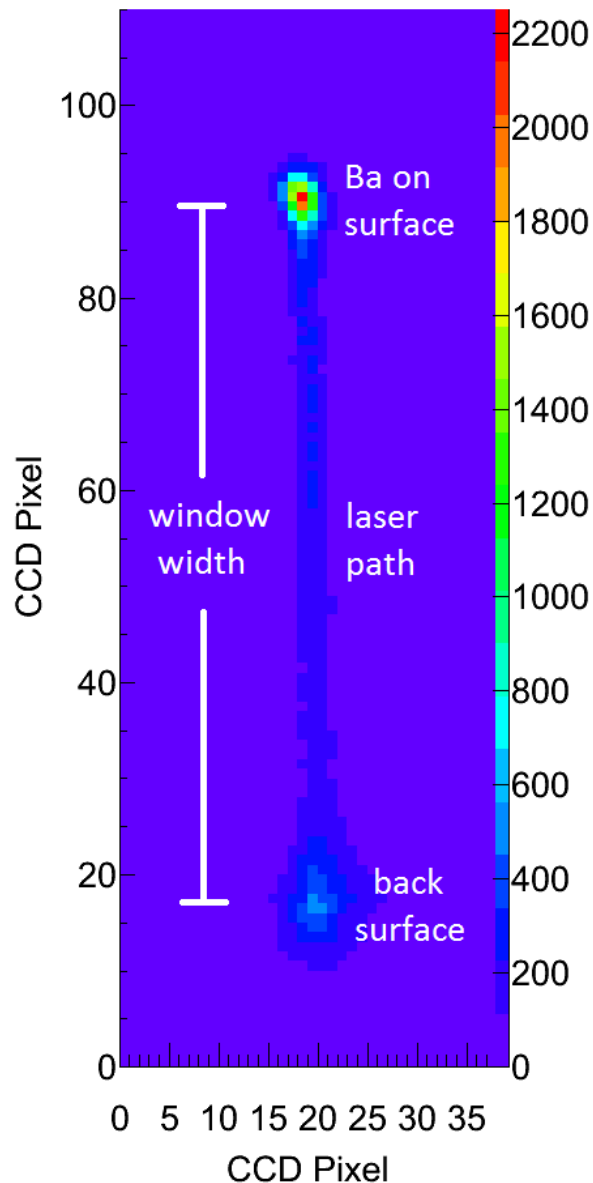
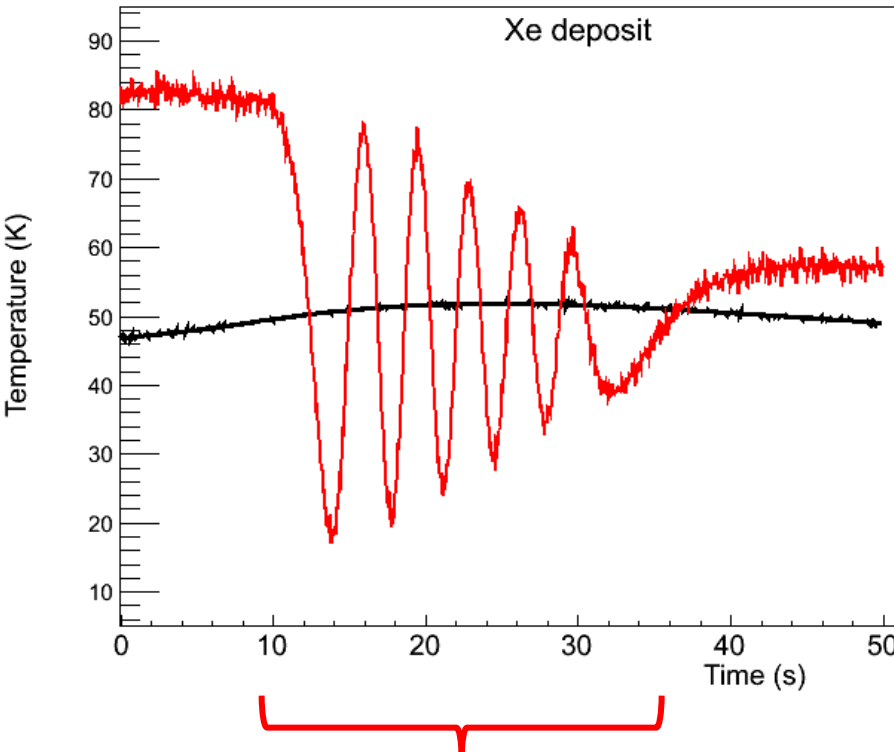


Image is from *above*

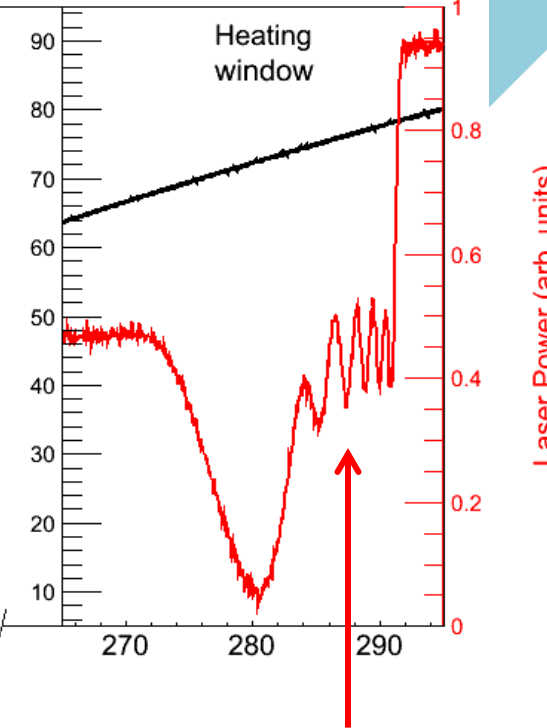


# Measuring Xe matrix growth rate using interference fringes:

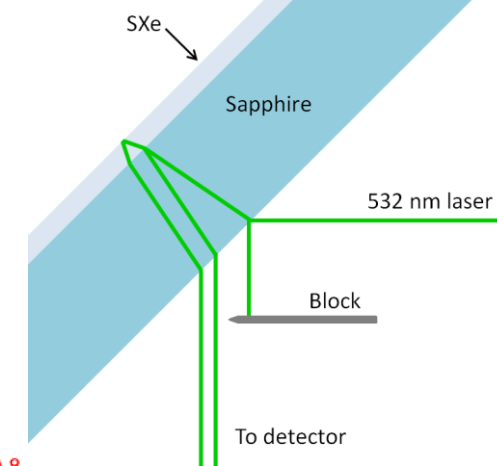


Xe deposit at 50 K

Deposition rate of  $\sim 30$  nm/s

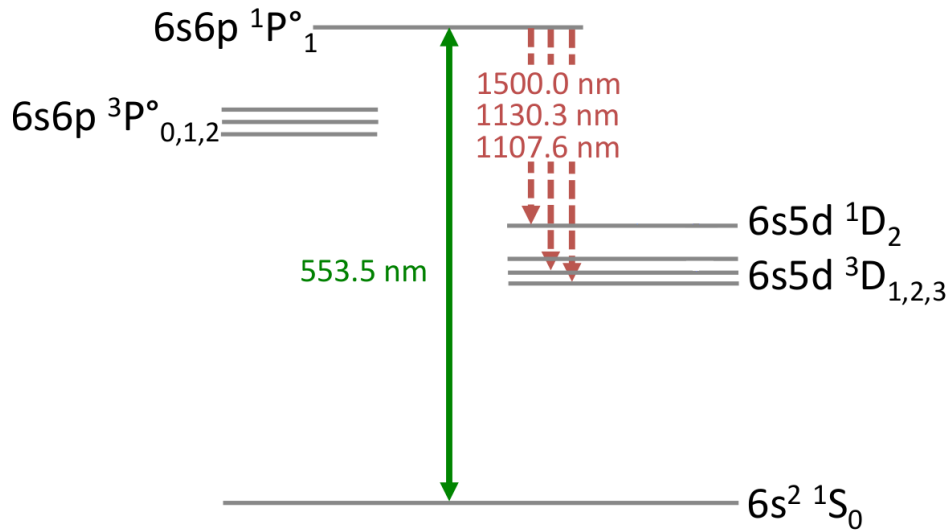


Observe same number of fringes  
when evaporating sample



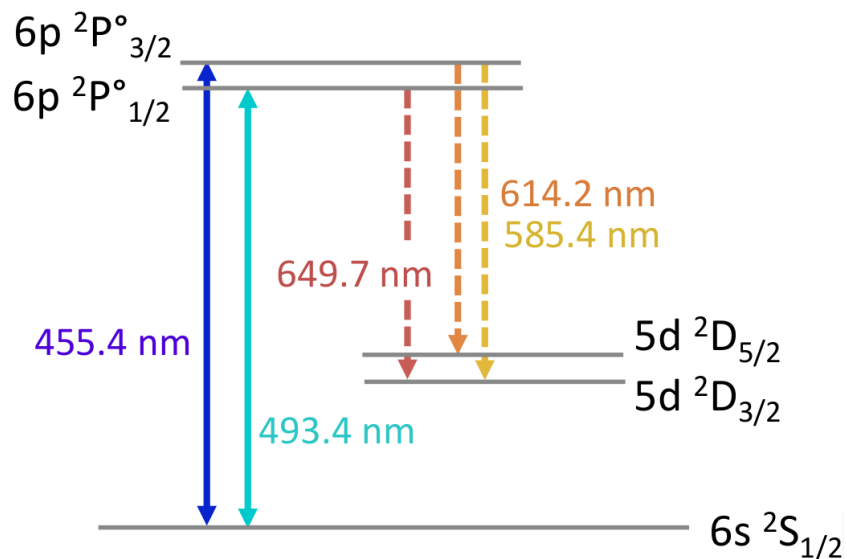
# Ba and Ba<sup>+</sup> Transitions in Vacuum

Ba

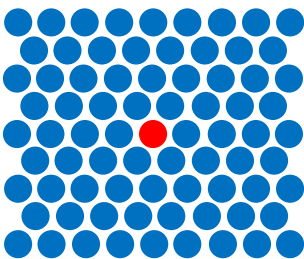


**~1 in 330** decays from  ${}^1P_1$  state  
are into metastable D states

Ba<sup>+</sup>

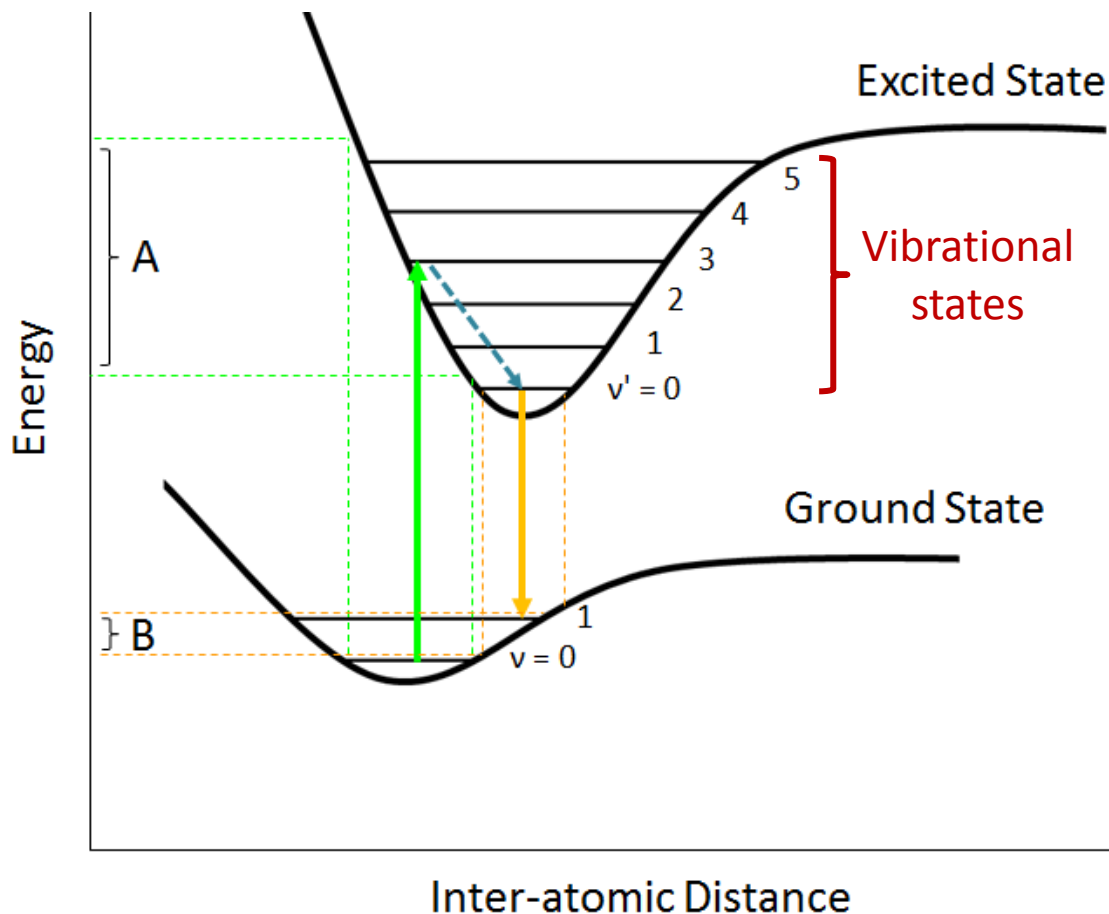


**~1 in 4** decays from  ${}^2P_{1/2}$  state  
are into metastable D state



Interactions with neighboring host atoms (xenon)

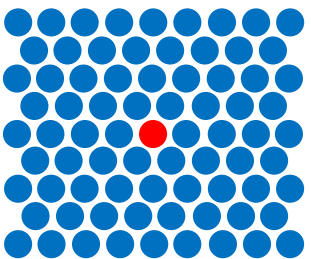
Ba/Xe interaction is different in ground vs. excited state:



**Franck-Condon principle:**  
Strongest excitation occurs to vibrational states whose wavefunctions overlap

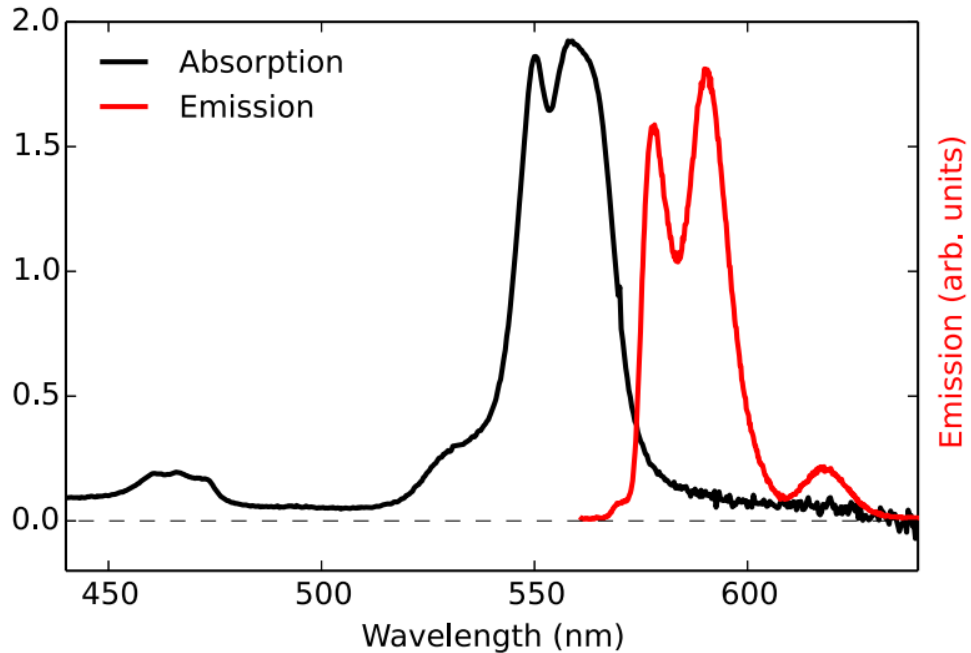


*Shifts and broadening in absorption (A) and emission (B)*



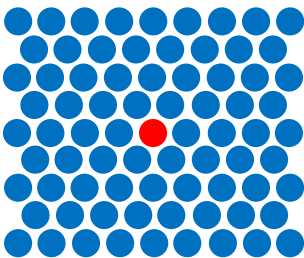
Interactions with  
neighboring host  
atoms (xenon)

Ba in solid xenon



- Excitation and emission are broadened
- Excitation is shifted from vacuum wavelength
- Emission is shifted from excitation

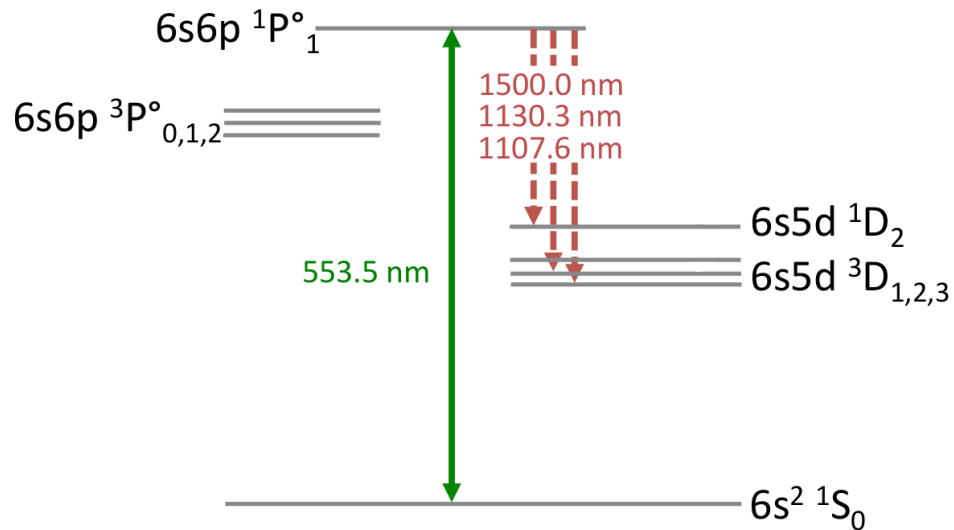
Phys. Rev. A **91**, 022505 (2015).



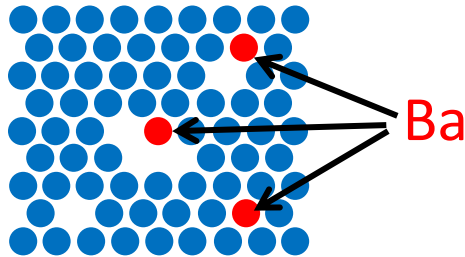
Interactions with  
neighboring host  
atoms (xenon)

Rate changes:

- Non-radiative, e.g. crossing of potential energy curves
- Radiative, e.g. parity change

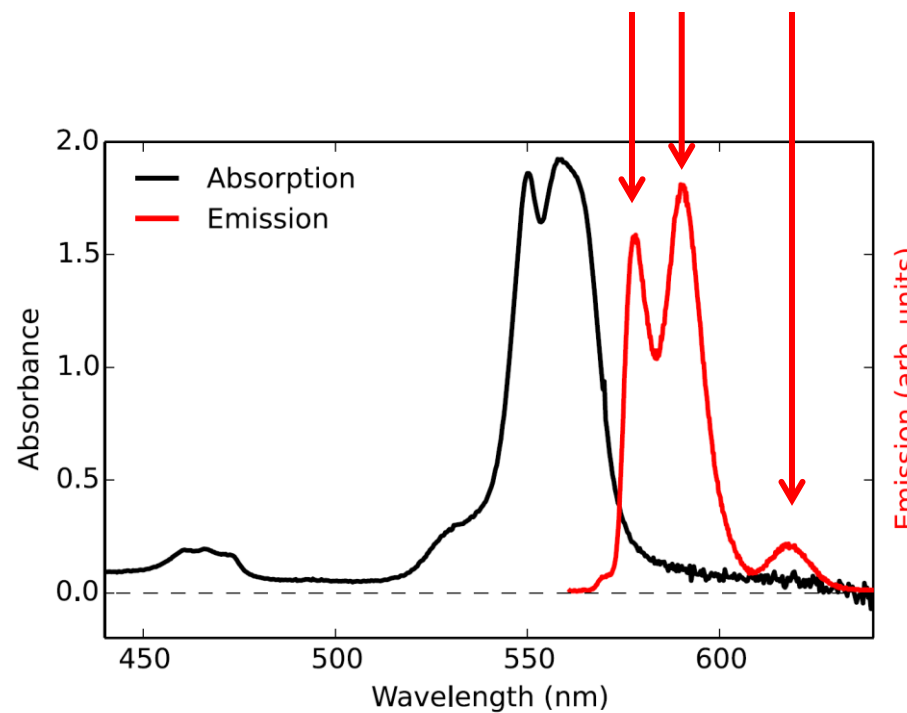


# Matrix Sites



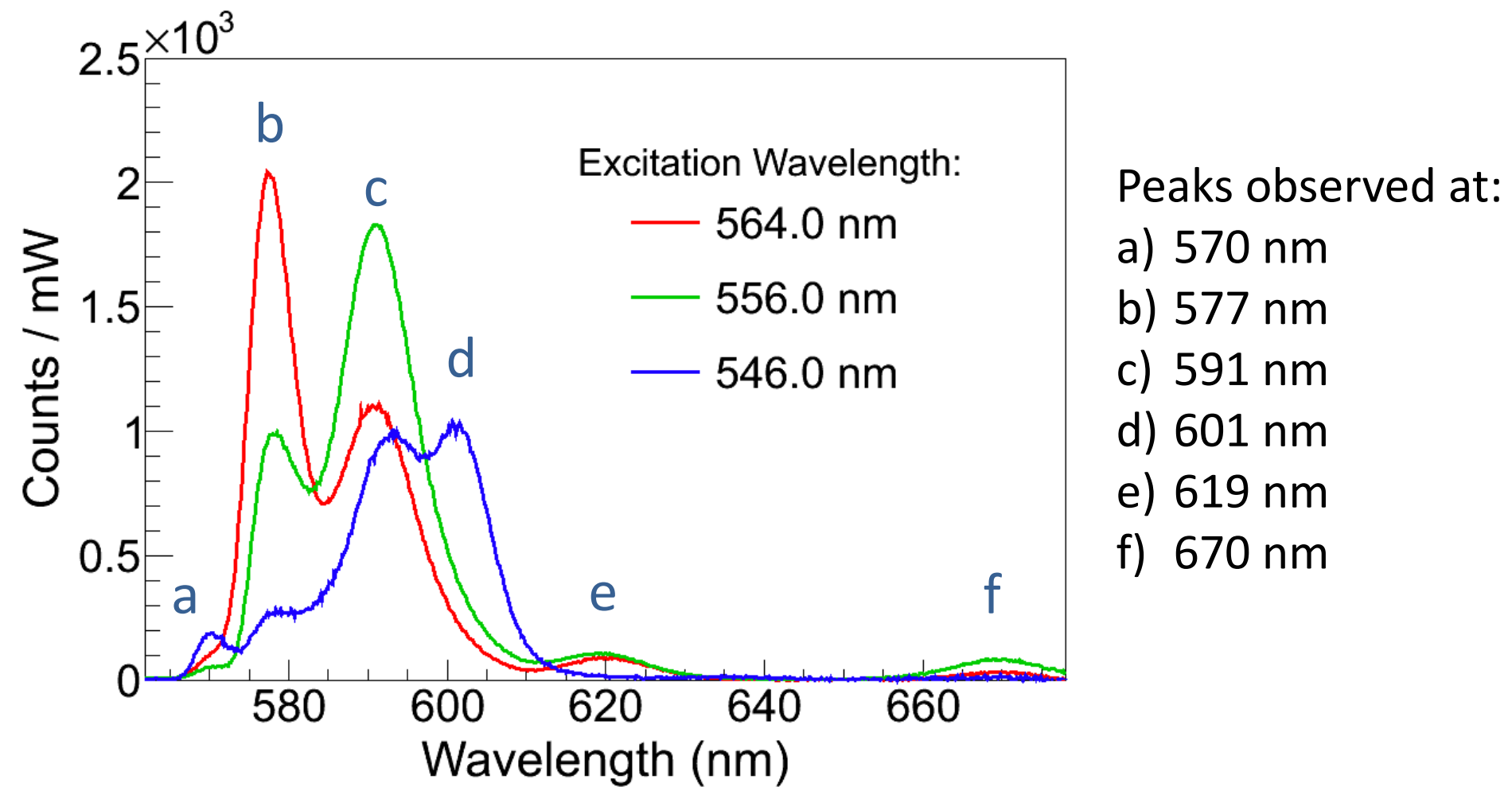
Matrix effects (shifts, broadening, and transition rates) can be matrix site dependent.

Emission from Ba occupying different sites

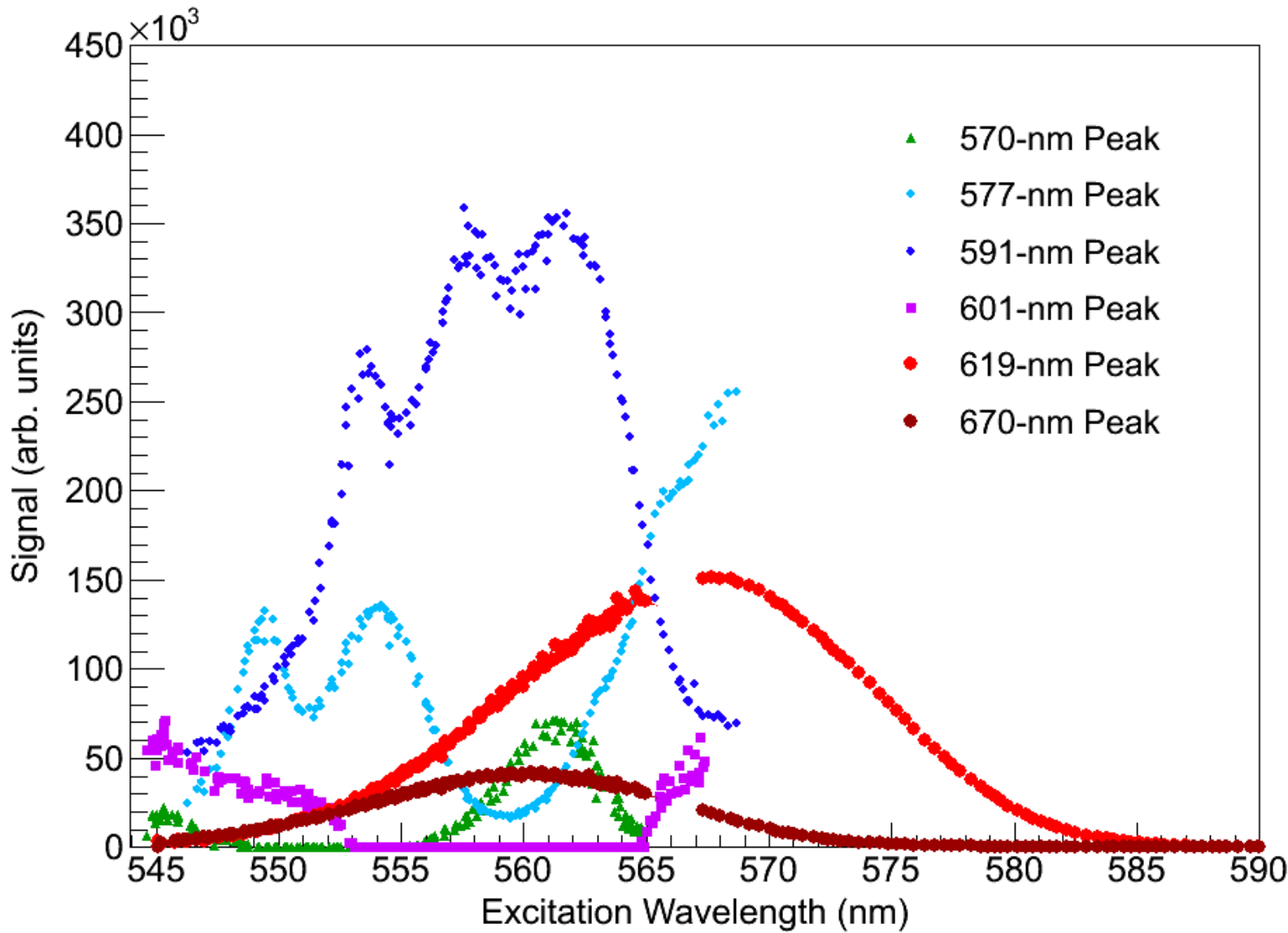


# Part 1: Spectroscopy

# Emission of Ba in Solid Xe

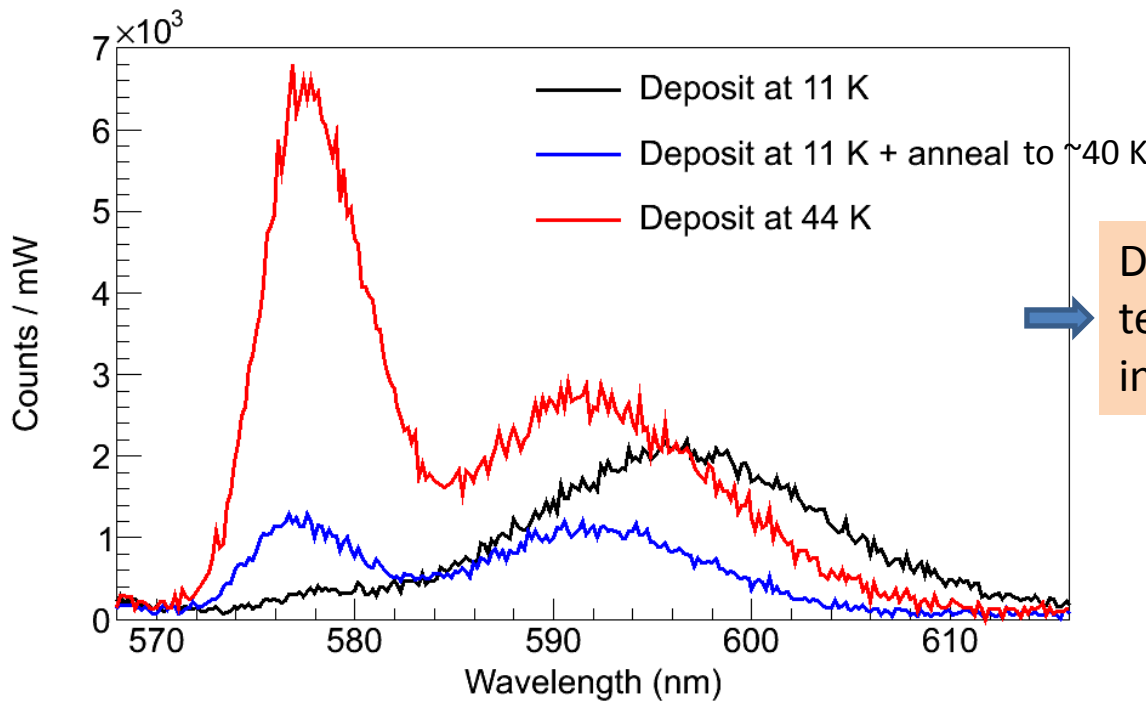


# Excitation Spectra of Ba Emission Peaks



# Thermal History Dependence

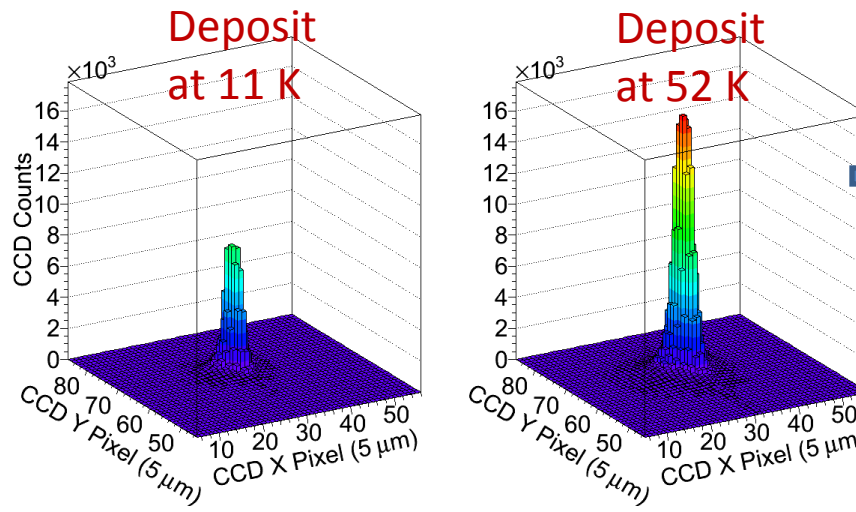
Matrix site populations can depend on thermal history:



Deposits at higher temperature ( $50 \pm 5$  K) result in larger 577-nm and 591-nm.

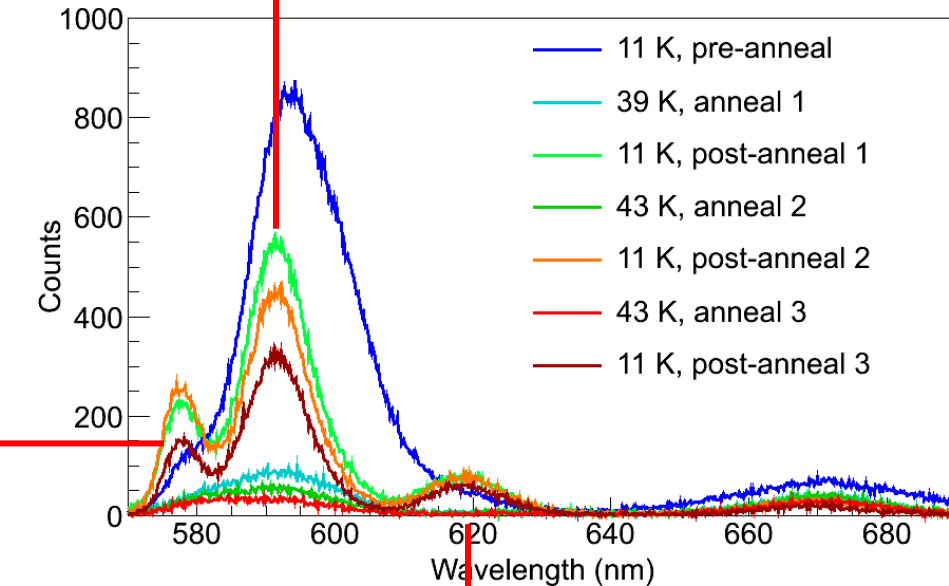
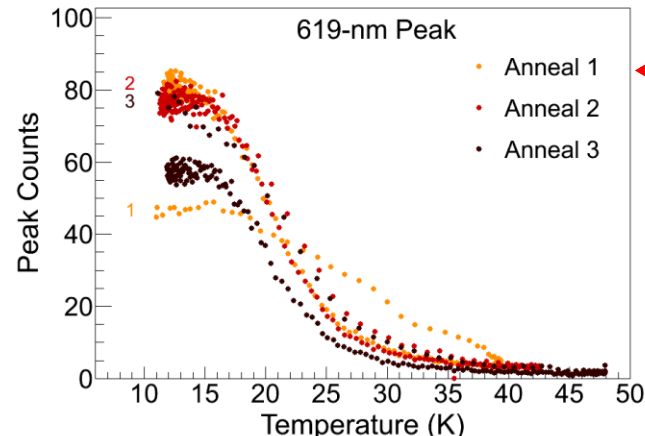
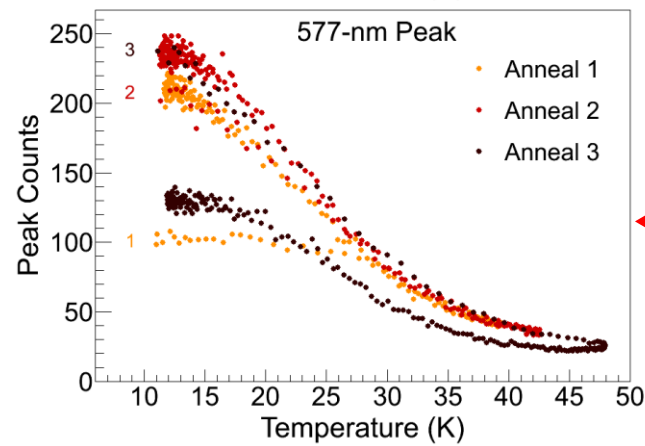
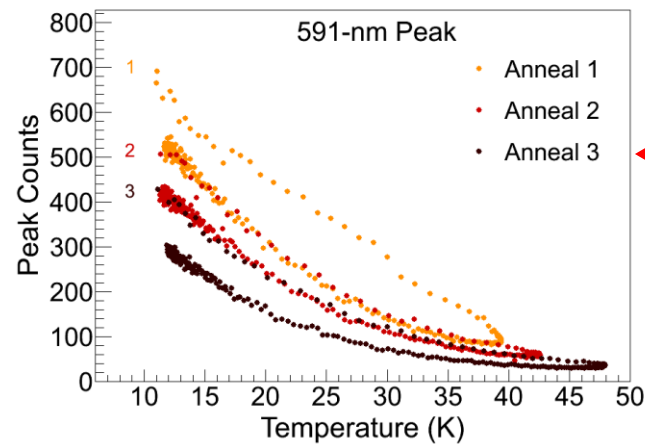
*All observation is at 11 K*

Images of 619-nm Ba fluorescence in focused laser (discussed later):



619-nm signal also higher w/  $50 \pm 5$  K deposit.

# Annealing

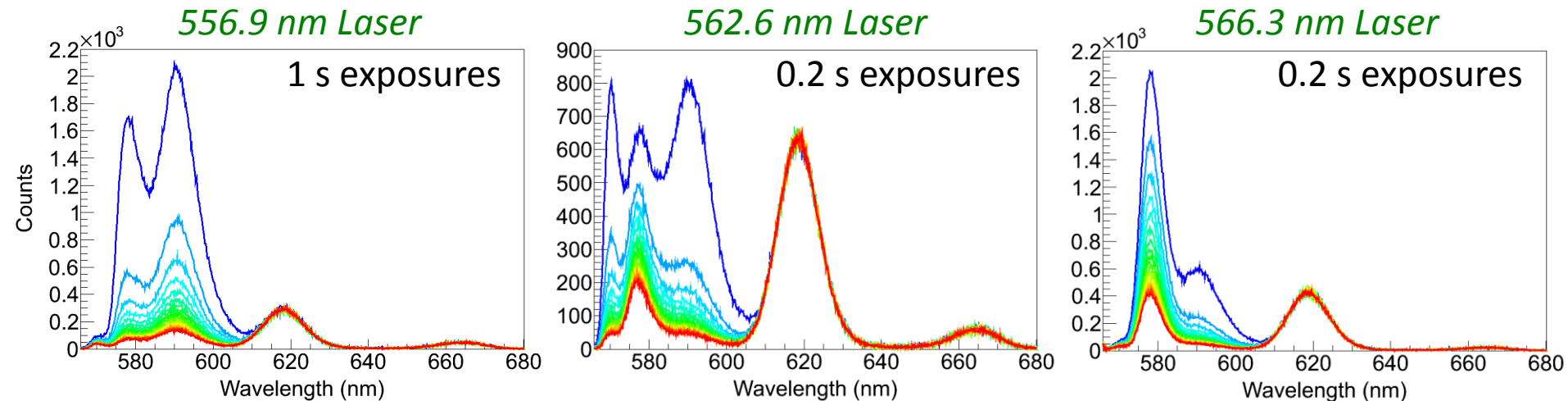


- Gain in 577-nm and 619-nm peaks after Cycle 1 (to 39 K), with modest loss in 591-nm.
- Loss in fluorescence after Cycle 3 (to 48 K).
- *Overall, fluorescence is highest at 11 K.*

# Bleaching

## Decay of Fluorescence w/ Laser Exposure

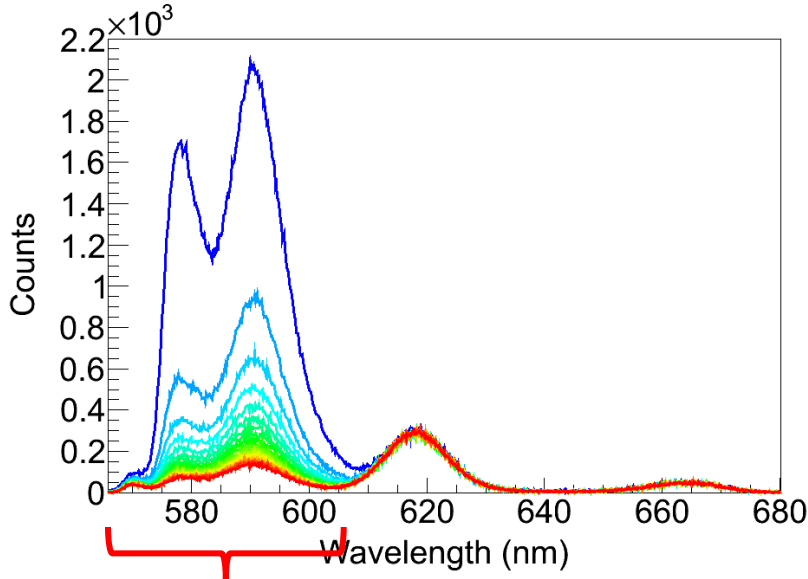
Spectra of Ba in SXe at different moments in time:  
*Every tenth exposure shown*



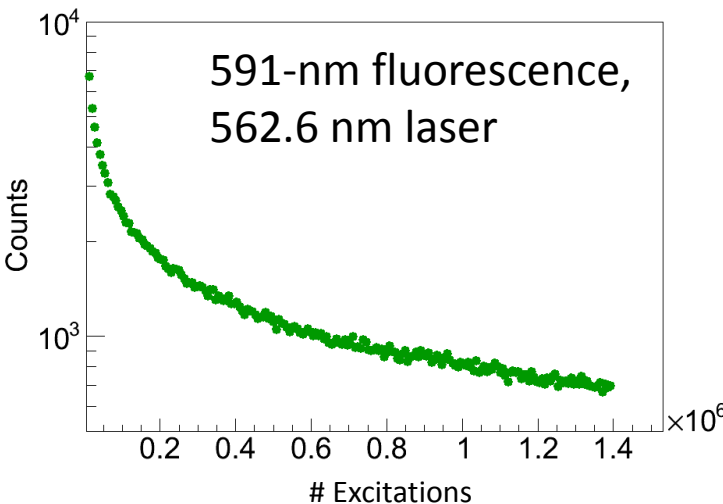
- Rapid bleaching in 570-nm, 577-nm, 591-nm peaks.
- 619-nm and 670-nm peaks **do not bleach** at this laser intensity

# Bleaching

## Decay of Fluorescence w/ Laser Exposure

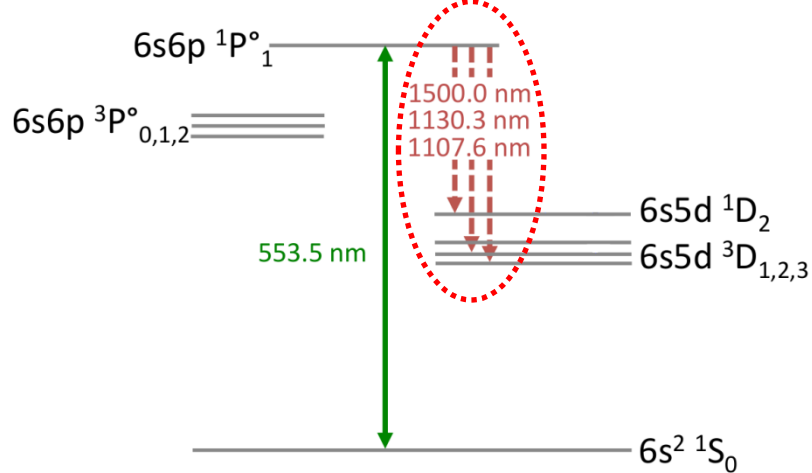


Bleaching is an obstacle for observing single atoms in these matrix sites:  
*need more photons/atom.*



What causes bleaching?

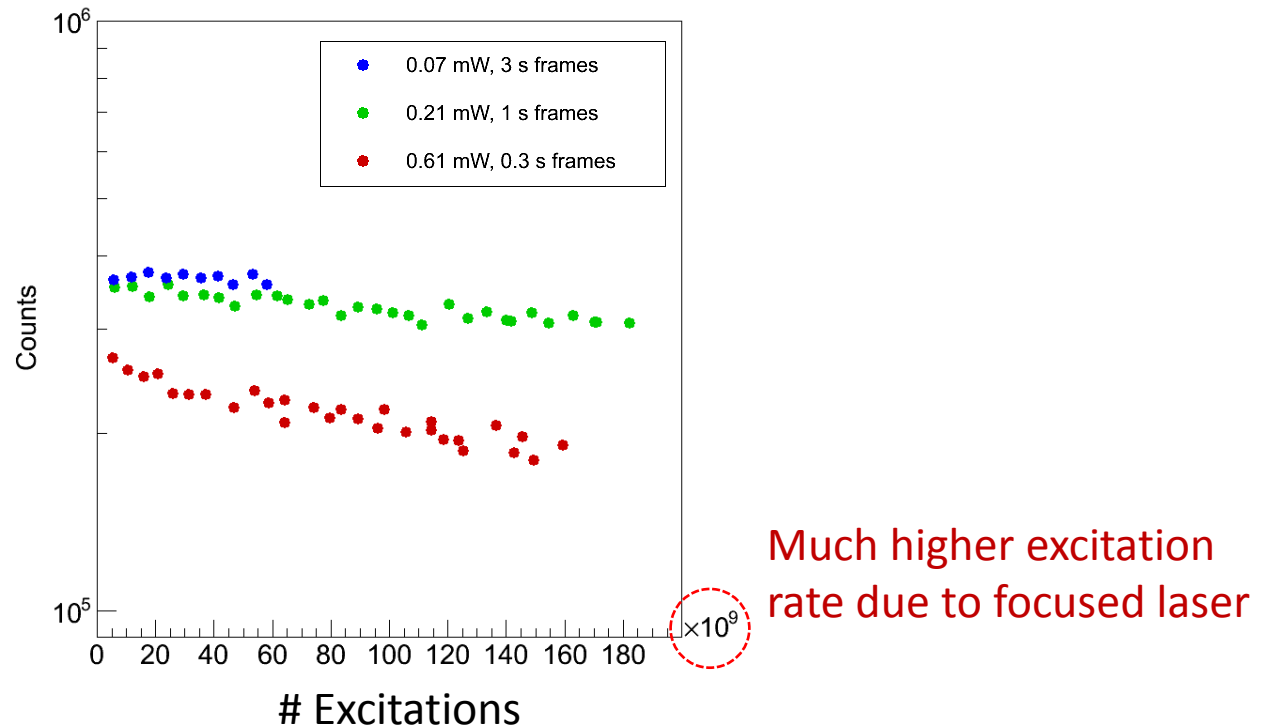
*Likely:* optical pumping into metastable states, as in Ba in vacuum:



Re-pumping with IR lasers may be required for continued fluorescence cycle w/ these peaks.

# Bleaching of 619-nm Peak

619-nm fluorescence counts from a focused laser:



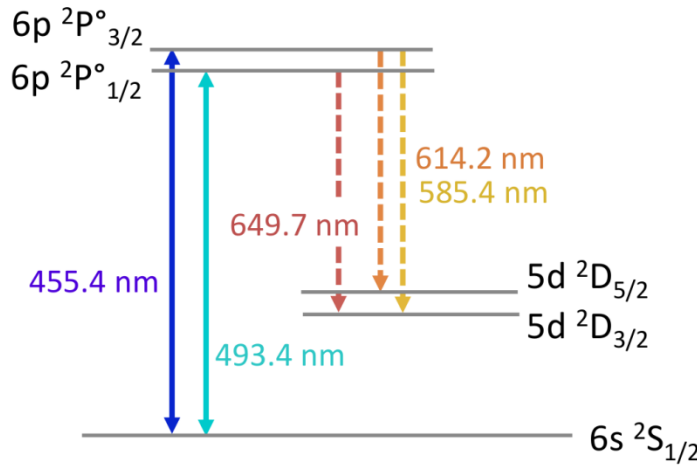
Though some bleaching is observed with the higher 0.61 mW laser power,  
the long-lasting 619-nm fluorescence is intriguing for single-atom detection  
w/o the need for re-pump lasers...

# Blue Excitation: Candidate Ba<sup>+</sup> Lines

Unknown: will some daughters remain ionized?

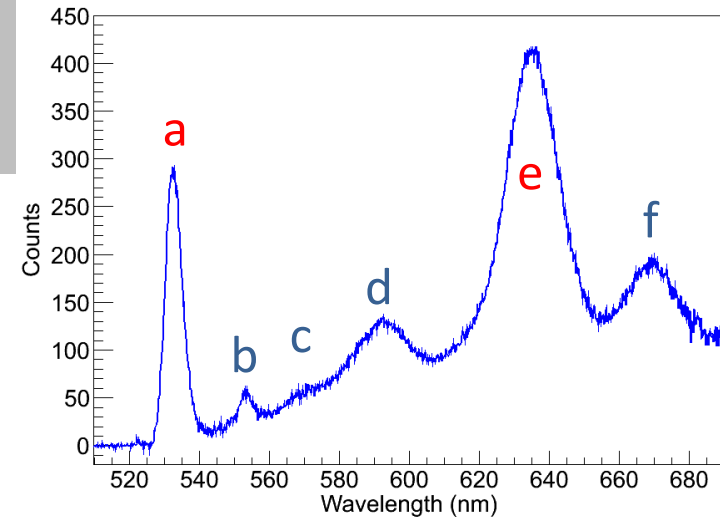
- a) 76% of beta decay daughters of  $^{214}\text{Pb}$  remain ionized in EXO-200 (*Phys. Rev. C* **92** (2015))
- b) Remain ionized in SXe on probe?

Ba<sup>+</sup> in vacuum:

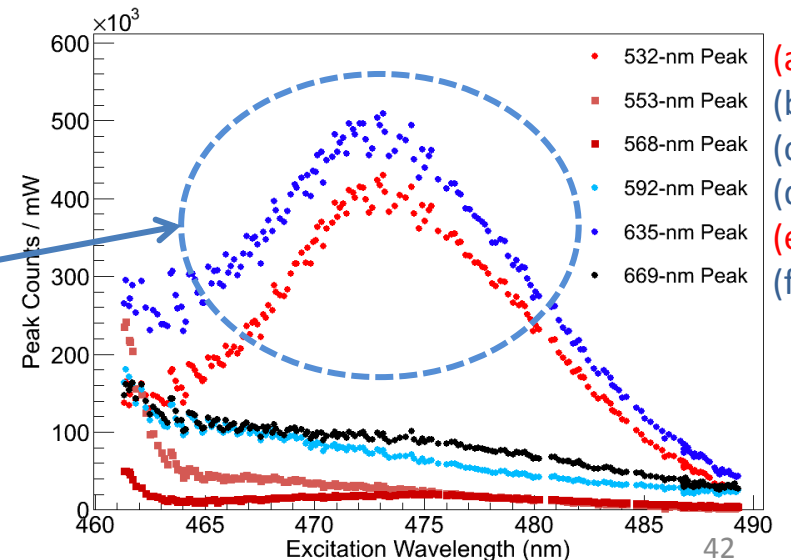


Similarity between excitation spectra for 532 nm line and 635 nm line suggests they are related, and could be fluorescence of P $\rightarrow$ S and P $\rightarrow$ D, respectively, for Ba<sup>+</sup>.

Emission of Ba<sup>+</sup> deposit w/ 468.25-nm excitation:



Excitation spectra for emission peaks:



# Part 2: Imaging

# Imaging Ba in SXe on Cold Sapphire Window

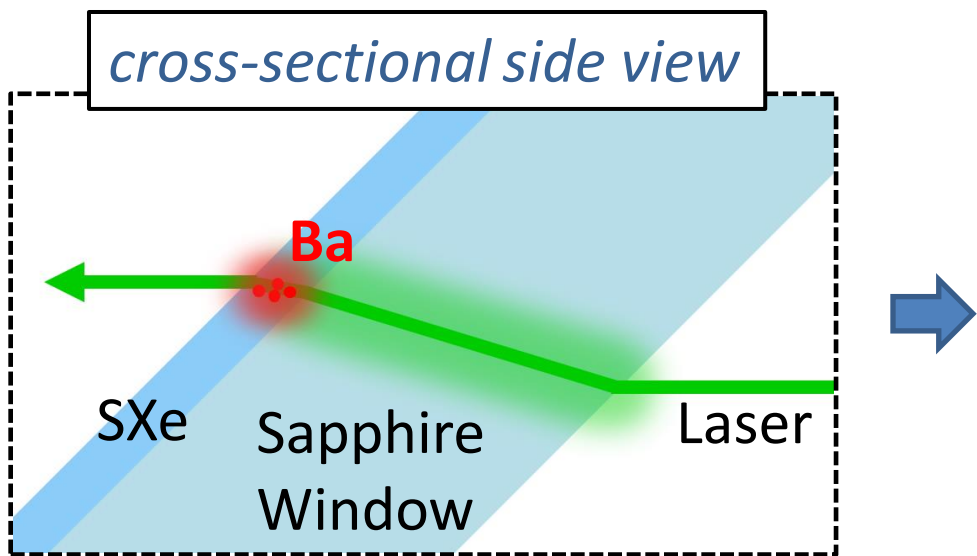
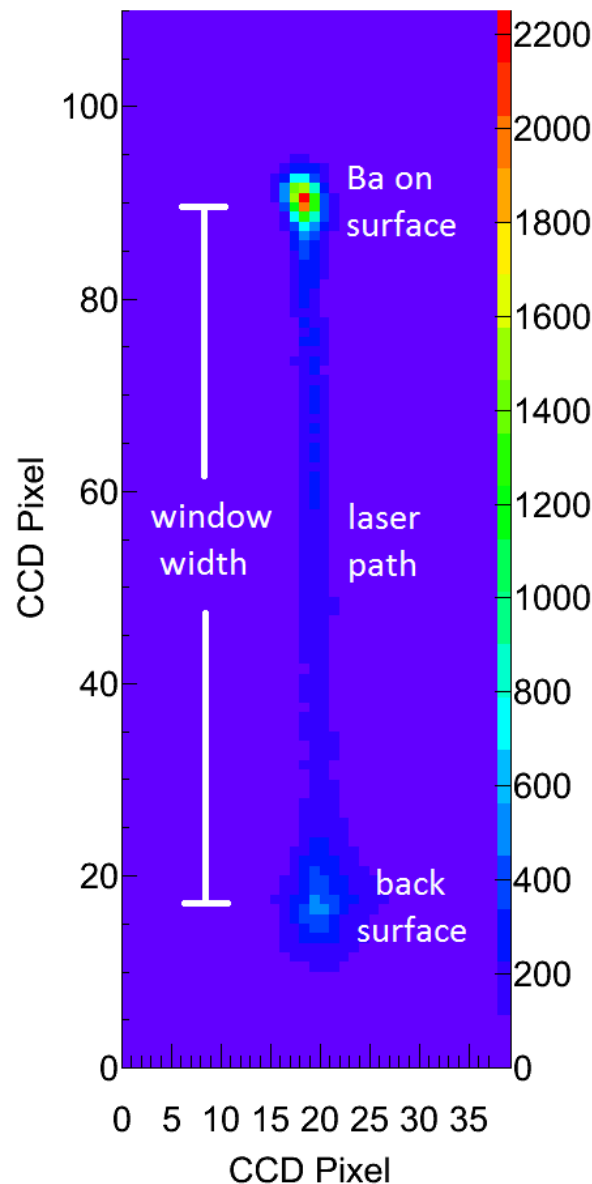
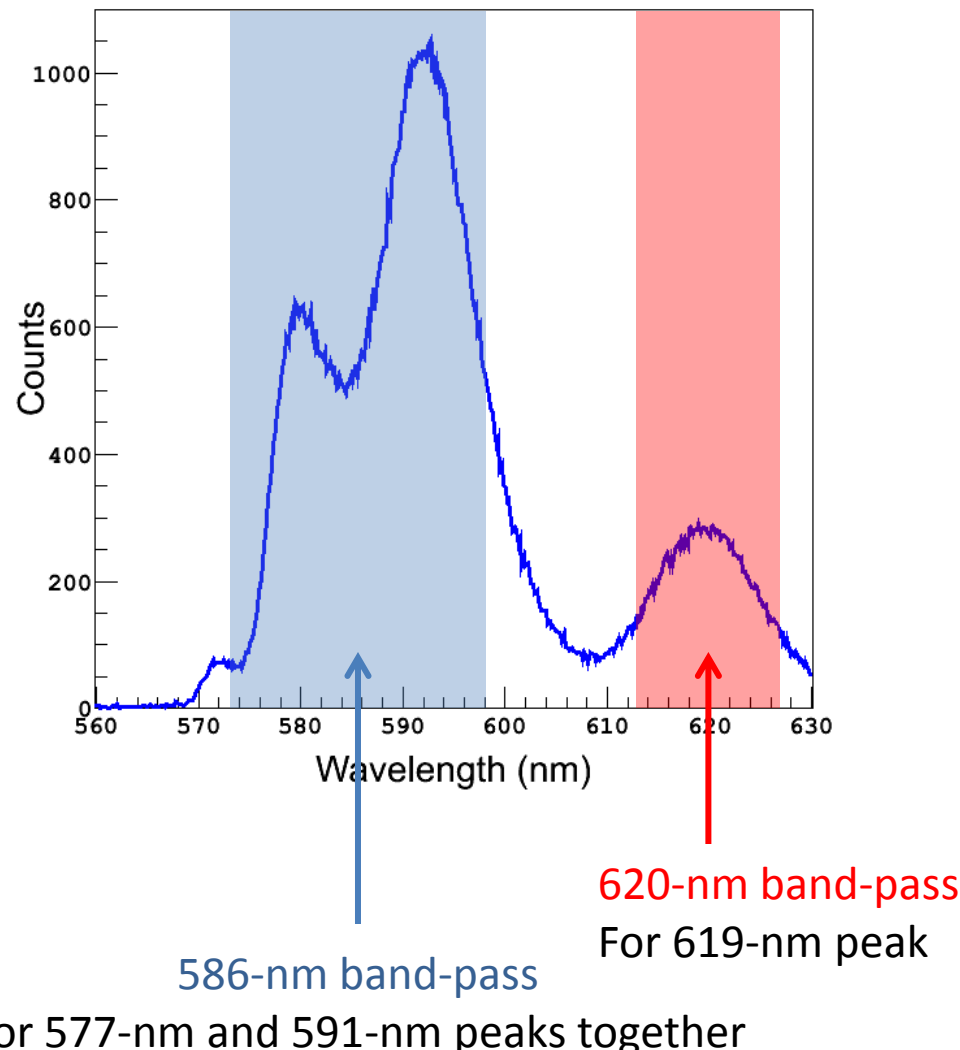


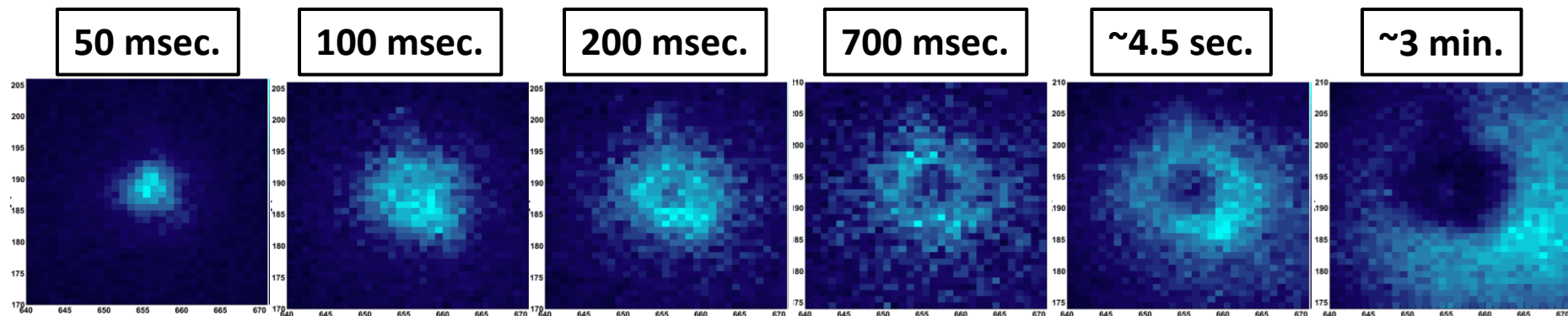
Image is from *above*



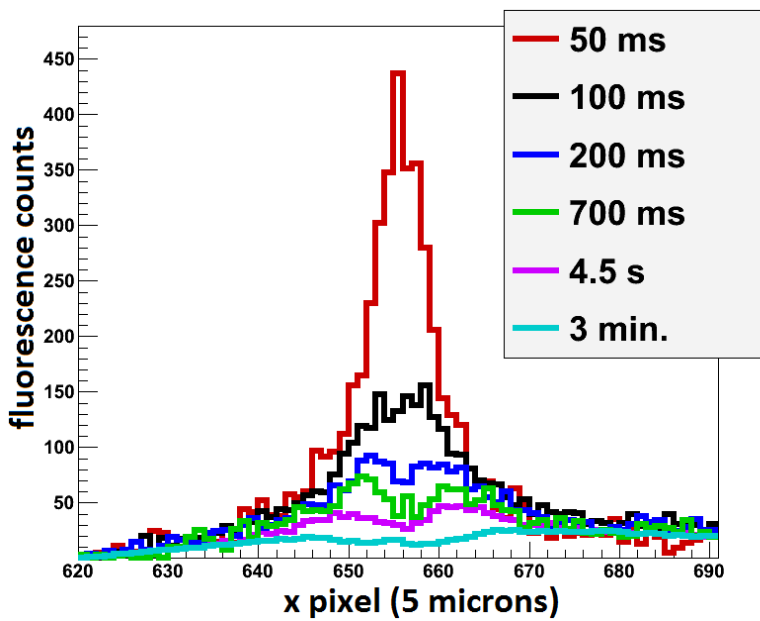
# Band-pass Filters for Imaging



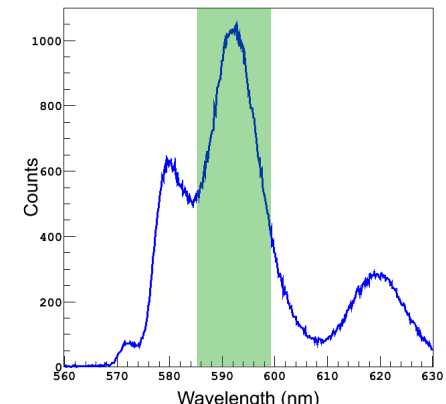
# Imaging 591-nm Fluorescence w/ Focused Laser, ~1 mW



Cross-section  
at focus position:

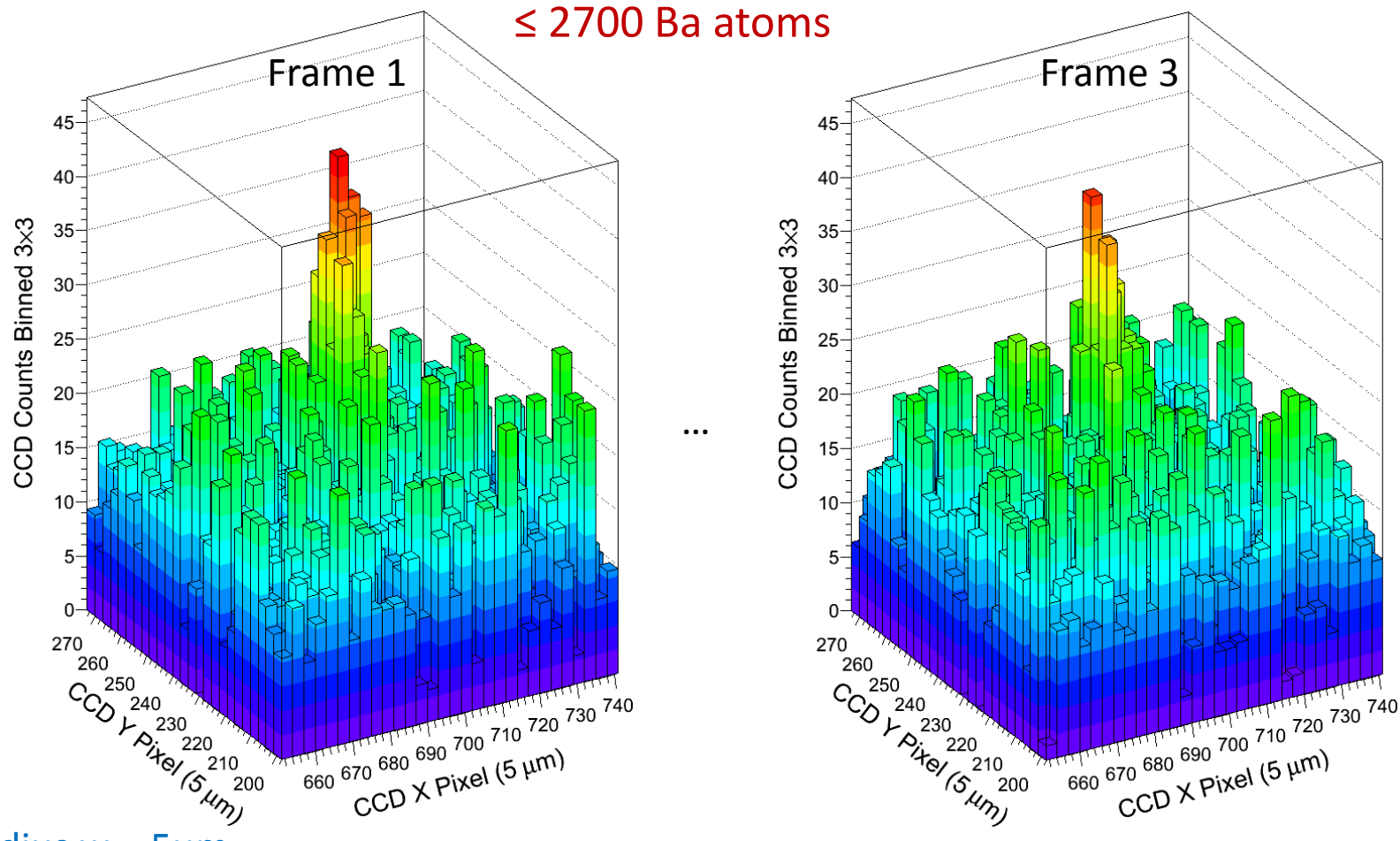


*These use a 590-nm band-pass filter:*



- Hole-bleaching occurs rapidly at high laser intensity.
- Need to use low laser power to image only atoms within focused laser region.

# Imaging 577-nm and 591-nm Fluorescence w/ Focused Laser (radius $w = 5\mu\text{m}$ ), 0.03 $\mu\text{W}$



- Only slight bleaching at this intensity in 100-s exposures
- Backgrounds are negligible at this intensity

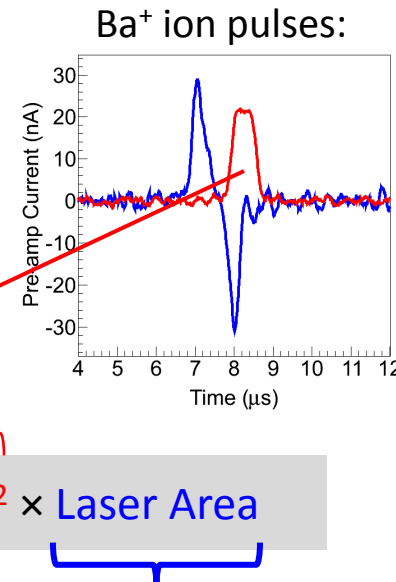
# Calculating # Ba atoms in focused laser region

Due to unknown neutralization fraction

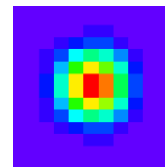
From calibrated Faraday signal

Per pulse of ion beam:

$$\# \text{atoms} \leq \# \text{ions} = [\text{charge}/(1.6 \times 10^{-19} \text{ C})]/\text{m}^2 \times \text{Laser Area}$$

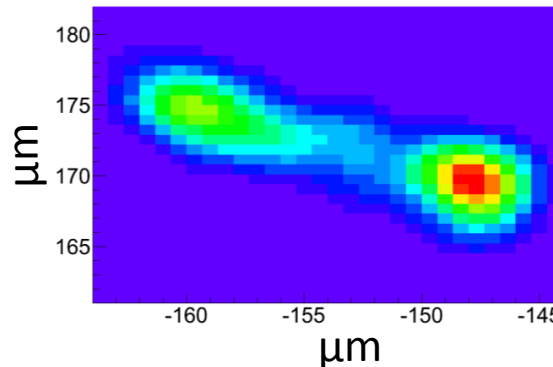


Simulated laser spot of radii  
 $w_x \times w_y = 2.06 \mu\text{m} \times 2.66 \mu\text{m}$ :



vibrations

Laser spot size  
overlain on cryostat  
vibration data:



Two definitions for number of atoms:

1) Those *instantaneously* illuminated by laser spot  
→  $8.6 \mu\text{m}^2$

2) *Total illuminated* over vibrations  
→  $40 \mu\text{m}^2$

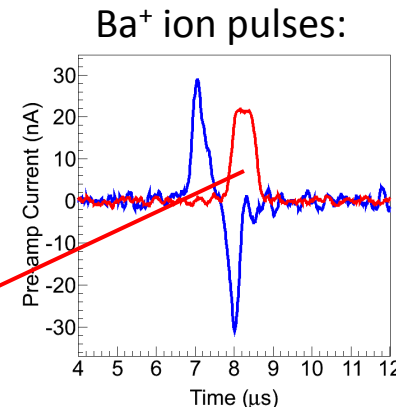
# Calculating # Ba atoms in focused laser region

Due to unknown neutralization fraction

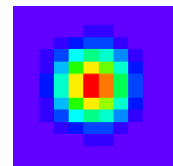
From calibrated Faraday signal

Per pulse of ion beam:

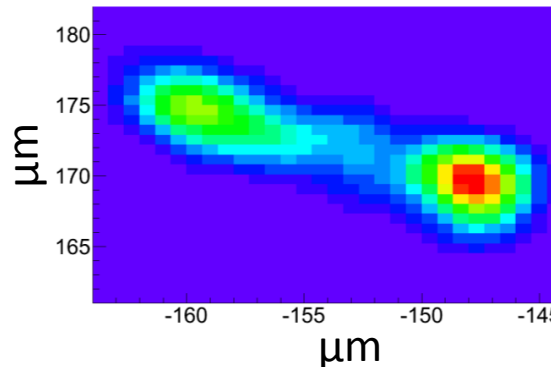
$$\# \text{atoms} \leq \# \text{ions} = [\text{charge}/(1.6 \times 10^{-19} \text{ C})]/\text{m}^2 \times \text{Laser Area}$$



Simulated laser spot of radii  
 $w_x \times w_y = 2.06 \mu\text{m} \times 2.66 \mu\text{m}$ :



Laser spot size overlaid on cryostat vibration data:



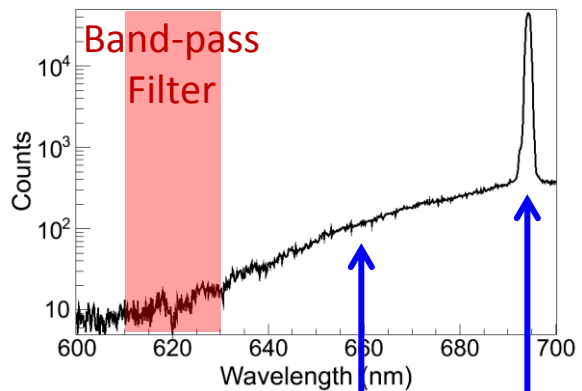
- Two definitions for number of atoms:
- 1) Those *instantaneously illuminated* by laser spot  
→  $8.6 \mu\text{m}^2$
  - 2) *Total illuminated* over vibrations  
→  $40 \mu\text{m}^2$

# Imaging 619-nm Fluorescence

Backgrounds become important at high laser intensity

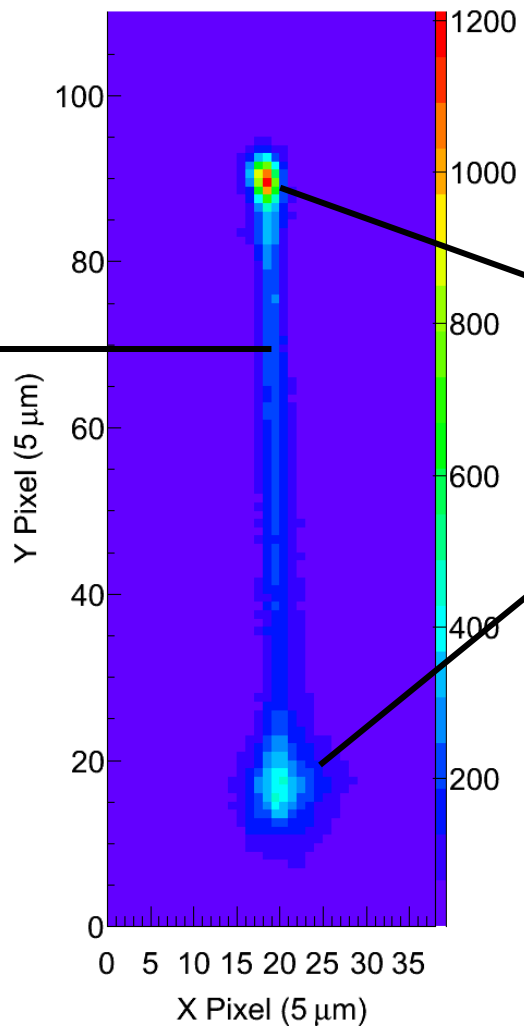
*Image w/ 620-nm  
band-pass filter:*

Sapphire Emission Spectrum:

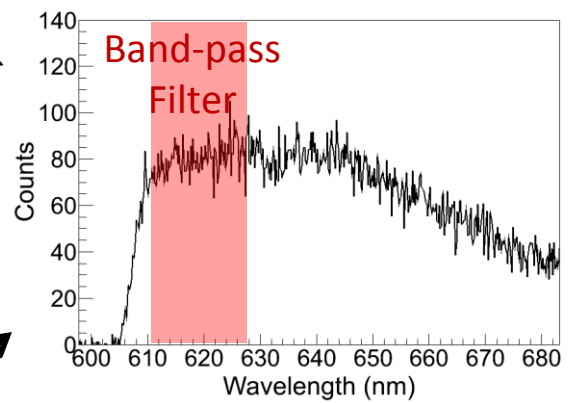


*Broad and sharp emission  
from Cr<sup>3+</sup> impurities in  
sapphire window*

- Minimized by high-purity windows
- Only low tail is passed by filter



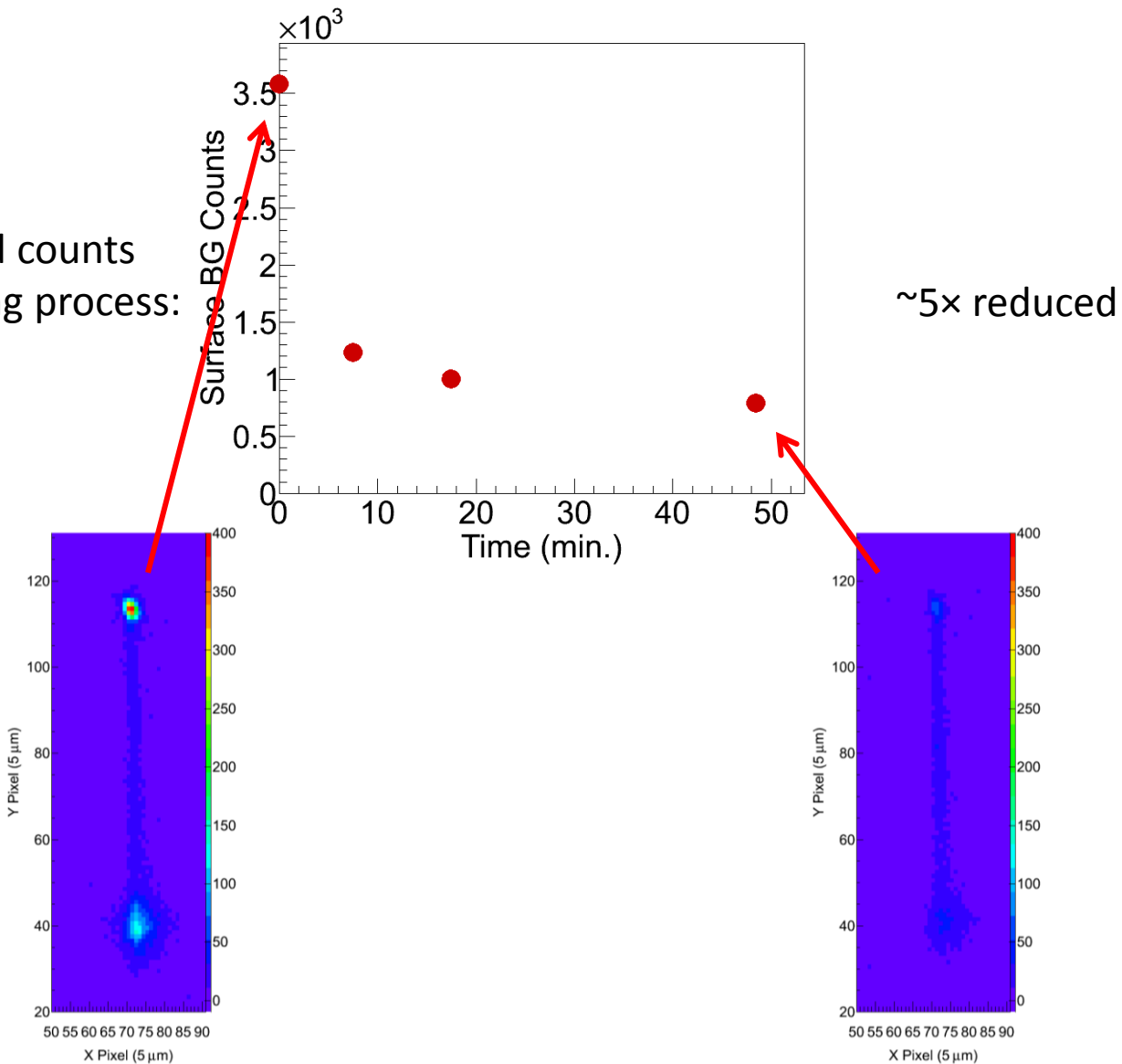
Surface Background Spectrum:



- Dominant background
- Bleaches with laser exposure – can be reduced

# Bleaching of the Surface Background

Surface background counts  
during pre-bleaching process:

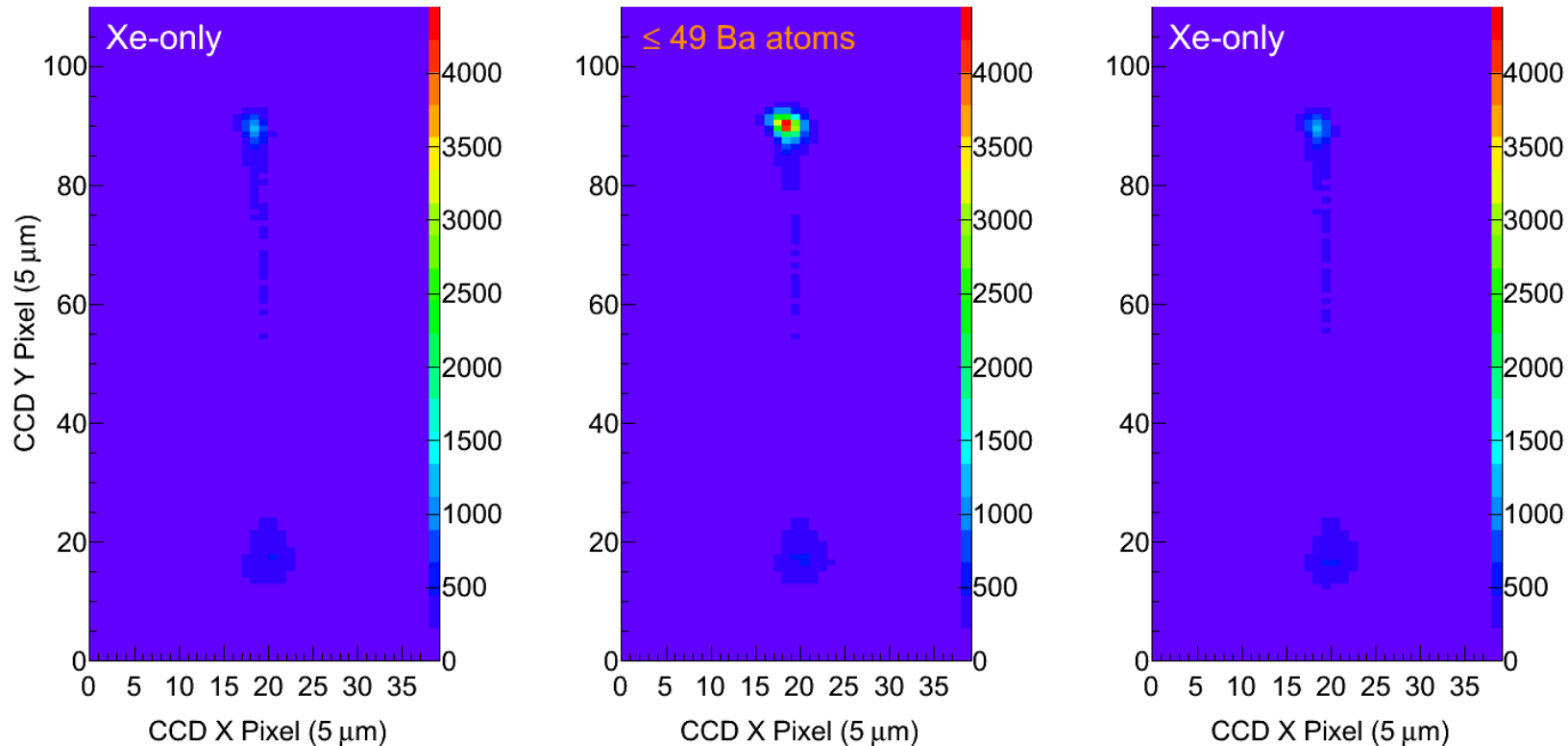


## Optimal conditions are determined:

- 1) Observe 619-nm peak w/ 570 nm laser
- 2) Deposit at ~50 K, observe at 11 K
- 3) Pre-bleach to lower surface background

# Imaging 619-nm Fluorescence

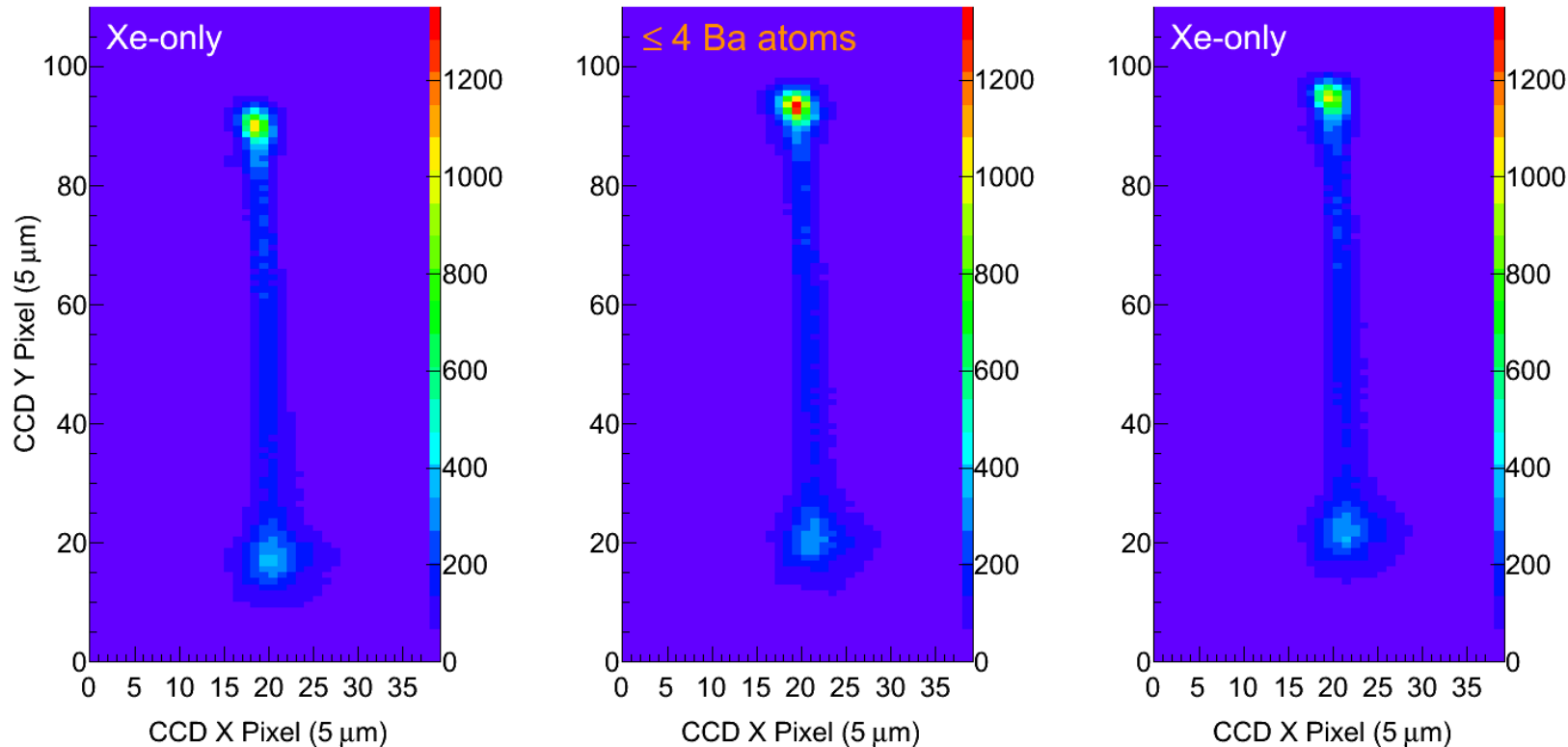
Xe-only deposits are observed in between  $\text{Ba}^+$  deposits  
to monitor surface background:



*Ba signal is clear over background*

# Imaging 619-nm Fluorescence

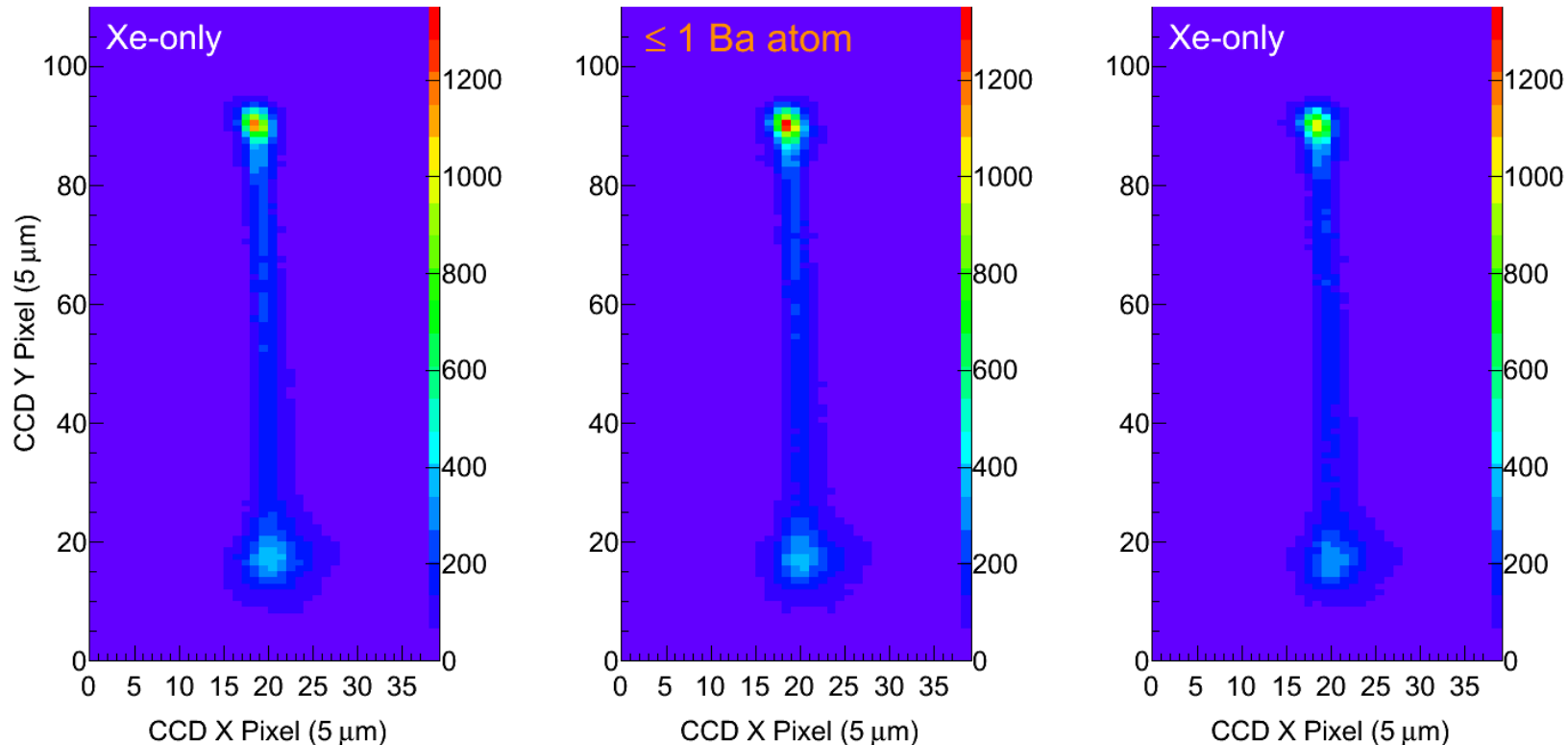
Xe-only deposits are observed in between  $\text{Ba}^+$  deposits  
to monitor surface background:



*Ba signal is clear over background*

# Imaging 619-nm Fluorescence

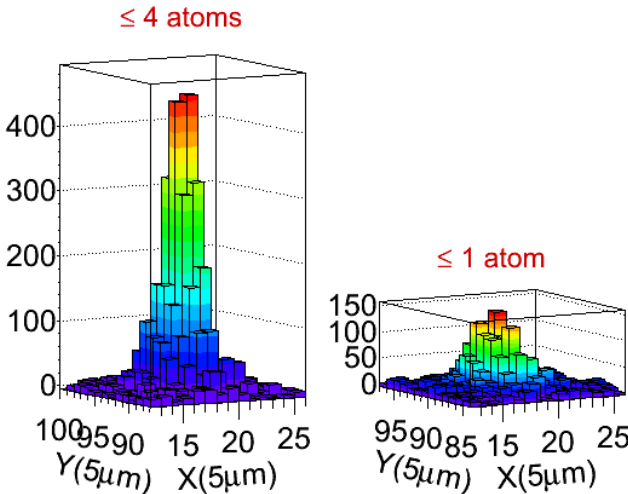
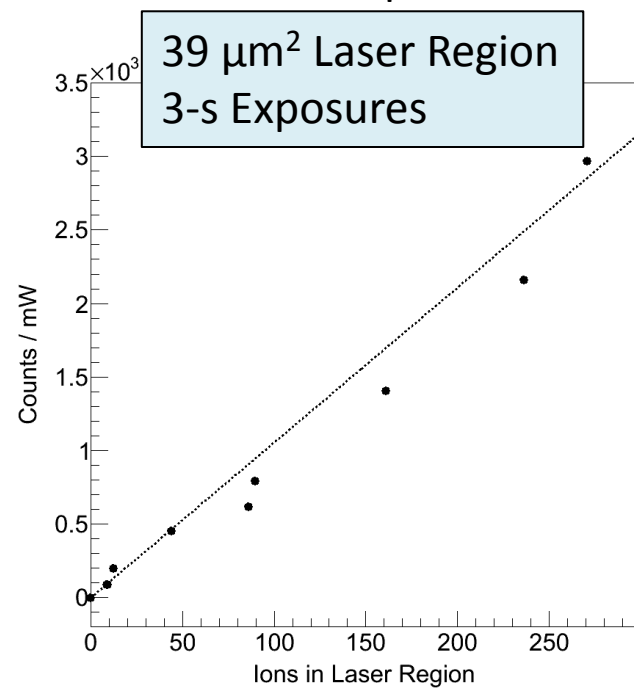
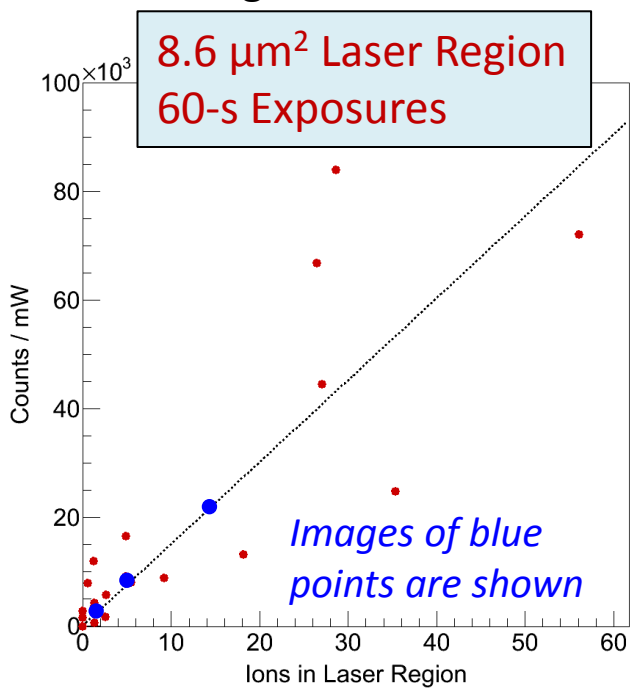
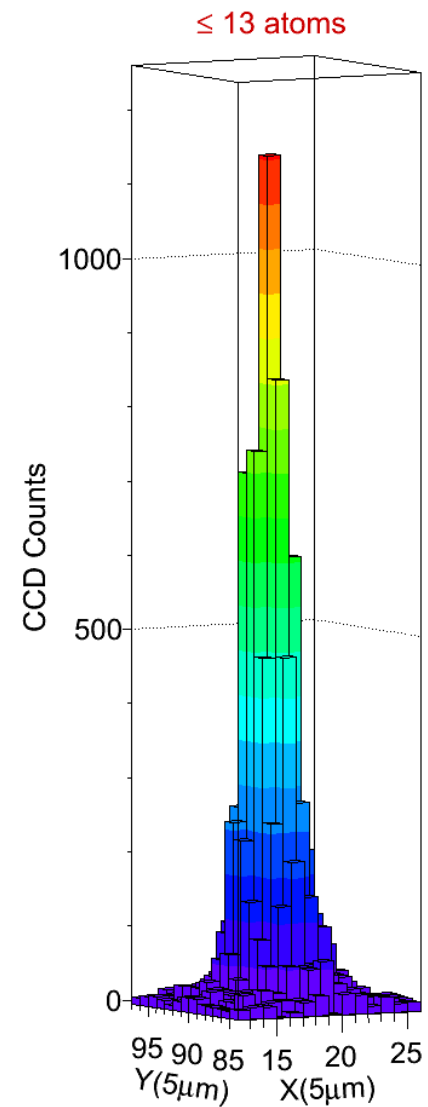
Xe-only deposits are observed in between  $\text{Ba}^+$  deposits  
to monitor surface background:



*Single-atom signal is distinguishable by eye!*

# Imaging 619-nm Fluorescence

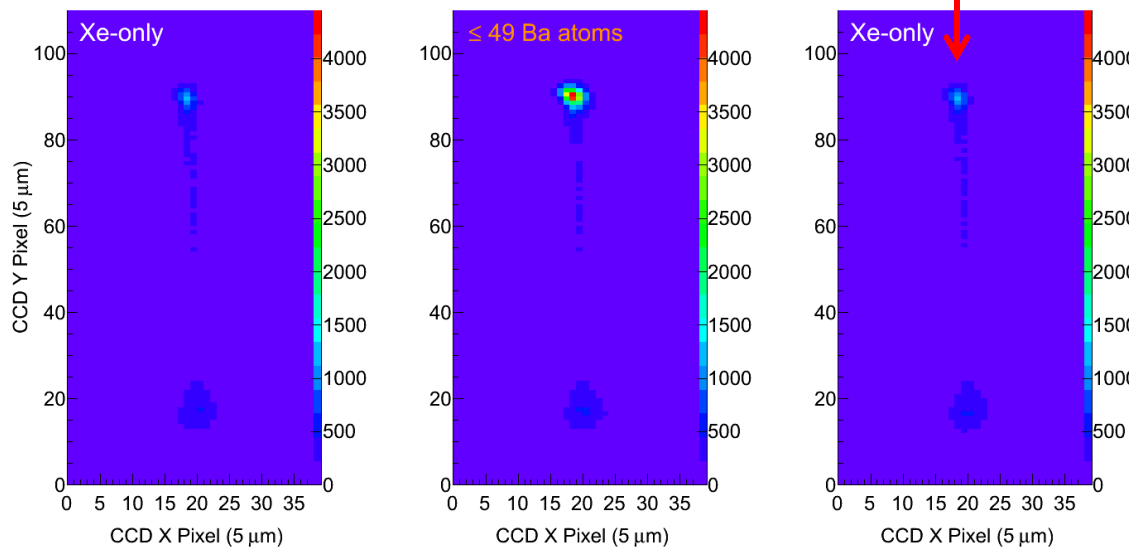
619-nm signal vs. ions in laser for two different experiments:



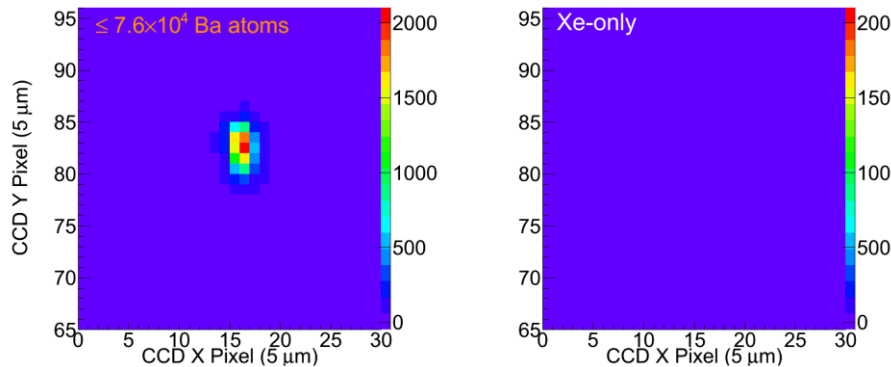
- $1500 \pm 160$  counts/mW from single atoms w/  $8.6 \mu\text{m}^2$  laser region, 60-s exposures
- Linear relationship rules out  $\text{Ba}_2$  molecule

# Imaging 619-nm Fluorescence

*No Ba signal after sample evaporation and re-deposit of Xe-only*



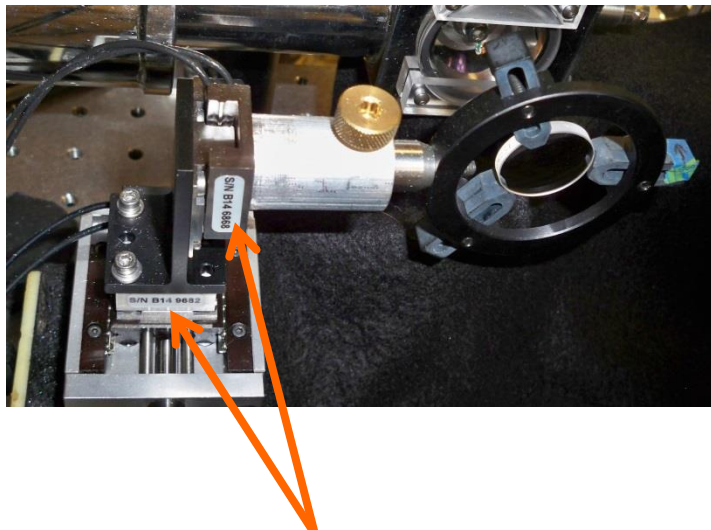
*Even in large Ba deposits:*



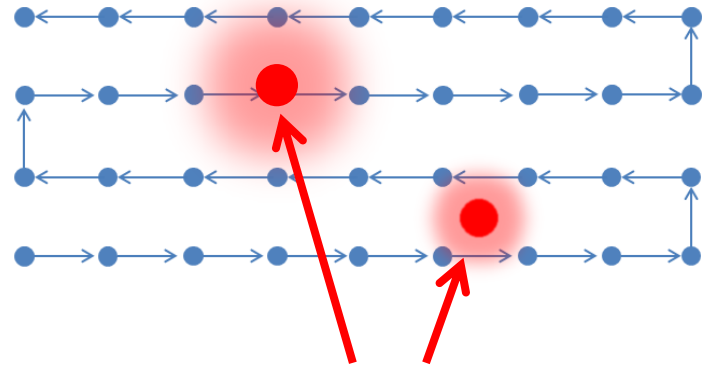
**Very important result for a Ba tagging cold probe in nEXO**

# Next Step: Scanned Images of Ba Atoms

Scan laser by scanning focusing lens:



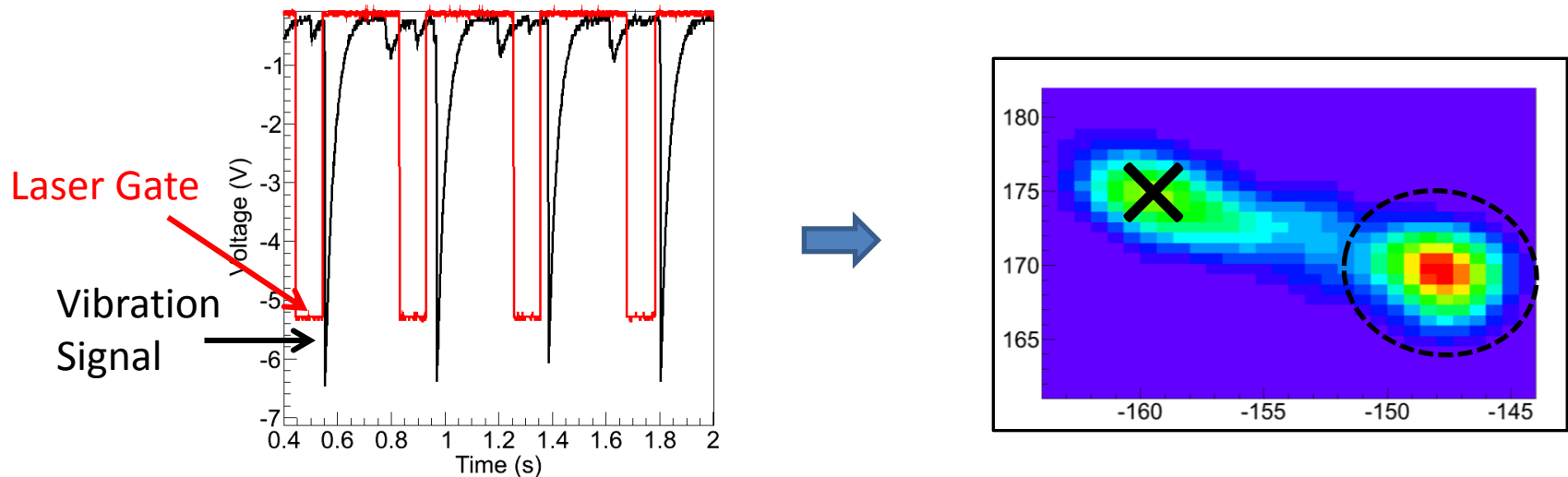
Each camera exposure is for a position in a grid:



See peaks as laser moves over single atoms

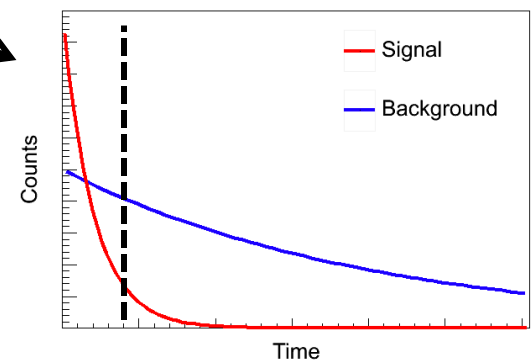
# Next Step: Scanned Images of Ba Atoms

- 1) Working on synchronizing laser gating w/ cryostat vibrations:



- 2) Possible methods to reduce surface background:

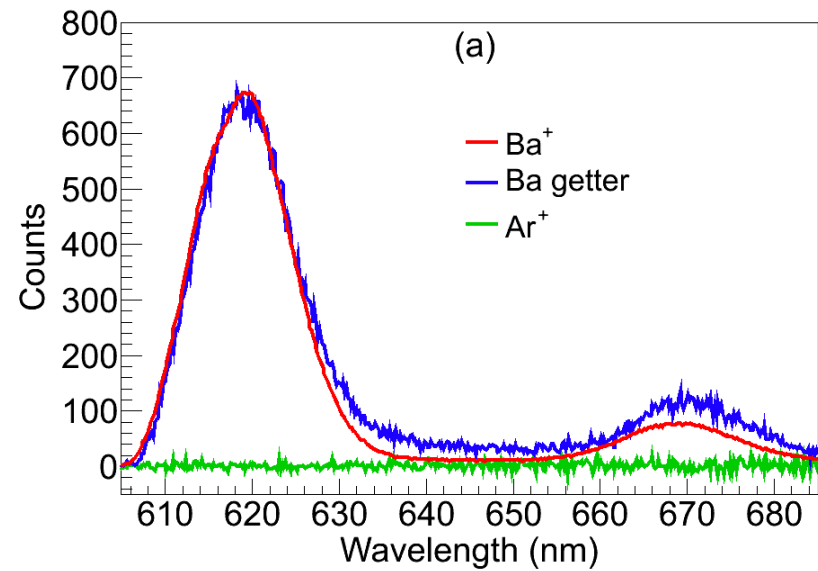
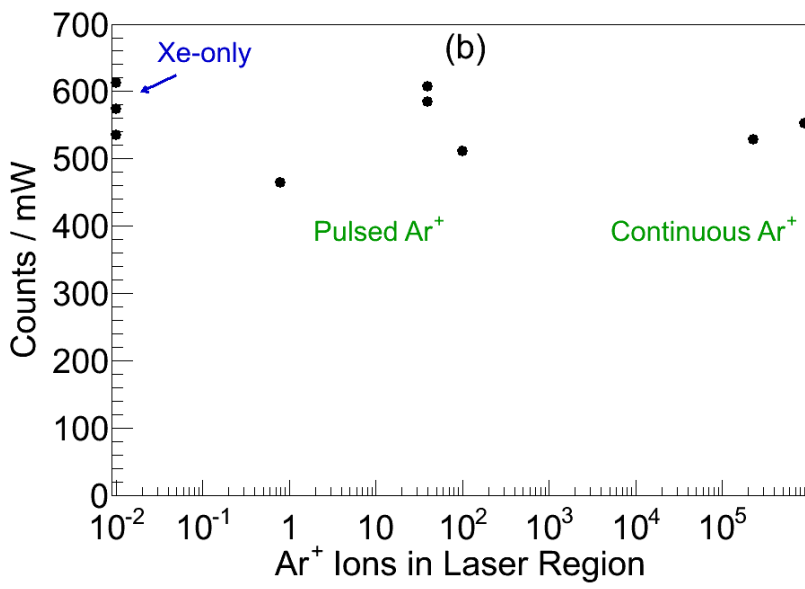
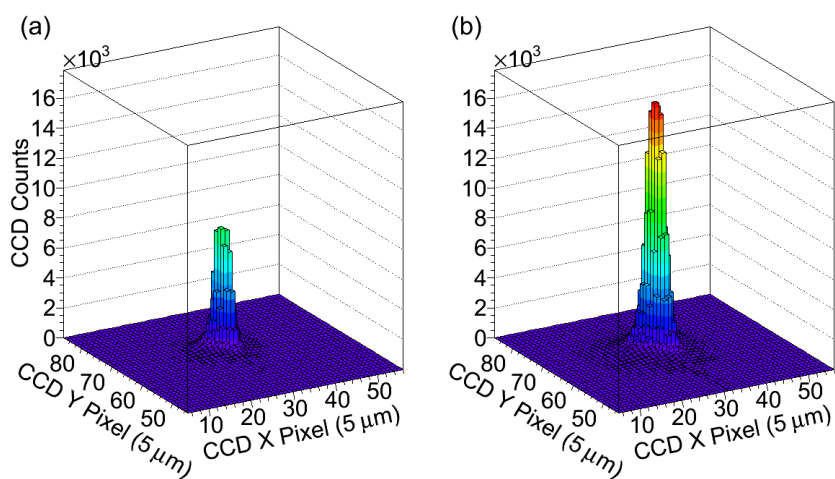
- Separation by fluorescence lifetimes
- Acid etching sapphire windows



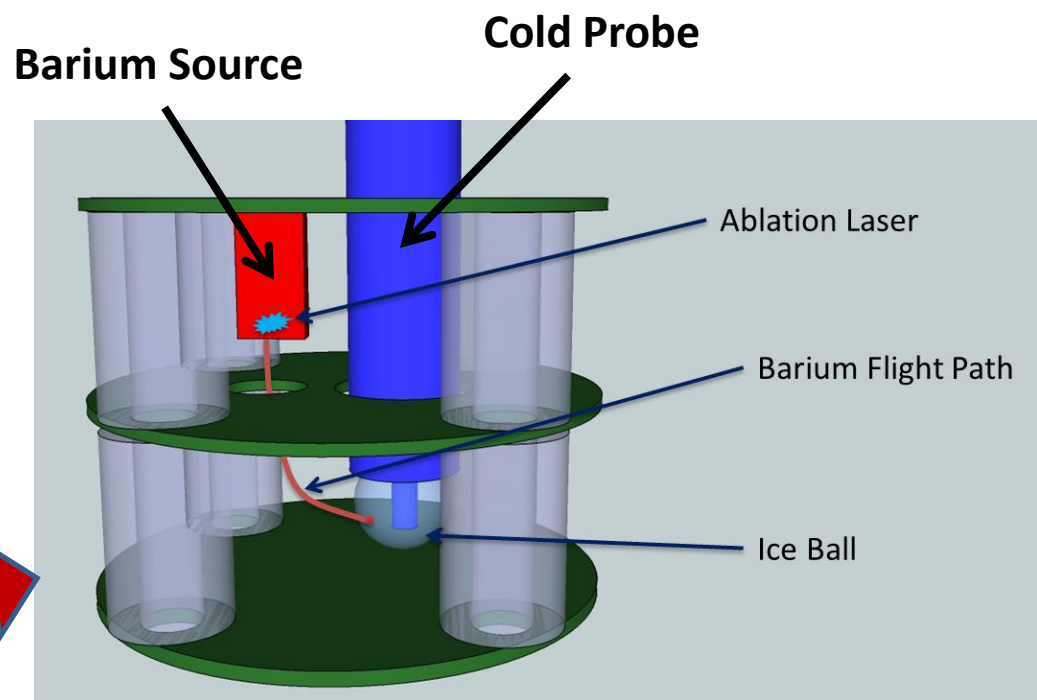
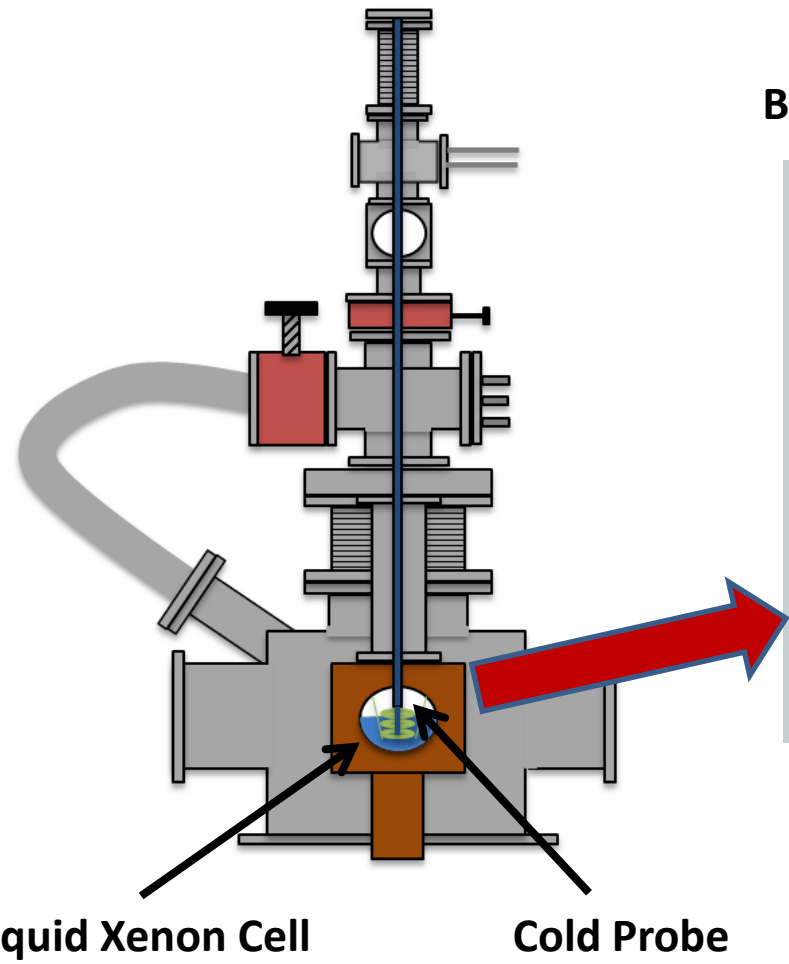
# Conclusions

- Spectroscopy of Ba in SXe has been studied with attention to:
  - Temperature history effects
  - Bleaching
- Imaging of Ba in SXe w/ sensitivity to:
  - $\sim 10^3$  atoms w/ 577- and 591-nm lines
  - Single atoms w/ 619-nm line!
- Single-atom level sensitivity is a major step toward Ba tagging in nEXO, and the future of neutrino physics!

Thx!

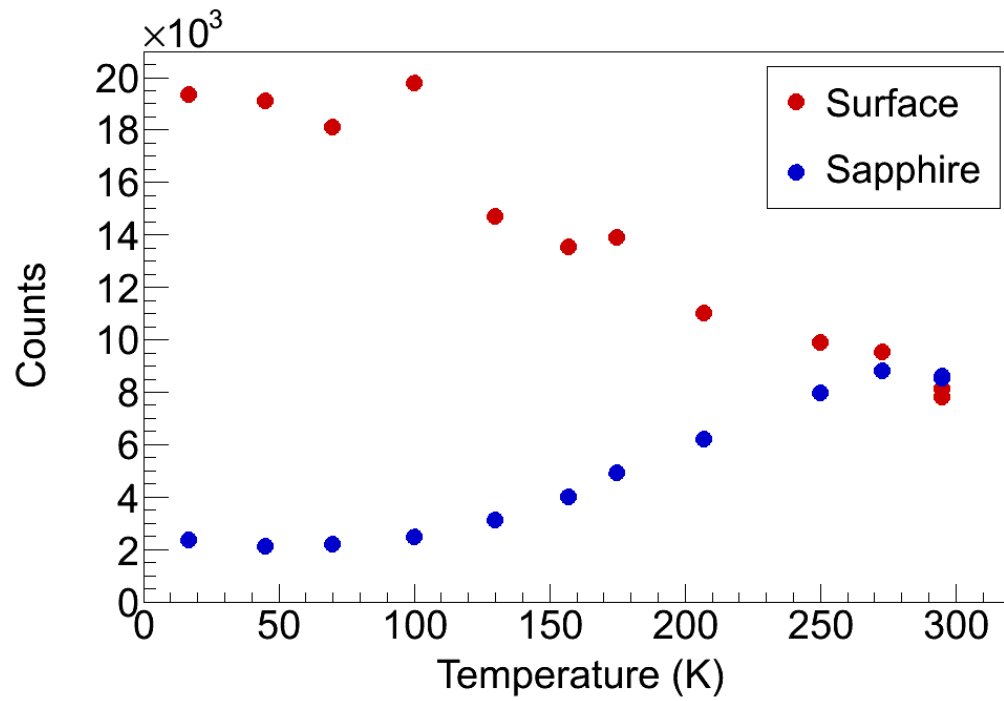


# Ion Extraction from Liquid Xenon

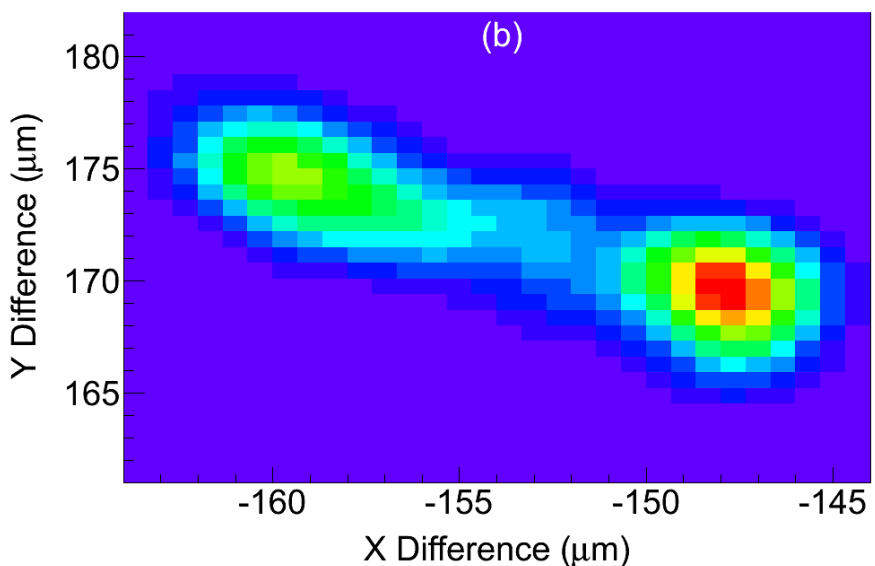
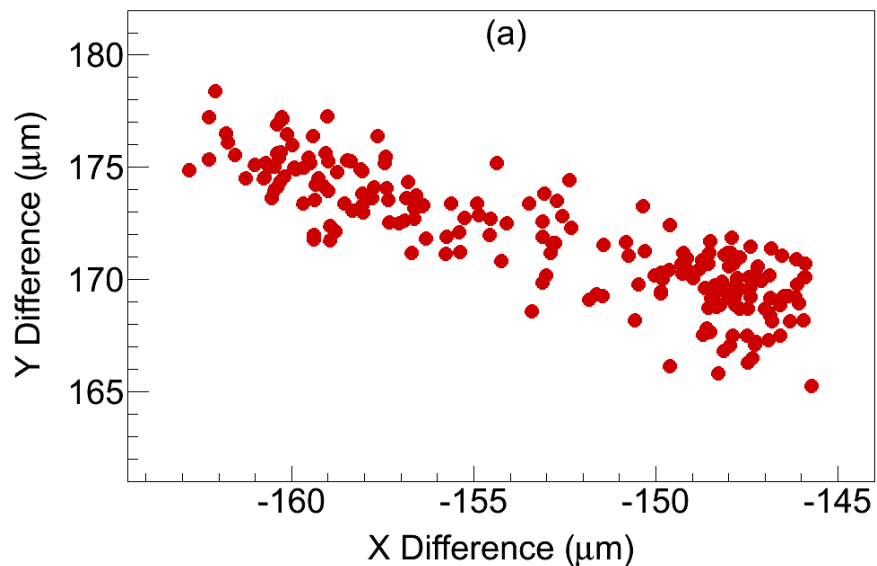


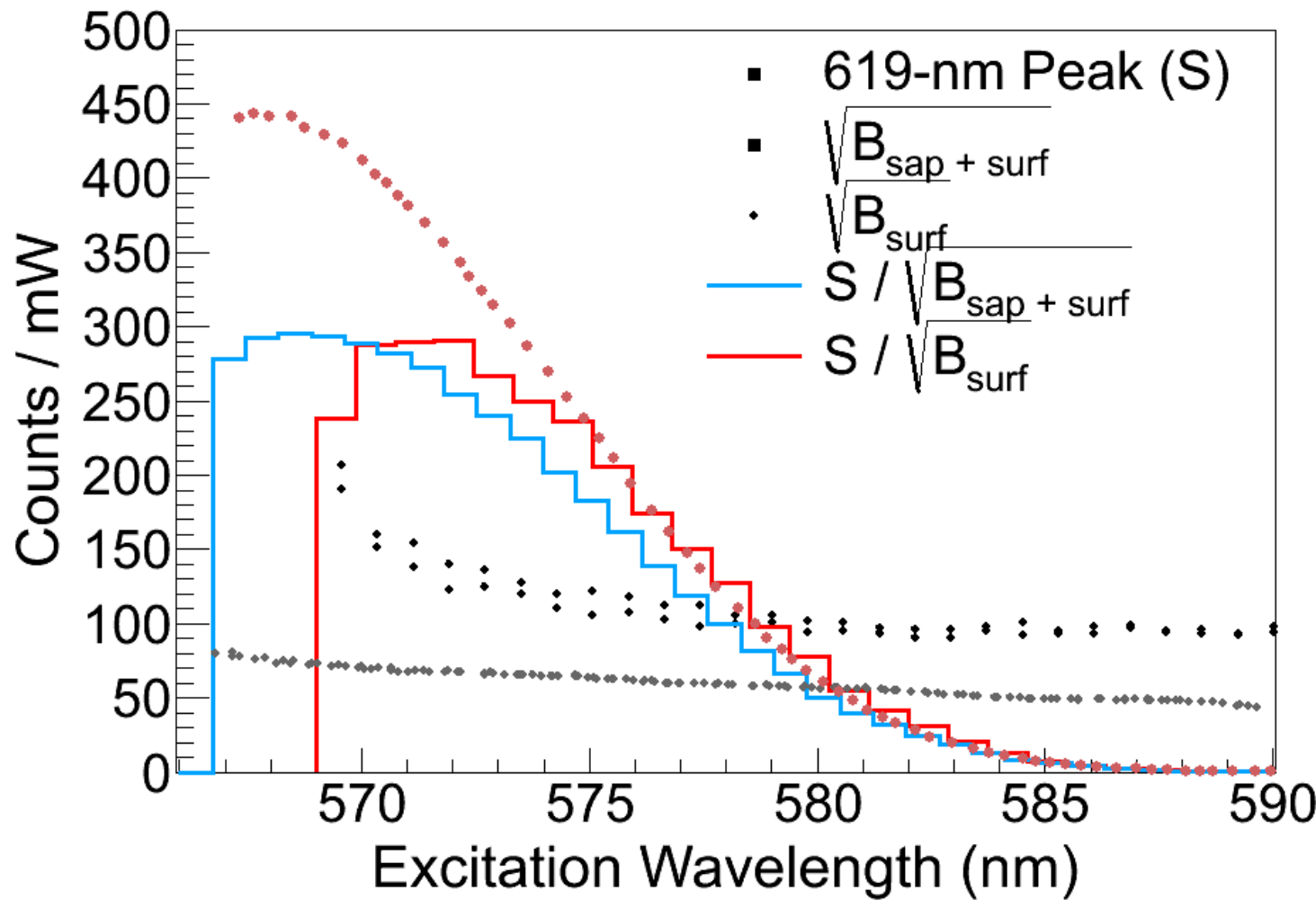
9.9 events in 2 sigma is consistent w/ null at 1.2 sigma level

## Backgrounds vs. Temperature:



## Cryostat Vibrations:





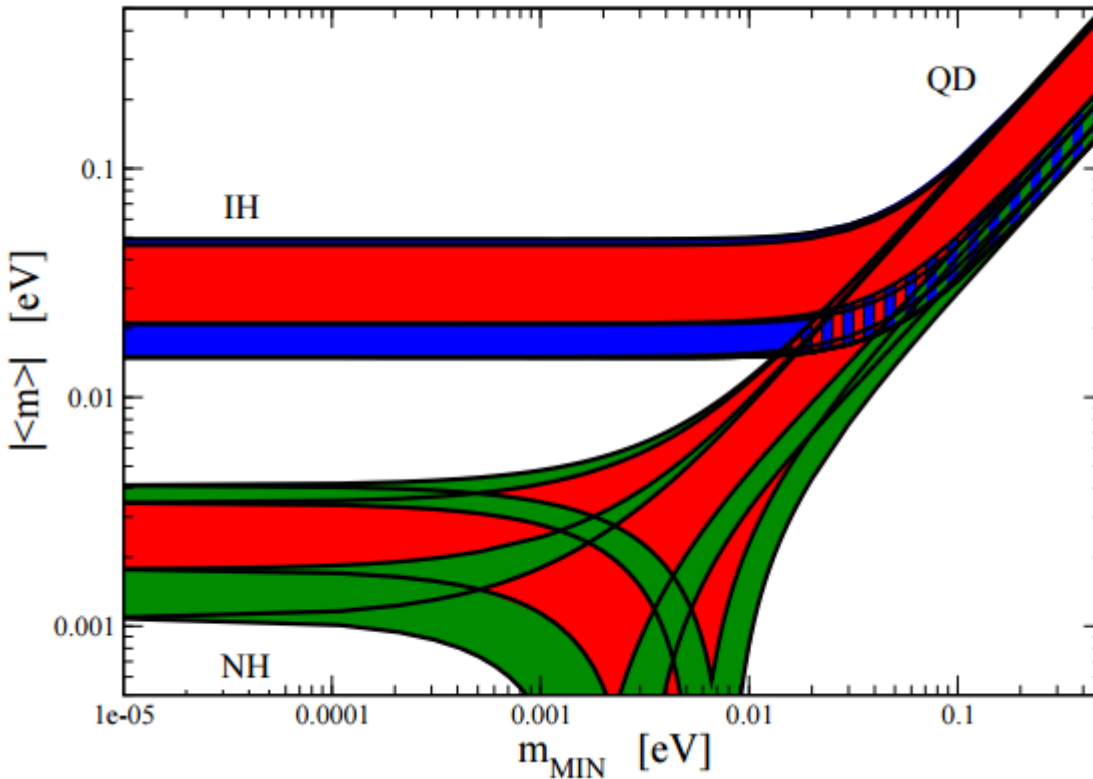
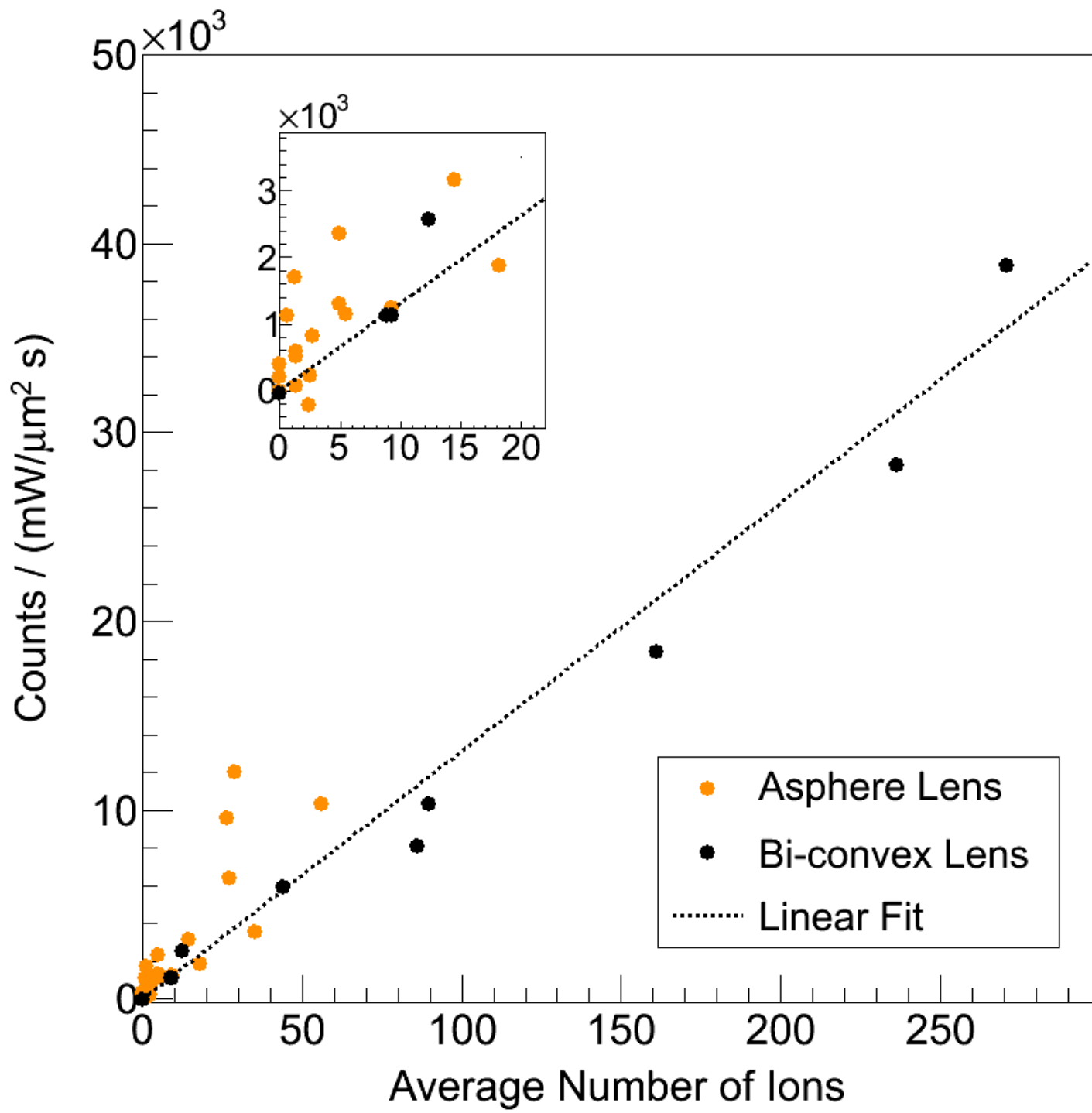


**Figure 14.10:** The effective Majorana mass  $|<m>|$  (including a  $2\sigma$  uncertainty), as a function of  $\min(m_j)$ . The figure is obtained using the best fit values and the  $2\sigma$  ranges of allowed values of  $\Delta m_{21}^2$ ,  $\sin^2 \theta_{12}$ , and  $|\Delta m_{31}^2| \cong |\Delta m_{32}^2|$  from Ref. 174. The phases  $\alpha_{21,31}$  are varied in the interval  $[0, \pi]$ . The predictions for the NH, IH and QD spectra are indicated. The red regions correspond to at least one of the phases  $\alpha_{21,31}$  and  $(\alpha_{31} - \alpha_{21})$  having a CP violating value, while the blue and green areas correspond to  $\alpha_{21,31}$  possessing CP conserving values. (Update by S. Pascoli of a figure from the last article quoted in Ref. 196.)



Parameter	Measurement ( $\pm 1\sigma$ )
$\Delta m_{21}^2$	$7.54^{+0.26}_{-0.22} \text{ } 10^{-5} \text{ eV}^2$
$ \Delta m^2 $	$2.43 \pm 0.06 \text{ (} 2.38 \pm 0.06 \text{) } 10^{-3} \text{ eV}^2$
$\sin^2 \theta_{12}$	$0.308 \pm 0.017$
$\sin^2 \theta_{23}$	$0.437^{+0.033}_{-0.023} \text{ (} 0.455^{+0.039}_{-0.031} \text{)}$
$\sin^2 \theta_{13}$	$0.0234^{+0.0020}_{-0.0019} \text{ (} 0.0240^{+0.0019}_{-0.0022} \text{)}$
$\delta/\pi$ ( $2\sigma$ range)	$1.39^{+0.38}_{-0.27} \text{ (} 1.31^{+0.29}_{-0.33} \text{)}$

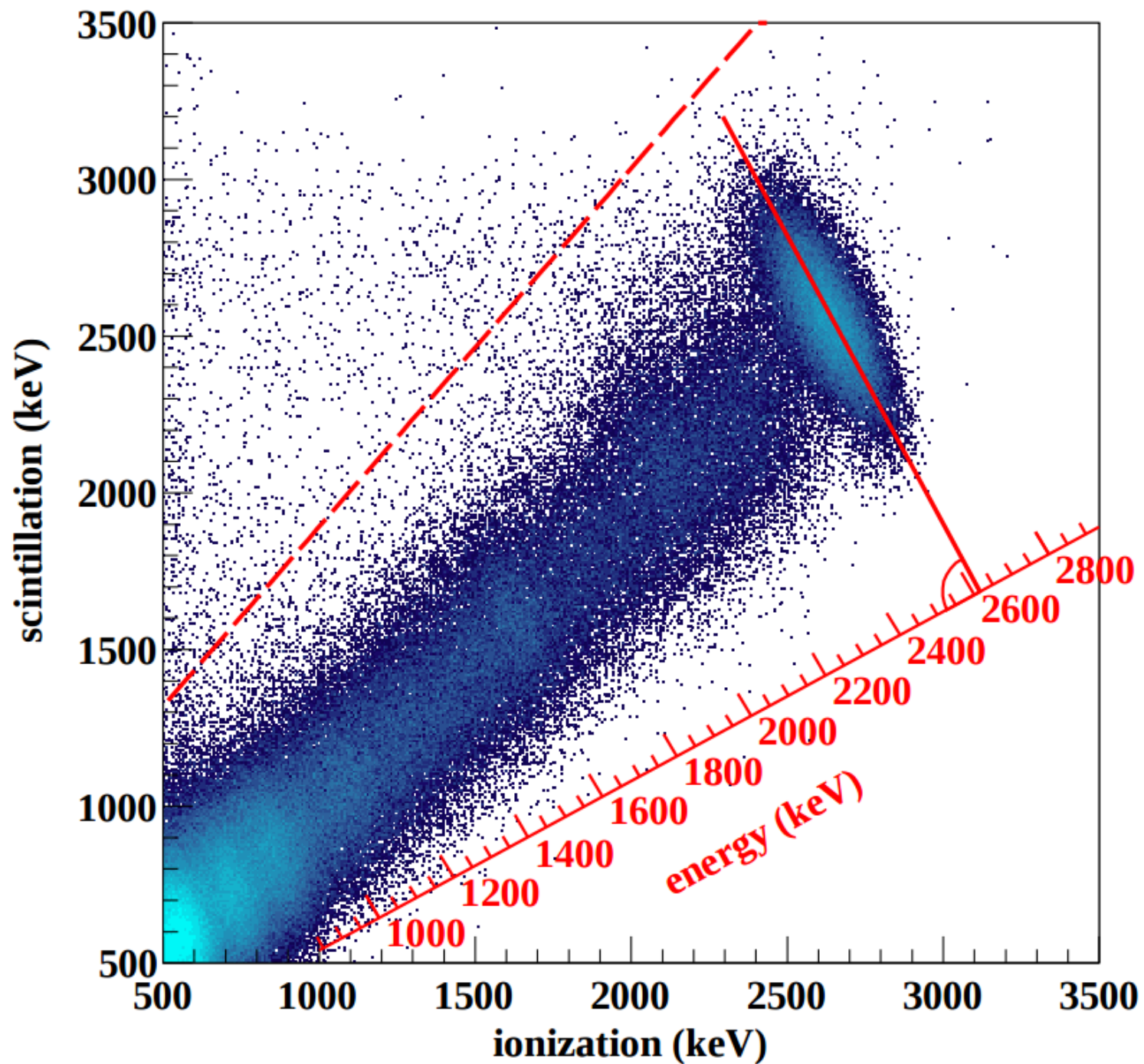
2012 Review by K. Nakamura, U. Tokyo, S.T. Petcov

**Table 14.7:** The best-fit values and  $3\sigma$  allowed ranges of the 3-neutrino oscillation parameters, derived from a global fit of the current neutrino oscillation data (from [174]). The values (values in brackets) correspond to  $m_1 < m_2 < m_3$  ( $m_3 < m_1 < m_2$ ). The definition of  $\Delta m^2$  used is:  $\Delta m^2 = m_3^2 - (m_2^2 + m_1^2)/2$ . Thus,  $\Delta m^2 = \Delta m_{31}^2 - \Delta m_{21}^2/2 > 0$ , if  $m_1 < m_2 < m_3$ , and  $\Delta m^2 = \Delta m_{32}^2 + \Delta m_{21}^2/2 < 0$  for  $m_3 < m_1 < m_2$ .

Parameter	best-fit ( $\pm 1\sigma$ )	$3\sigma$
$\Delta m_{21}^2$ [ $10^{-5}$ eV $^2$ ]	$7.54^{+0.26}_{-0.22}$	$6.99 - 8.18$
$ \Delta m^2 $ [ $10^{-3}$ eV $^2$ ]	$2.43 \pm 0.06$ ( $2.38 \pm 0.06$ )	$2.23 - 2.61$ ( $2.19 - 2.56$ )
$\sin^2 \theta_{12}$	$0.308 \pm 0.017$	$0.259 - 0.359$
$\sin^2 \theta_{23}$ , $\Delta m^2 > 0$	$0.437^{+0.033}_{-0.023}$	$0.374 - 0.628$
$\sin^2 \theta_{23}$ , $\Delta m^2 < 0$	$0.455^{+0.039}_{-0.031}$	$0.380 - 0.641$
$\sin^2 \theta_{13}$ , $\Delta m^2 > 0$	$0.0234^{+0.0020}_{-0.0019}$	$0.0176 - 0.0295$
$\sin^2 \theta_{13}$ , $\Delta m^2 < 0$	$0.0240^{+0.0019}_{-0.0022}$	$0.0178 - 0.0298$
$\delta/\pi$ ( $2\sigma$ range quoted)	$1.39^{+0.38}_{-0.27}$ ( $1.31^{+0.29}_{-0.33}$ )	$(0.00 - 0.16) \oplus (0.86 - 2.00)$ $((0.00 - 0.02) \oplus (0.70 - 2.00))$

$$U = \begin{pmatrix} c_{12}c_{13} & s_{12}c_{13} & s_{13}e^{-i\delta} \\ -s_{12}c_{23} - c_{12}s_{23}s_{13}e^{i\delta} & c_{12}c_{23} - s_{12}s_{23}s_{13}e^{i\delta} & s_{23}c_{13} \\ s_{12}s_{23} - c_{12}c_{23}s_{13}e^{i\delta} & -c_{12}s_{23} - s_{12}c_{23}s_{13}e^{i\delta} & c_{23}c_{13} \end{pmatrix} \begin{pmatrix} 1 & 0 & 0 \\ 0 & e^{i\alpha_1/2} & 0 \\ 0 & 0 & e^{i\alpha_2/2} \end{pmatrix}$$

$$U = \begin{bmatrix} U_{e1} & U_{e2} & U_{e3} \\ U_{\mu 1} & U_{\mu 2} & U_{\mu 3} \\ U_{\tau 1} & U_{\tau 2} & U_{\tau 3} \end{bmatrix}$$



tritium

<2.3 eV

Planck: sum < 0.23

.2 eV limit